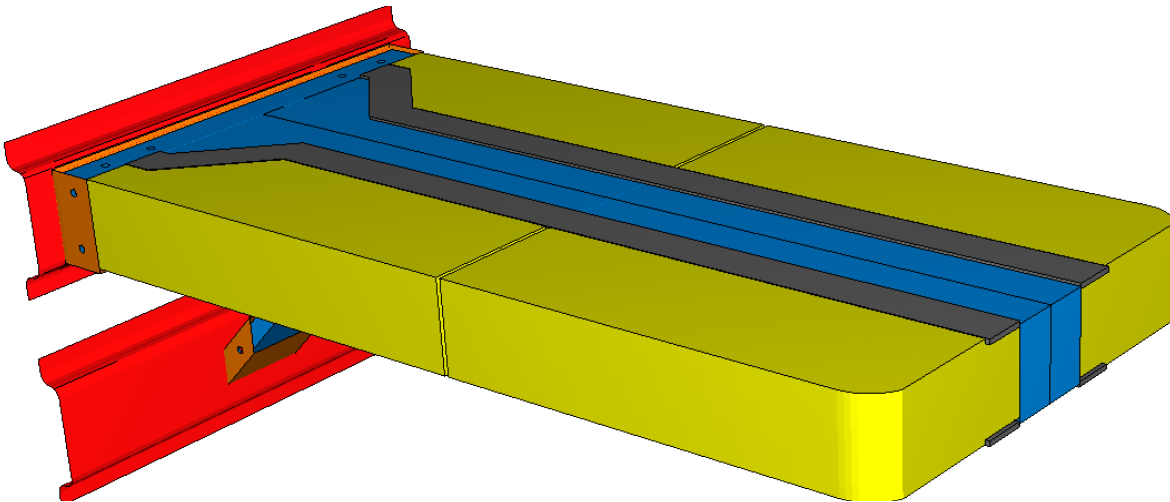




U.S. Department of
Transportation
**Federal Railroad
Administration**

Workstation Table Engineering Model Design, Development, Fabrication, and Testing

Office of Railroad
Policy and Development
Washington, DC 20590



NOTICE

This document is disseminated under the sponsorship of the Department of Transportation in the interest of information exchange. The United States Government assumes no liability for its contents or use thereof. Any opinions, findings and conclusions, or recommendations expressed in this material do not necessarily reflect the views or policies of the United States Government, nor does mention of trade names, commercial products, or organizations imply endorsement by the United States Government. The United States Government assumes no liability for the content or use of the material contained in this document.

NOTICE

The United States Government does not endorse products or manufacturers. Trade or manufacturers' names appear herein solely because they are considered essential to the objective of this report.

REPORT DOCUMENTATION PAGE			<i>Form Approved</i> OMB No. 0704-0188	
Public reporting burden for this collection of information is estimated to average 1 hour per response, including the time for reviewing instructions, searching existing data sources, gathering and maintaining the data needed, and completing and reviewing the collection of information. Send comments regarding this burden estimate or any other aspect of this collection of information, including suggestions for reducing this burden, to Washington Headquarters Services, Directorate for Information Operations and Reports, 1215 Jefferson Davis Highway, Suite 1204, Arlington, VA 22202-4302, and to the Office of Management and Budget, Paperwork Reduction Project (0704-0188), Washington, DC 20503.				
1. AGENCY USE ONLY (Leave blank)		2. REPORT DATE May 2012		3. REPORT TYPE AND DATES COVERED Technical Report
4. TITLE AND SUBTITLE Workstation Table Engineering Model, Design, Development, Fabrication, and Testing				5. FUNDING NUMBERS
6. AUTHOR(S) Richard Stringfellow ¹ and Robert Rancatore ¹				
7. PERFORMING ORGANIZATION NAME(S) AND ADDRESS(ES) U.S. Department of Transportation Research and Innovative Technology Administration John A. Volpe National Transportation Systems Center 55 Broadway Cambridge, MA 02142-1093				8. PERFORMING ORGANIZATION REPORT NUMBER
9. SPONSORING/MONITORING AGENCY NAME(S) AND ADDRESS(ES) U.S. Department of Transportation Federal Railroad Administration Office of Railroad Policy and Development Washington, DC 20590				10. SPONSORING/MONITORING AGENCY REPORT NUMBER DOT/FRA/ORD-12/06
11. SUPPLEMENTARY NOTES ¹ TIAX LLC 15 Acorn Park Cambridge, MA 02140 a) FRA Program Manager: Jeffrey Gordon				
12a. DISTRIBUTION/AVAILABILITY STATEMENT This document is available to the public through the FRA Web site at http://www.fra.dot.gov .				12b. DISTRIBUTION CODE
13. ABSTRACT (Maximum 200 words) This research effort is focused on providing a workstation table design that will reduce the risk of occupant injuries due to secondary impacts and to compartmentalize the occupants to prevent impacts with other objects and/or passengers seated across from them. The table must be capable of protecting the passengers in a seating arrangement with the table located between facing seats. Included in this study are the design, fabrication, quasi-static testing, and delivery of the table for subsequent testing in the crash energy management (CEM) full-scale test. Finite element analyses of the table components and multibody dynamic analyses of the occupant response were performed to help guide the design and predict whether the occupant injury risk for the newly designed table meets the requirements. Four tables were fabricated; two were included in the CEM full-scale train-to-train test in March 2006, and two were constructed for use in quasi-static and dynamic sled tests. To date, only the quasi-static tests and the CEM full-scale test have been performed.				
14. SUBJECT TERMS Crashworthiness, workstation table, quasi-static testing, crash energy management, full-scale test, finite element analysis				15. NUMBER OF PAGES 121
				16. PRICE CODE
17. SECURITY CLASSIFICATION OF REPORT Unclassified	18. SECURITY CLASSIFICATION OF THIS PAGE Unclassified	19. SECURITY CLASSIFICATION OF ABSTRACT Unclassified	20. LIMITATION OF ABSTRACT	

METRIC/ENGLISH CONVERSION FACTORS

ENGLISH TO METRIC

LENGTH (APPROXIMATE)

1 inch (in)	=	2.5 centimeters (cm)
1 foot (ft)	=	30 centimeters (cm)
1 yard (yd)	=	0.9 meter (m)
1 mile (mi)	=	1.6 kilometers (km)

AREA (APPROXIMATE)

1 square inch (sq in, in ²)	=	6.5 square centimeters (cm ²)
1 square foot (sq ft, ft ²)	=	0.09 square meter (m ²)
1 square yard (sq yd, yd ²)	=	0.8 square meter (m ²)
1 square mile (sq mi, mi ²)	=	2.6 square kilometers (km ²)
1 acre = 0.4 hectare (he)	=	4,000 square meters (m ²)

MASS - WEIGHT (APPROXIMATE)

1 ounce (oz)	=	28 grams (gm)
1 pound (lb)	=	0.45 kilogram (kg)
1 short ton = 2,000 pounds (lb)	=	0.9 tonne (t)

VOLUME (APPROXIMATE)

1 teaspoon (tsp)	=	5 milliliters (ml)
1 tablespoon (tbsp)	=	15 milliliters (ml)
1 fluid ounce (fl oz)	=	30 milliliters (ml)
1 cup (c)	=	0.24 liter (l)
1 pint (pt)	=	0.47 liter (l)
1 quart (qt)	=	0.96 liter (l)
1 gallon (gal)	=	3.8 liters (l)
1 cubic foot (cu ft, ft ³)	=	0.03 cubic meter (m ³)
1 cubic yard (cu yd, yd ³)	=	0.76 cubic meter (m ³)

TEMPERATURE (EXACT)

$$[(x-32)(5/9)]^{\circ}\text{F} = y^{\circ}\text{C}$$

METRIC TO ENGLISH

LENGTH (APPROXIMATE)

1 millimeter (mm)	=	0.04 inch (in)
1 centimeter (cm)	=	0.4 inch (in)
1 meter (m)	=	3.3 feet (ft)
1 meter (m)	=	1.1 yards (yd)
1 kilometer (km)	=	0.6 mile (mi)

AREA (APPROXIMATE)

1 square centimeter (cm ²)	=	0.16 square inch (sq in, in ²)
1 square meter (m ²)	=	1.2 square yards (sq yd, yd ²)
1 square kilometer (km ²)	=	0.4 square mile (sq mi, mi ²)
10,000 square meters (m ²)	=	1 hectare (ha) = 2.5 acres

MASS - WEIGHT (APPROXIMATE)

1 gram (gm)	=	0.036 ounce (oz)
1 kilogram (kg)	=	2.2 pounds (lb)
1 tonne (t)	=	1,000 kilograms (kg)
	=	1.1 short tons

VOLUME (APPROXIMATE)

1 milliliter (ml)	=	0.03 fluid ounce (fl oz)
1 liter (l)	=	2.1 pints (pt)
1 liter (l)	=	1.06 quarts (qt)
1 liter (l)	=	0.26 gallon (gal)

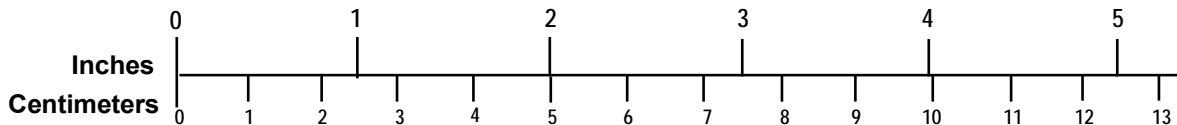
$$1 \text{ cubic meter (m}^3\text{)} = 36 \text{ cubic feet (cu ft, ft}^3\text{)}$$

$$1 \text{ cubic meter (m}^3\text{)} = 1.3 \text{ cubic yards (cu yd, yd}^3\text{)}$$

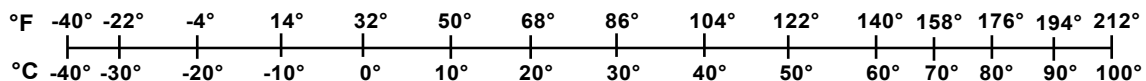
TEMPERATURE (EXACT)

$$[(9/5) y + 32]^{\circ}\text{C} = x^{\circ}\text{F}$$

QUICK INCH - CENTIMETER LENGTH CONVERSION



QUICK FAHRENHEIT - CELSIUS TEMPERATURE CONVERSION



For more exact and or other conversion factors, see NIST Miscellaneous Publication 286, Units of Weights and Measures. Price \$2.50 SD Catalog No. C13 10286

Updated 6/17/98

Preface

The John A. Volpe National Transportation Systems Center (Volpe Center) is conducting research in support of the Federal Railroad Administration (FRA) Passenger Equipment Safety Program to minimize injuries and fatalities during train accidents. This report describes the development of a fixed workstation table that was designed to reduce the risk of occupant injuries caused by impacts with tables during train collisions and to compartmentalize the occupants to prevent impacts with other objects and/or passengers seated across from them. Included in this research were the design, fabrication, quasi-static testing, and delivery of the table design for subsequent testing in the full-scale train-to-train impact test by using rail cars that incorporate crash energy management (CEM). Finite element analyses of the table components and multibody dynamic analyses of the occupant response were performed to help guide the design and predict whether the occupant injury risk for the newly designed table meets the requirements. Four tables were fabricated; two were included in the CEM full-scale train-to-train test in March 2006, and two were constructed for use in quasi-static and dynamic impact tests. The results of these tests are described in separate reports.

The project team included the Volpe Center, TIAX LLC, Taylor Raynauld Amar Associates, CVID Consulting Services LLC, Simula Aerospace, and Altair Engineering, Inc.

This work was performed as part of the FRA's Equipment Safety Research Program sponsored by the Office of Research and Development. The authors would like to thank Dr. Tom Tsai, and Mr. Eloy Martinez, former Program Managers, Mr. Jeff Gordon, current Program Manager, Ms. Claire Orth, former Division Chief, Equipment and Operating Practices Research Division, Office of Research and Development, FRA, and current Division Chief, Kevin Kesler, for their support.

The authors would like to thank Mr. Daniel Parent, Mechanical Engineer, from the Structures and Dynamics Division, Volpe Center, for his guidance, support, and assistance throughout the program.

Contents

Executive Summary	1
1. Introduction	2
2. Design Requirements	2
2.1 Introduction	2
2.2 Regulations and Standards	2
2.3 Collision Requirements	3
2.3.1 Collision Scenarios	4
2.4 Table Attachment Requirements	5
2.5 Geometric Requirements	5
2.6 Occupant Protection Requirements	7
3. Review of Existing Table Designs	8
3.1 Introduction	8
3.2 Development of Contact List	8
3.3 Identification of Key Table Features	9
3.4 Existing Table Design Strategies	9
4. Table Concepts and Selection	12
4.1 Introduction	12
4.2 Concept Generation and Selection	12
4.3 Concept Development	15
4.3.1 Materials Selection	15
5. Component Testing	21
5.1 Preliminary Crush Tests	21
5.1.1 Preliminary Honeycomb Crush Tests	21
5.1.2 Preliminary Composite Panel Crush Tests	23
5.2 Vertical Strength Tests	26
5.2.1 Single Panel Attached with Screws to C-Channel	26
5.2.2 Single Panel Bonded to C-Channel	27
5.2.3 Five-Block Panel	28
5.3 Composite Panel Crush Tests	29
5.3.1 Four-Inch Honeycomb/Melamine Panels	29
5.3.2 Two-Inch Honeycomb/Melamine Panels	32
6. Table Model Development and Analyses	35

6.1	Finite Element Models and Analyses	35
6.1.1	Honeycomb Crush	36
6.1.2	Table Crush Models	40
6.1.3	Vertical Service Load Model	45
6.2	MADYMO Model and Analyses	48
6.2.1	Eight-G Acceleration Pulse Results	51
6.2.2	CEM Acceleration Pulse Results.....	53
7.	Quasi-Static Tests.....	55
7.1	Introduction.....	55
7.2	Test Facilities and Setup	55
7.2.1	Quasi-Static Test Frame	56
7.2.2	Quasi-Static Test Setup	56
7.3	Quasi-Static Test Procedures	59
7.3.1	Service Load Tests	61
7.3.2	Longitudinal Crush Test.....	62
7.4	Test Results	64
7.4.1	Horizontal Service Load Test.....	66
7.4.2	Vertical Service Load Tests	66
7.4.3	Collision Strength under Horizontal Loading	67
8.	Table Design.....	74
8.1	Table Attachment Method	74
8.2	Table Frame and Structure.....	75
8.3	Table Crush Elements	76
8.4	Crush Element Attachment.....	77
8.5	Tabletop Attachment.....	78
9.	Fabrication.....	81
9.1	Fabrication Process	81
9.1.1	Honeycomb Panel Preparation and Installation	82
9.1.2	Tabletop Attachment	84
9.1.3	Tabletop Attachment Modifications.....	85
9.1.4	Tabletop Edges	87
9.2	Shipping	87
10.	Summary and Conclusions	88
11.	References	90

Illustrations

Figure 1. An 8g Peak, 250-Millisecond Triangular Acceleration Pulse	4
Figure 2. The Ideal Design Table Load/Crush Curve for a Single Seated Position	4
Figure 3. Workstation Table Geometry Specifications (top view)	6
Figure 4. Workstation Table Geometry Specifications (side view).....	6
Figure 5. A Georgia Rail Workstation Table.....	11
Figure 6. A Colorado Rail Car Table.....	11
Figure 7. SMTC Workstation Tables.....	11
Figure 8. A Schematic of the Crushable Table Concept Selected for Development.....	15
Figure 9. The Ideal Force/Crush Curve Used to Select the Material and Design the Table.....	16
Figure 10. A Typical Force/Crush Curve for an Aluminum Honeycomb	18
Figure 11. A Photograph of an Aluminum Honeycomb Element of the Type Used in the Table Design (the directions T, L, and W are indicated)	19
Figure 12. A Quasi-Static Crush Test Showing the Melamine Top Folding at the Grooved Location and Pulling Away from the Honeycomb as It Is Crushed.....	20
Figure 13. The Load-Crush Curve for Hexcel HexWeb CRIII 1/4-5052-.004 when Crushed in the L Direction	22
Figure 14. A Hexcel HexWeb CRIII 1/4-5052-.004 Aluminum Honeycomb Specimen before Crush (above) and during Crush (below)	23
Figure 15. A 4- by 4- by 10-Inch-Tall Honeycomb/Melamine Sandwich Panel before Crush Testing	24
Figure 16. A 4- by 4-Inch by 10-Inch-Tall Composite Panel with the Melamine Bonded to the Honeycomb with Contact Cement.....	25
Figure 17. A Comparison of the Crush Strengths of the 0.625- by 1.5- by 6-Inch Honeycomb- Only Specimen and the 4- by 4- by 10-Inch Composite Specimen	25
Figure 18. The Table Specimen Mounted in the Instron before the First Vertical Load Test.....	26
Figure 19. A 350-Pound-Force (1.56 kN) Load Is Applied to a Single-Block Panel that Has Been Bonded to the C-Channel	28

Figure 20. The Five-Block Panel under a Load of 350 lbf	29
Figure 21. A Series of Images from the Five-Panel Crush Test	30
Figure 22. A Sequence of Images Showing Crush of Single-Block Panel	31
Figure 23. A Comparison of the Measured Load-Crush Curves for the Two Honeycomb Panels	31
Figure 24. A 2-Inch-Wide Honeycomb/Melamine Composite Test Panel Clamped to Supporting Angle Irons, Shown in the Instron before Testing	32
Figure 25. A 2-Inch-Wide Honeycomb/Melamine Composite Test Panel Shown during Crush	33
Figure 26. A Comparison of the Load-Crush Curves for Two 2-Inch-Wide Honeycomb/ Melamine Panels and Two Honeycomb-Only	34
Figure 27. The Mesh Developed to Simulate Crush of a Honeycomb Block along Its L Direction	37
Figure 28. Uniform Crush of the Honeycomb Block between Two Flat Plates	37
Figure 29. Crush of the Honeycomb Block with a Centrally Located, Rigid Indenter	38
Figure 30. Crush of the Split Honeycomb Block with a Centrally Located, Rigid Indenter	39
Figure 31. The Deformed Honeycomb Block for a Crush of 7 in	39
Figure 32. A Comparison of the Load-Crush Response Predicted by the Continuum Honeycomb Model with the Idealized Curve Determined from Tests	40
Figure 33. The Finite Element Model for the Workstation Table: (a) Table Frame Only; (b) Honeycomb Blocks and Spacers Added; (c) Melamine and Rigid Indenter Added	41
Figure 34. The Separation-Strength Curve Assumed for the Contact Cement	42
Figure 35. The Predicted Deformation of the Workstation Table after 6 in of Indenter Motion	43
Figure 36. The Predicted Deformation of the Workstation Table after 6 in of Indenter Motion (top view showing outline of undeformed mesh; melamine not shown)	43
Figure 37. The Distribution of Mises Stress at an Indenter Displacement of approximately 6 in (a total load of about 5,000 lbf)	44
Figure 38. The Distribution of Equivalent Plastic Strain at an Indenter Displacement of approximately 6 in (a total load of about 5,000 lbf)	44

Figure 39. Load-Displacement Curves for the Window-Side and Aisle-Side Indenters	45
Figure 40. The Mesh for the Vertical Service Load Model (the load is applied to the region highlighted in red)	46
Figure 41. The Distribution of Vertical Displacement for a 350–Pound-Force Vertical Load	47
Figure 42. The Distribution of Mises Stress for a 350–Pound-Force Vertical Load	47
Figure 43. An Image of the MADYMO Model of the Crushable Table with Two 50th-Percentile THOR ATDs Seated at the Table	49
Figure 44. The Table Crush Response Used in the MADYMO Occupant Interaction Model	50
Figure 45. The 8g Peak, 250-Millisecond Triangular Acceleration Pulse Used in the MADYMO Analyses	50
Figure 46. The Predicted CEM Train-to-Train Acceleration Pulse Used in the MADYMO Analyses	51
Figure 47. The Predicted Force vs. Crush Response of the Table for the 8g Acceleration Pulse Scenario for (a) the Aisle Occupant and (b) the Window Occupant	52
Figure 48. The Predicted Force vs. Crush Response of the Table for the CEM Acceleration Pulse Scenario for (a) the Aisle Occupant and (b) the Window Occupant	54
Figure 49. The Quasi-Static Test Frame with the Table Setup for Testing	57
Figure 50. A Dial Gage Was Used to Measure Table Displacement in the Horizontal Service Load Test (left) and the Vertical Service Load Test (right)	57
Figure 51. Two String Pots Were Used to Measure Table Displacement in the Crush Strength Test	58
Figure 52. Three 10,000–Pound-Force Triaxial Load Cells Were Used to Measure the Wall Attachment Loads, Shown Here from a Side View of the Table-to-Wall Attachment	58
Figure 53. Load Application Sites for the Three Tests	60
Figure 54. The 10,000–Pound-Force Load Cell, the Load Application Plate, and the Foam Piece Used to Distribute the Compressive Force on the Edge of the Table	61
Figure 55. Two Hydraulic Cylinders Are Prepositioned to Separately Apply Load to the Table in Service Load Test	62
Figure 56. Two Hydraulic Cylinders Prepositioned to Apply Horizontal Load to the Table through Two Load Applicators Representing 50th-Percentile Male Abdomens in Test 3	63

Figure 57. The Load Applicator Was Sized to Represent a 50th-Percentile Male Abdomen	63
Figure 58. The Orientation of the Wall Attachment Load Cells When Viewed from Inside the Rail Car, Standing at the Aisle-Side Edge of the Table	65
Figure 59. Pre- and Posttest Photographs of the Horizontal Service Load Test (Test No. 060028)	66
Figure 60. Pre- and Posttest Photographs of the Vertical Service Loading Tests (No. 060029 and No. 060030).....	67
Figure 61. A Series of Photos (1–6) Showing Progression of Table Crush during Test No. 060031	68
Figure 62. The Measured Table Force vs. Deflection Curves for the Inboard (above) and Outboard (below) Load Applicator Positions for the Horizontal Crush Test (Test No. 060031)	70
Figure 63. A Pretest Photograph Showing the Experimental Setup for the Horizontal Crush Test (Test No. 060031).....	71
Figure 64. A Posttest Photograph of the Horizontal Crush Test (Test No. 060031)	71
Figure 65. A Posttest Photograph Showing the Crushed Honeycomb Core after the Horizontal Crush Test (Test No. 060031)	72
Figure 66. Posttest Photographs of Crushed Honeycomb Core after Test No. 060031 (left) and Test No. 060032 (right)	73
Figure 67. An Isometric View of the Crushable Table with Its Mounting Support Brackets	74
Figure 68. An Exploded View of the Crushable Table Showing all the Table Components	76
Figure 69. Results from a Crush Test Showing the Honeycomb Pulling in from the Sides during the Crush	77
Figure 70. A Photograph of the Table Crush Elements Installed in the I-Beam Showing the Recessed Areas.....	78
Figure 71. The Finished Surface (top side) of the Melamine Tabletop	79
Figure 72. Examples of Grooves Machined into the Backside of the Melamine Sheets.....	79
Figure 73. Locations of the Grooves that Are Cut into the Back Side of the Melamine.....	80
Figure 74. An Assembled Table Showing the Neoprene Edge and Marine Guard	80
Figure 75. A Welded I-Beam before Being Welded to the Box Beam.....	82
Figure 76. The Finished Weldment for Table A Installed in the Mounting Brackets	83

Figure 77. The Second Side of Table A Is Prepared for Curing.....	84
Figure 78. A Melamine Sheet Prepared for Bonding to the Frame and Honeycomb Inserts for Table A	84
Figure 79. The Underside of the Melamine Top with the Revised Groove Pattern Masked in Preparation of Spraying the Contact Cement	85
Figure 80. The Tabletop following the Spraying of the Contact Cement in the Revised Lamination Process—the Neoprene Spacers Are in Place.....	86
Figure 81. A Finished Prototype Crushable Workstation Table.....	87

Tables

Table 1. List of Industry Contacts.....	9
Table 2. Dimensional Ranges for Tables Used in Metrolink, Amtrak, and MBTA Vehicles	10
Table 3. The Table Concepts Evaluation Matrix	14
Table 4. Average Crush Strength for Aluminum Honeycomb Samples.....	22
Table 5. Results of the First Vertical Load Test	27
Table 6. Results of the Second Vertical Load Test.....	27
Table 7. Table Crush and Occupant Response Measurements for the 8g Acceleration Scenario	52
Table 8. Table Crush and Occupant Response Measurements for the CEM Acceleration Scenario	53
Table 9. Quasi-Static Test Instrumentation	59
Table 10. Quasi-Static Test Series Requirements.....	60
Table 11. Quasi-Static Test Results	64
Table 12. Peak Loads Recorded at the Three Wall Attachment Points for Each Test	65
Table 13. Average Mechanical Properties for the A572-65 Steel Used to Fabricate the Table Frame Structure	81

Executive Summary

In support of the Federal Railroad Administration (FRA) Equipment Safety Research Program, the John A. Volpe National Transportation Systems Center (Volpe Center) has been conducting research to improve structural crashworthiness of passenger rail cars and occupant protection for passengers. Described in this report is the development of a workstation table designed to reduce passenger injury risk and to compartmentalize the occupants. The prototype table developed in this project demonstrates the feasibility of a crushable table designed to protect occupants when seated in a “facing seats” configuration (also known as open bay seats) with the table between the facing seats.

A set of requirements was first developed to guide the table design. These requirements included the quasi-static and dynamic loading conditions, maximum injury assessment reference values for several body components, (e.g., head, chest, and abdomen), and the level of compartmentalization. The requirements included the ability to compartmentalize and reduce the injury risk below specified maximum limits for two 50th-percentile males seated on one side of a workstation table. The table and occupants were subjected to a standard 8g, 250-millisecond (ms) triangular acceleration pulse used to test rail equipment.

Preliminary design concepts for table elements to absorb energy and protect the occupant were generated in several broad categories, including crushable table, pivoting table, energy-absorbing mounts, and inflatable devices. The aim of the concepts that were generated was to reduce the injury risk to passengers by absorbing enough of the impact energy through deformation of some component of the table and to compartmentalize the occupant to avoid impacts with other objects or occupants. The table concepts were ranked in order of potential for achieving the design requirements, feasibility, and cost. On the basis of the rankings, one concept was then selected for detailed design. The selected concept used a crushable edge and was intended to offer equal occupant protection independent of the seating position. The attachments to the car were cantilevered and needed to be capable of withstanding the load applied by two seated occupants during the collision. Finite element analyses were performed to guide the detailed design and verify that the workstation table could withstand the operating loads without permanent deformation. Occupant response analyses were also performed to predict the reduction in injury risk that the improved workstation table design could achieve.

Nondestructive quasi-static tests were performed to show that the table design met the service load requirements. In addition, destructive crush tests were performed to obtain the actual force/crush response of the table and to show that the mounting arrangement met the attachment strength requirements. The measured force/crush response was used to model the planned occupant experiments in a full-scale train-to-train impact test using rail cars modified to incorporate crash energy management (CEM). Modeling results indicated that the tables met the injury assessment reference value (IARV) requirements set for the improved table design.

1. Introduction

The Volpe Center has been supporting FRA in conducting research and development studies to improve rail equipment crashworthiness. Areas for improvement are sometimes identified during accident investigations conducted by FRA's forensic accident investigation team. As an example, the investigation of an inline collision between a passenger train and a freight train in Placentia, CA, on April 23, 2002, which resulted in two fatalities and several injuries for occupants seated at workstation tables [1], identified workstation tables as an area in which occupant protection strategies can reduce the risk of fatal and serious injuries on passenger rail cars [2].

This project addresses this concern by developing a crushable workstation table that reduces passenger injury risk and compartmentalizes the occupants. The prototype table designed in this project will help to protect occupants during a collision when seated in a "facing seats" configuration (also known as open bay seats) with the table between the facing seats.

2. Design Requirements

2.1 Introduction

The design requirements for the improved workstation table were derived from industry and Federal requirements, and they provide the basis for selecting and evaluating various design options. The Workstation Table Design Requirements, shown in Appendix A, include collision, operational, and fabrication requirements.

2.2 Regulations and Standards

The workstation table requirements were written to satisfy the applicable government and industry regulations and standards found in Title 49 Code of Federal Regulations (CFR) Part 238, Section 233 [3] and the United Kingdom (UK) Association of Train Operating Companies (ATOC) Vehicles Standard AV/ST9001.10 [4]. The maximum injury criteria values are derived from 49 CFR Part 571, Section 208 [5]. Although the CFR does not explicitly state the requirements for tables, some of the key requirements used in this project for the workstation design were based on some of its regulations for other rail equipment. These include the following:

- The table must be attached to an existing passenger car by way of seat rails on the floor and/or rails on the wall of the carbody, taking care not to impede occupant ingress/egress.
- The hardware used to attach the table to the carbody must not require modification of the seat rails and must conform to 49 CFR Part 238, Section 233, Article (d): "To the extent possible, all interior fittings in a passenger car, except seats, shall be recessed or flush-mounted."
- Sharp edges or corners shall be avoided or padded to mitigate consequences of an impact with such surfaces.

The requirements and recommended practices from the UK ATOC Vehicles Standard AV/ST9001.10 were used as a guide to help identify requirement categories to be included. The magnitudes of the applied quasi-static forces were modified to be consistent with other existing requirements in the CFR. For example, the UK standard requires that a ± 224 -pound-force (lbf) ($\pm 1,000$ Newton (N)) vertical quasi-static force be applied anywhere on the table with less than 0.050 inches (in) (1.1 millimeters (mm)) of permanent deformation of the table. Likewise, it requires that a ± 336 lbf (1,500 N) horizontal force be applied with no permanent deformation. The key requirements for this project are the following:

- Permanent deformation of the table shall be less than 0.050 in (1.1 mm) following application of a 350 lbf (1,557 N) downward vertical load applied over a 5- by 5-inch (0.13 by 0.13 meters (m)) area at any point on the top surface of the table. The load and area of application were chosen to represent a person(s) standing on the table.
- Permanent deformation of the table shall be less than 0.050 in (1.1 mm) following application of a 500-pound-force (2,224 N) longitudinal (i.e., the direction of travel of the vehicle) load applied over a minimum 8- by 3.5-inch (0.20 by 0.09 m) area at any point on the table edge. The load and area of application were chosen to represent a person(s) pushing on the table with his/her feet.
- The crush/displacement of the table edge shall occur in a controlled fashion in the longitudinal direction, shall compartmentalize the occupant, and shall prevent head impacts with the table.
- The table shall not enter the space of the facing occupant nor interfere with his/her egress.

2.3 Collision Requirements

The following collision requirements guided the design of the improved workstation table:

- The table must reduce the injury risk for a 50th-percentile male experiencing an 8g peak, 250-millisecond duration triangular acceleration pulse, as shown in Figure 1.
- The minimum force necessary to cause permanent table edge crush is 750 lbf (3.3 kiloNewton (kN)).
- The maximum force experienced by the occupant caused by impact with the table is 2,200 lbf (9.8 kN).

Though not a design requirement, the idealized force/crush curve for an individual seat position of the table is shown in Figure 2. This force/crush characteristic meets the collision requirements defined above in computer models and was used to guide the design process.

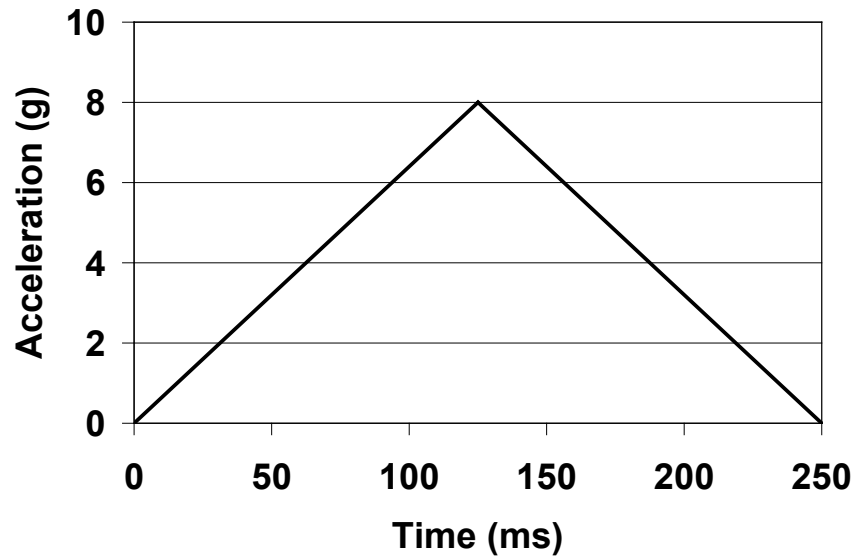


Figure 1. An 8g Peak, 250-Millisecond Triangular Acceleration Pulse

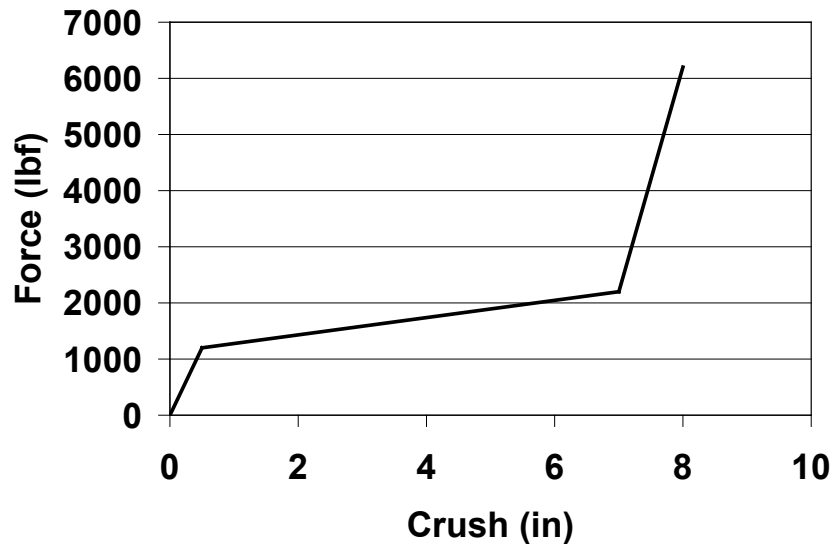


Figure 2. The Ideal Design Table Load/Crush Curve for a Single Seated Position

2.3.1 Collision Scenarios

Two collision scenarios were identified to be used during the design tasks, one ideal and one nonideal scenario. The workstation table design was required to meet both scenarios.

2.3.1.1 Ideal Collision Scenario

The ideal collision scenario involves a facing seat arrangement with a seat pitch of 65 in (1.65 m). The table is positioned between the facing seats with two, seated 50th-percentile males on one side of the table. An 8g peak, 250-millisecond acceleration pulse is applied to the table and occupants.

2.3.1.2 Nonideal Collision Scenario

The nonideal collision case differs from the ideal case in that one 50th-percentile male is seated directly between the window and the aisle seats, essentially straddling the seats. This scenario was considered to ensure that the table design does not pose a more serious threat to a person moving from one seat to the other.

2.4 Table Attachment Requirements

An important aspect of the table design was that its mounting must not fail, which would allow the table to become a free-flying object that could injure passengers. The following attachment requirements focused on ensuring the table remains attached to the carbody:

- The table must be attached to an existing passenger car by way of seat rails on the floor and/or rails on the wall of the carbody, taking care not to impede occupant ingress/egress.
- The table attachments to the floor and/or wall must not experience significant permanent deformation under a quasi-static horizontal load of 500 lbf (2,225 N) applied on a minimum 8- by 3.5-inch (0.20 by 0.09 m) area in a longitudinal direction at the aisle-side edge of the tabletop.
- The table attachments to the floor and/or wall must not experience permanent deformation under loading from two 50th-percentile male occupants subjected to an 8g peak, 250-millisecond duration triangular acceleration pulse.

2.5 Geometric Requirements

The table must meet several geometric requirements that were based on typical industry practice with regard to size and location relative to the seated occupants as well as features like the table edge. The geometric requirements for the table include the following:

- The edge must be a minimum of 2 in (51 mm) in thickness. The corners of the table edge must be rounded to a minimum radius of 0.188 in (5.1 mm).
- The depth must be at least 16 in (0.41 m) but no more than 20 in (0.51 m).
- The overall size must be small enough to allow occupants to slide easily into the seats, and yet large enough to be functional.
- The underside must be at least 28 in (0.74 m) but no more than 32 in (0.81 m) from the floor.
- The top of the table must be level and continuous. It must be centered between the facing seats and span the entire width of both the aisle and window seats.

No part of the table may occupy the space necessary for an occupant to be seated at any of the seats surrounding the table. The diagrams shown in Figure 3 and Figure 4 illustrate the spatial requirements of the table with respect to the seats and occupants. Depth and width are depicted

in Figure 3 below. The height is the vertical dimension form the floor to the underside of the table. The thickness is the vertical dimension of the tabletop.

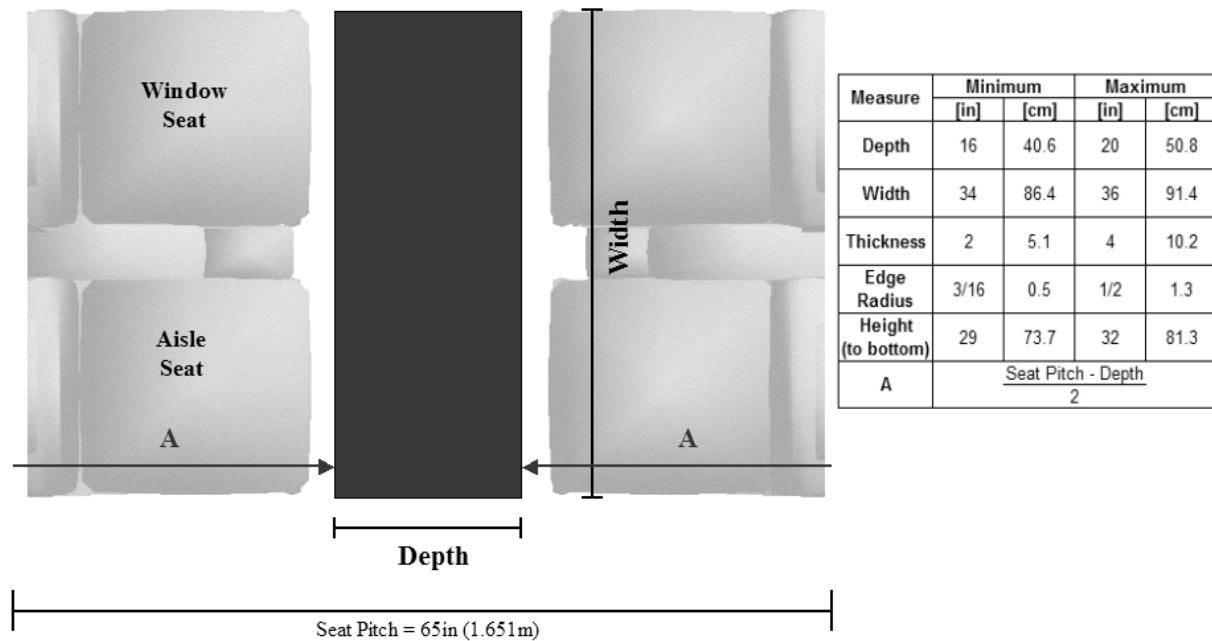


Figure 3. Workstation Table Geometry Specifications (top view)

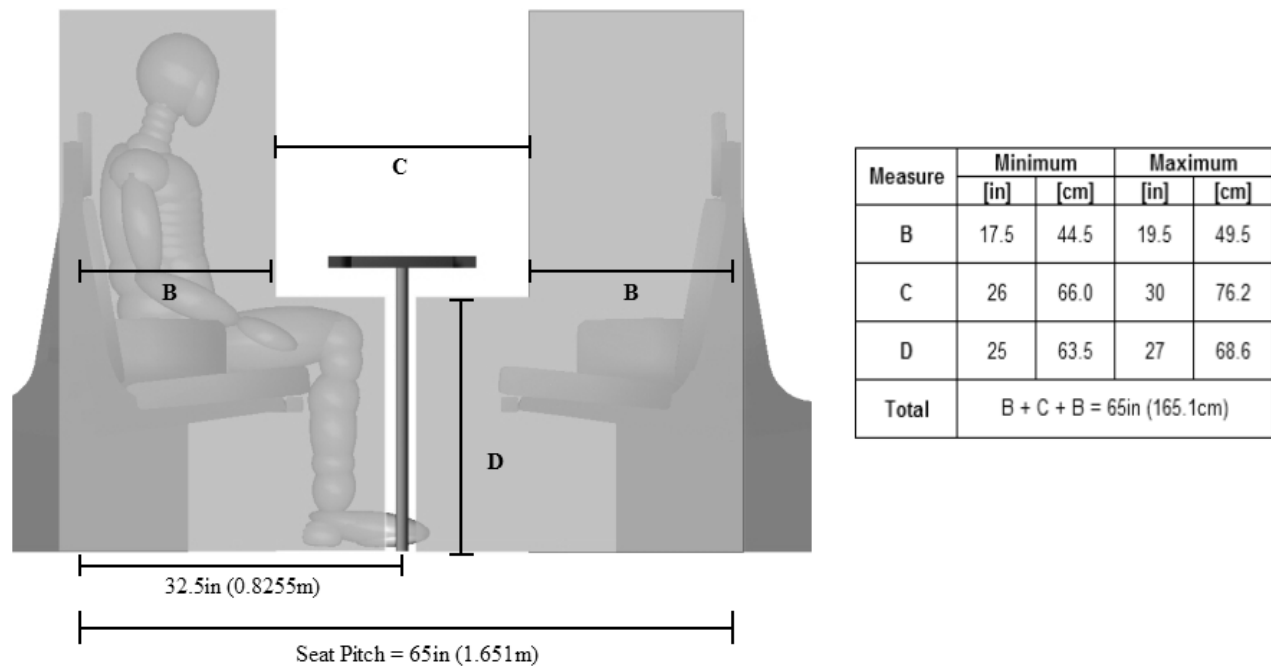


Figure 4. Workstation Table Geometry Specifications (side view)

2.6 Occupant Protection Requirements

The primary purpose of a table is to provide a functional work surface for passengers seated at a table. Without interfering with table functionality, requirements have been added to also protect the occupant by providing compartmentalization and reducing the injury risk when the occupant impacts the table edge during a collision. To increase the collision protection offered by workstation tables, the following requirements have been defined for a sled test with an 8g, 250-millisecond crash pulse, as described in Appendix A:

- Both occupants seated at the table must be compartmentalized. Successful compartmentalization requires that the resting position of the occupant after the impact be between the initial seating position and the workstation table.
- The head, torso, or arms of either occupant must not impact the seats opposite the table.
- Injury criteria limits (as measured on instrumented ATDs in dynamic tests) include the following:
 - a) The Head Injury Criteria, HIC15, must not exceed 700;
 - b) The neck injury criteria, Nij, must not exceed 1.0;
 - c) The neck tension must not exceed 938 lbf (4,170 N);
 - d) The chest deceleration must not exceed 30g over a 3-millisecond clip;
 - e) The chest compression must not exceed 2.36 in (60 mm);
 - f) The chest viscous criterion must not exceed 2.62 feet (ft)/second (s) (0.8 m/s);
 - e) and f) are measured at the sternum;
 - f) is calculated using a torso depth of 9 in (0.229 m), with a scale factor of 1.3;
 - g) The abdominal compression must not exceed 2.75 in (70 mm); and
 - h) The upper abdominal viscous criterion must not exceed 4.10 ft/s (1.25 m/s);
 - g) and h) are measured at the upper abdomen/lower CRUX of the Test device for Human Occupant Restraint (THOR);
 - g) and h) are measured at the lower CRUX of the Hybrid 3RS;
 - f) is calculated using torso depth of 9 in (0.229 m), with a scale factor of 1.3.

Detailed requirements can be found in Appendix A.

3. Review of Existing Table Designs

3.1 Introduction

A review of existing workstation tables was conducted in an effort to better understand the state-of-the-art passenger car workstation table design. This review had two primary objectives: (1) to identify and document the geometry, fabrication, and attachment parameters of existing workstation tables to establish a baseline from which an energy-absorbing table could be designed and optimized for installation compatibility and ease of use; and (2) to understand the design strategies that others have used for improved crashworthiness workstation tables.

The next several sections describe the approach used during the review of existing tables with photographs of some of the tables identified.

3.2 Development of Contact List

A list of rail industry contacts was generated that included names, companies, email addresses, and telephone numbers. The contacts include rail car manufacturers and operators, internal fittings supply companies, and European leasing and operating companies. Table 1 lists the contact names and companies. The individuals on the list were contacted by telephone and/or through a survey letter to gather information concerning the crashworthiness of existing tables. Tables B1, B2, and B3 in Appendix B contain additional contact information and brief summaries of the discussions with each person.

Table 1. List of Industry Contacts

Name	Company	Name	Company
Rail Car Manufacturers/Operators			
Gordon Campbell	LDK Engineering, Inc, (for Bombardier)	Blair Slaughter	Amtrak
Ned Parker	Colorado Railcar, CO	Pat Malin	Amtrak
Neil Harwood, Chief Engineer	Alstom	Andre Gagne	Bombardier
Ralph Dolinger (Steve Roman)	LTK Engineering Services	Telis Kakaris	Metrolink
European Leasing Companies (TLC)			
Barrie Cottam, Engineering Mgr. – Fleet	Metronet BCV, Ltd., UK		
European Operating Companies (TOC)			
Clive Burrows, Director of Engineering	First Group, UK	John Benyon	AEA Technology Rail
Jim Lupton, Head of Engineering and Research	Rail Safety and Standards Board (RSSB)	David Sawyer, Engineering Director	South West Trains, UK
Roy Windle	Atomic Energy Association Technology Rail (AEAT)		
Interior Fitting Supply Companies			
Terry Soesbee, President	RailPlan International, Baltimore, MD	Gilles Le Masson	Syndicat Mixte des Transport en Commun (SMTC), France
Emmit Lonergan	Frank Ralphs, Buffalo, NY	Ken Ullman, Engineering	Cattco USA
Morley Smith	GSM Design	Claude Martin, Engineering Director	Compin

3.3 Identification of Key Table Features

Several key categories were defined to organize information gathered about existing tables. These categories include geometry and construction of the tables, manufacturing methods, attachment methods to the rail car, and other crashworthiness features. Table B2 in Appendix B presents a summary of the features of existing tables for each of the categories listed above. Although all of the tables meet the existing regulations and standards, none of them was designed to purposely crush and absorb energy and provide compartmentalization.

3.4 Existing Table Design Strategies

Each individual listed in Table 1 was contacted, and their respective information was documented. Tables B2 and B3 in Appendix B summarize the information gathered on existing passenger car workstation tables.

Overall, several table and attachment design strategies were documented. Design strategies were originally targeted for passenger comfort in terms of ingress and egress, as well as for operational usefulness. Recently, however, strategies for crashworthiness and passenger safety have been incorporated into some table and attachment designs. Some of the features associated with these designs include the following:

- A sacrificial table attached to a highly structural, secure attachment that provides compartmentalization. The table is of traditional ply-metal construction encased in a phenolic-based laminate material with a marine edge to prevent liquid spills from rolling onto the floor. The attachment is very rugged, with a double stainless steel tube that bolts to the floor and bends 90 degrees beneath the table and extends to the wall mount (Metrolink).
- A thin, honeycomb-core table that is lightweight offers some local crushability and operational rigidity and is attached structurally to seat tracks on the wall and the floor to provide compartmentalization (Acela).
- Energy absorption is designed into the attachment and not into the table (SMTC).
- The tabletop length spans from the wall to the aisle seat inboard arm rest to offer potential protection for both seated passengers.

Specific dimensions were obtained for tables provided by Metrolink, Amtrak, and the Massachusetts Bay Transportation Authority (MBTA). Table 2 shows a summary of the table dimensions.

Table 2. Dimensional Ranges for Tables Used in Metrolink, Amtrak, and MBTA Vehicles

Table Parameter	Dimensions
Length	30.4–53.7 in (0.77–1.36 m)
Width	16–24 in (0.41–0.61 m)
Depth	0.75–1.0 in (19–25 mm)
Distance from top of table to floor	27.12–29.75 in (0.69–0.76 m)
Seat pitch	42–69 in (1.07–1.75 m)
Distances to table leg	26–27 in (0.66–0.69 m) from wall to table leg, 28.9 in (0.73 m) from table leg to car center line

Several existing tables are pictured in Figures 5 through 7. Of the safety strategies described previously, however, only the table length spanning both seat widths is depicted by these photos.



Figure 5. A Georgia Rail Workstation Table



Figure 6. A Colorado Rail Car Table



Figure 7. SMTC Workstation Tables

4. Table Concepts and Selection

4.1 Introduction

The goal of this project was to design a workstation table that could protect seated occupants by compartmentalizing them and reducing the injury risk caused when they impact the table edge during a collision. Accident investigations have shown that a narrow, stiff tabletop can severely injure the internal organs in the abdomen, potentially resulting in fatalities. Some important considerations of any energy-absorbing table include the force to which the occupant is subjected, the area over which the force is applied, and the region of the body that will be impacted. Associated with these are the constraints on the table design. Some of the constraints include the following:

- The table must remain fastened to the rail car,
- The table must not deflect more than a specified amount, and
- The table must keep the occupant compartmentalized.

These and other requirements mentioned previously require innovative ideas that become the basis for a design. The next several sections summarize the process used to generate ideas, the concepts that were identified, and in more detail, the table design that was tested in the CEM full-scale train-to-train test.

4.2 Concept Generation and Selection

Two concept generation sessions were held to generate ideas that could be used individually and/or combined to develop a crashworthy table. Engineers and scientists with varied backgrounds used their experience to identify, discuss, and build upon ideas that could help protect occupants seated at a table in a rail car that is involved in an inline collision. Before the sessions, the participants were presented with an overview of the problem and the issues related to it. They were shown test videos of onboard experiments in full-scale impact tests of conventional and CEM cars with conventional tables installed. The general requirements of the table and occupant interactions were described.

The first session was conducted at TIAX LLC (TIAX) and included participants from TIAX, CVID Consulting Services LLC (CVID), Technical Metal Specialties, Inc., and the Volpe Center. The second session took place at Transportation Technology Center, Inc. (TTCI), in Pueblo, CO, where team members from TIAX were joined by participants from the Volpe Center, Louis T. Klauder and Associates (LTK), and Metrolink. The purpose of these sessions was to identify and document the ideas, which included energy-absorbing methods to tabletop features, materials, and attachment features. Operational issues, such as the need to support tabletop and edge loads, and the use of an aisle-side support and/or knee bolsters and their effects on occupant ingress/egress and comfort also were discussed.

A set of criteria was identified and used to later rank the ideas and are shown across the top of Table 3. The ideas were screened and combined with the appropriate table concept. Every team member ranked each idea with respect to its ability to fulfill the program requirements and meet

the criteria. The overriding requirement of the table concept was for it to absorb enough energy in some manner to protect the occupants while keeping them compartmentalized.

Four basic table concepts were identified as being capable of meeting the requirements. These concepts feature different methods for absorbing energy and compartmentalizing the occupant:

- A crushable table material,
- Energy absorption at the table mount,
- Inflatable protection, and
- Energy absorption with a pivoting table.

For each of these general concepts, several different specific mechanisms for absorbing energy and/or compartmentalizing the occupant were identified. Twelve evaluation factors were identified and weighted according to importance. Each specific mechanism was rated on a scale from 0 to 5 and multiplied by the appropriate weighting factor. The weighted ratings were summed, with the highest value indicating the most promising mechanism. Table 3 provides this information in an evaluation matrix. This matrix was used by the team to rate the table concepts. The results of the rating were presented to the Volpe Center along with a recommended concept to be analyzed and designed.

Table 3. The Table Concepts Evaluation Matrix

	Energy Absorbed (efficiency)	Crush Efficiency (distance)	Vertical Load Requirement	Weight	Requires Active Control	Impact Load Distribution	Effects Ingress or Egress	Complexity of Design	Material Cost	Manufacturability Ease	Single Occupant Issues	Maintenance Required	SUM
RATING	5	4.5	4	3.5	1.25	5	3.5	2.5	1.75	2.25	4	2.25	
Crushable Table													
Center crushing	17.5	15.75	14	12.25	4.6875	20	17.5	6.25	5.6875	5.0625	14	8.4375	164
Edge crushing	20	13.5	10	12.25	4.6875	20	14	11.25	5.6875	8.4375	16	8.4375	167
Honeycomb Vertical	20	18	18	15.75	4.6875	20	14	11.25	3.9375	8.4375	16	8.4375	181
Honeycomb Horizontal	20	15.75	8	17.5	4.6875	17.5	14	11.25	3.9375	7.3125	16	8.4375	163
Tubes Lateral	17.5	15.75	10	12.25	4.6875	20	14	8.75	5.6875	5.0625	14	8.4375	159
Tubes Longitudinal	22.5	13.5	10	12.25	4.6875	20	14	8.75	5.6875	6.1875	14	8.4375	159
Tubes Vertical	17.5	15.75	18	10.5	4.6875	20	14	8.75	5.6875	5.0625	16	8.4375	167
Scored Metal	7.5	13.5	12	14	4.6875	15	14	5	3.9375	3.9375	14	8.4375	135
Foam filled, shape driven	15	13.5	14	17.5	4.6875	20	14	6.25	5.6875	7.3125	16	8.4375	161
Metal Cutting	17.5	15.75	16	12.25	4.6875	17.5	14	6.25	3.9375	2.8125	10	8.4375	148
Energy Absorbing Mounts													
Spring and Damper	15	9	16	14	4.6875	15	14	6.25	3.0625	3.9375	10	6.1875	135
Multiple mounts	15	13.5	18	8.75	4.6875	12.5	12.25	6.25	2.1875	2.8125	10	6.1875	130
Metal cutting	15	15.75	20	8.75	4.6875	12.5	14	7.5	3.9375	2.8125	8	7.3125	140
Crushable	12.5	15.75	14	14	4.6875	12.5	14	8.75	5.6875	3.9375	10	7.3125	143
Shock Absorber	15	11.25	16	7	4.6875	12.5	15.75	8.75	3.0625	3.9375	10	6.1875	132
Inflatable Protection													
Edge Inflatable	15	11.25	16	14	0.9375	22.5	12.25	7.5	1.3125	5.0625	16	3.9375	147
Knee bolster trigger	7.5	9	14	10.5	0.9375	20	8.75	5	1.3125	3.9375	10	2.8125	111
Sensor trigger	15	13.5	16	15.75	0.9375	15	14	6.25	1.3125	5.0625	12	2.8125	133
Knee Bolster - padded	7.5	6.75	14	12.25	2.1875	20	7	7.5	3.0625	6.1875	16	7.3125	127
Knee Bolster - resilient	5	6.75	14	12.25	2.1875	17.5	8.75	7.5	3.0625	6.1875	16	7.3125	122
Knee Bolster with inflatable	10	9	14	12.25	0.9375	22.5	7	6.25	1.3125	3.9375	14	3.9375	123
Undertable inflatable, individual	12.5	11.25	14	10.5	0.9375	25	7	5	1.3125	2.8125	16	3.9375	132
Undertable inflatable, per side	12.5	11.25	14	8.75	0.9375	25	7	5	1.3125	2.8125	14	3.9375	128
Pivoting Table													
Single pivot per side	17.5	4.5	14	12.25	3.4375	17.5	8.75	2.5	3.0625	1.6875	12	5.0625	122
Double pivot per side	12.5	6.75	12	8.75	3.4375	17.5	8.75	2.5	3.0625	1.6875	12	5.0625	114
Crushing pivot	12.5	6.75	12	12.25	3.4375	12.5	8.75	2.5	3.0625	1.6875	10	5.0625	111
Metal cutting pivot	17.5	6.75	14	8.75	3.4375	15	8.75	2.5	3.0625	1.6875	10	5.0625	117
Rotational Spring pivot	15	6.75	10	12.25	3.4375	15	8.75	2.5	3.9375	1.6875	10	6.1875	116

4.3 Concept Development

On the basis of the results of the evaluation, the crushable table material concept was selected for development. Figure 8 shows a schematic of the crushable table concept. This concept meets the requirements of protecting one or two seated occupants, regardless of their seated location.

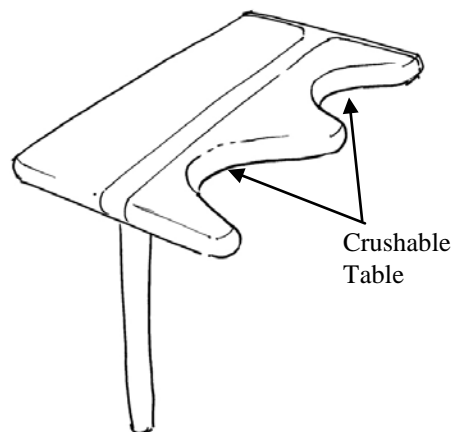


Figure 8. A Schematic of the Crushable Table Concept Selected for Development

4.3.1 Materials Selection

One of the challenges for this concept was to find a table core material that would absorb the required amount of energy and meet vertical and lateral operational load requirements but still crush at a lower level force so that the occupant injury levels would be acceptable. Another challenge was to find a tabletop material that met the flammability and loading requirements, performed as intended for a table, and yet deformed while the table crushed without adversely increasing the crush force on the occupant.

Certain requirements limited the peak force allowed to crush the table and the distance the table could crush. Figure 9 shows the desired ideal force/crush curve used to guide the design of the table for a single seated position (also shown previously in Figure 2). Note that the force increases significantly after 7 in of crush occurs as the honeycomb bottoms out. Details on the development of this curve are described in Section 5 Component Testing. Attaching the table to the rail car wall without using an aisle support was also desirable.

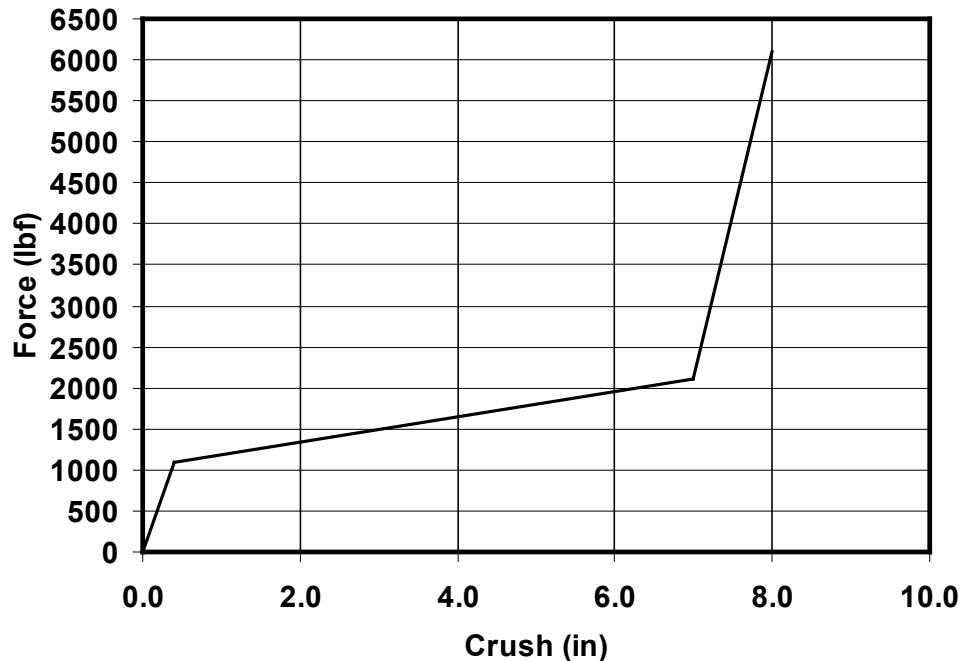


Figure 9. The Ideal Force/Crush Curve Used to Select the Material and Design the Table

4.3.1.1 Energy-Absorbing Material

Several component crush analyses were conducted to determine the range of material properties the crushable material needed to exhibit to function as a table as well as an energy absorber. The initial search was for materials in the 25–100 pounds per square inch (psi) (0.17–0.69 megapascals (MPa)) compression strength range. Several materials were identified in the search, and these were down-selected on the basis of availability, cost, fabrication issues, and ability to meet the requirements. One of the important requirements for material selection was flammability. Numerous energy-absorbing materials were eliminated on the basis of their inability to meet the flammability requirements.

Because of budget and schedule limitations, the selected material had to not only meet the load requirements, but also be readily available. Aluminum honeycomb has shown to be an excellent energy-absorbing material and was used successfully in both the pushback coupler and roof energy absorbers in the CEM coach and cab car crush zones [6]. A feature of aluminum honeycomb that lends itself to energy absorbing applications is its ability to crush at a relatively constant force and attain a high efficiency of crush (60–70 percent). Figure 10 shows a typical force/crush curve for aluminum honeycomb. Such behavior maximizes the amount of energy that can be absorbed for a given crush distance.

Aluminum honeycomb is known to have a much higher crush strength in its “T” (thickness) direction, as shown in Figure 11, than in the two lateral directions—the “L” (longitudinal or “ribbon”) and “W” (width or transverse) directions. A review of the crush strengths of available aluminum honeycomb materials did not identify any that had a sufficiently low-level crush strength in its T direction to satisfy the requirements.

Another issue related to the orientation of the honeycomb is how the vertical load requirements for the table are met. On the basis of the need to provide strength and stiffness to resist vertical loads, the team decided to investigate crushing the material along its weaker L direction, with the stronger T direction oriented vertically. The vertical orientation of the much stronger T direction provided much more bending resistance to the honeycomb than it would have had if oriented differently. This bending resistance was viewed as critical to providing the required vertical strength.

With this configuration in mind, two different aluminum honeycomb materials were procured and tested to determine the strength and force/crush properties of the aluminum honeycomb in its lateral directions (see Section 5). The results of the tests indicated that such an orientation would allow for both crush and operational load requirements to be met.

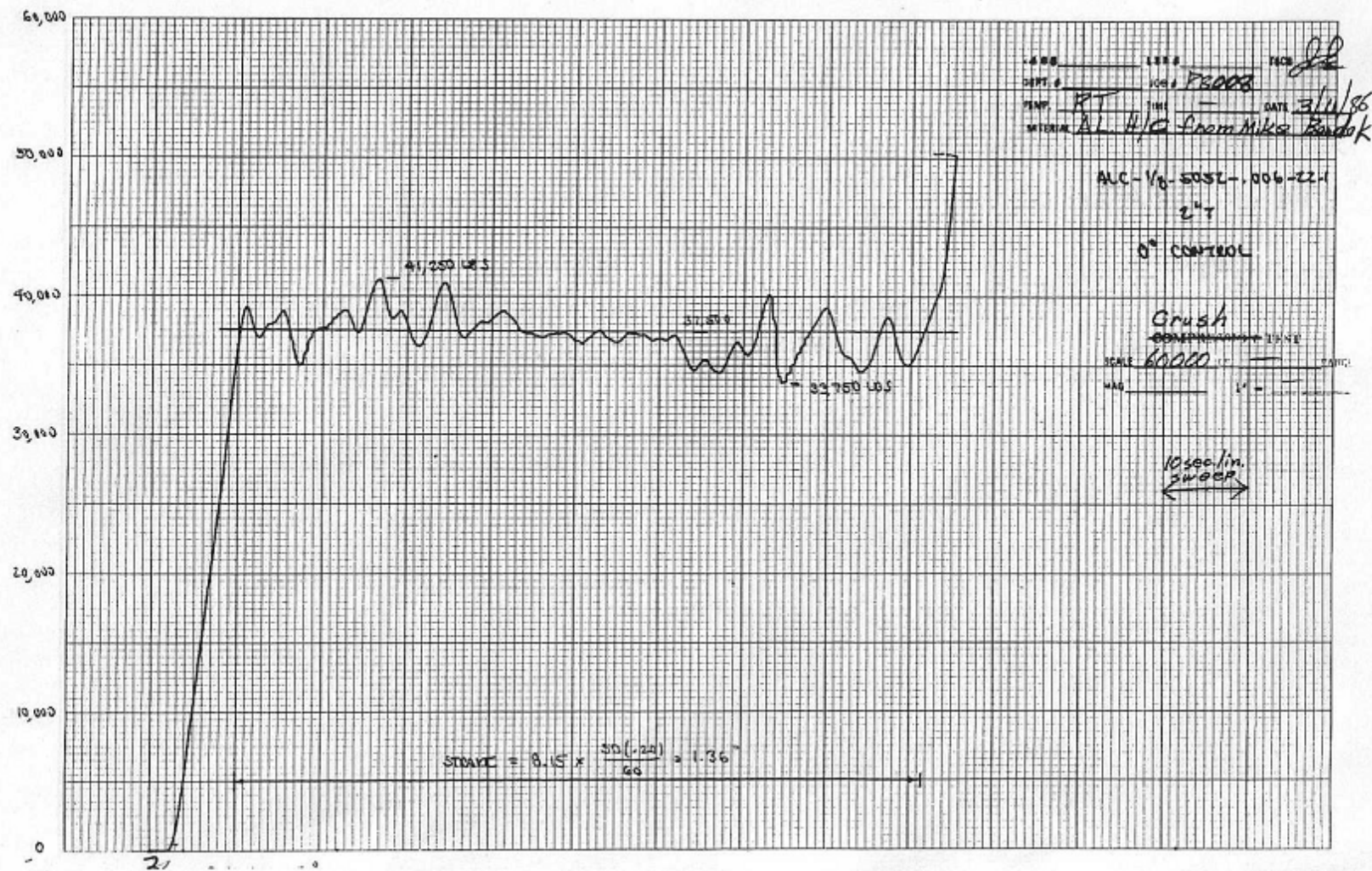


Figure 10. A Typical Force/Crush Curve for Aluminum Honeycomb

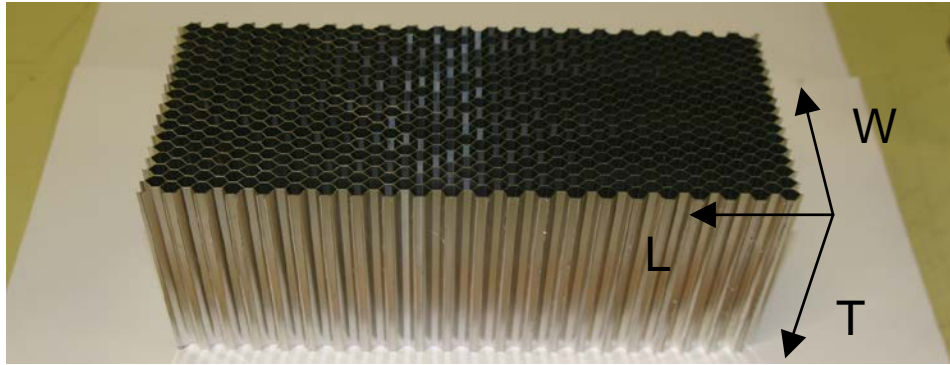


Figure 11. A Photograph of an Aluminum Honeycomb Element of the Type Used in the Table Design (the directions T, L, and W are indicated)

4.3.1.2 Tabletop Material

A literature review was performed to find a suitable tabletop material. Some of the performance requirements for the tabletop are provided below. The tabletop must:

- Provide a flat, durable surface
- Meet flammability and vandalism requirements
- Be capable of folding or moving out of the way while the table crushes
- Provide no additional harm to the occupant (i.e., cutting, etc.)
- Minimize any increase in the force/crush response of the table

Few materials were found that could provide all of the performance requirements directly. One material that meets the operational and hazard requirements and is currently used on rail car tables is melamine. Melamine is a stiff and brittle material that can be bonded to other materials. By selectively weakening the melamine by cutting shallow grooves into its underside, the melamine was shown through testing that it would fold at the grooves and break out of the way with a minimal increase in the crush force of the table. Melamine was selected as the tabletop material on the basis of these results. Figure 12 shows a grooved melamine that was bonded to the aluminum honeycomb and has deformed as intended during a test crush of a honeycomb element.



Figure 12. A Quasi-Static Crush Test Showing the Melamine Top Folding at the Grooved Location and Pulling Away from the Honeycomb as It Is Crushed

5. Component Testing

This section describes the tests that were performed to support the development of the workstation table design. Most of the tests were conducted at TIAX's facilities. Because of limitations in the load capacity of the Instron test equipment at TIAX, one set of tests was performed at Massachusetts Materials Research, Inc. (MMR), in West Boylston, MA. The tests that most influenced the development of the design included the following:

- Preliminary crush tests of aluminum honeycomb material samples to help select the specific honeycomb product to determine the orientation of the honeycomb in the table and to establish its force/crush characteristics
- Crush tests of 4-inch-square by 10-inch-high blocks of honeycomb with melamine sheets bonded to them
- Strength tests on bonded honeycomb/melamine panels that mimicked the vertical service load requirement
- Crush tests of 4-inch-wide honeycomb/melamine composite panels (MMR tests)
- Crush tests of 2-inch-wide honeycomb/melamine composite panels

All of these tests were quasi-static, and a description of each is presented in the sections that follow.

5.1 Preliminary Crush Tests

5.1.1 Preliminary Honeycomb Crush Tests

The initial series of tests focused on evaluating the crush performance of two aluminum honeycomb samples that had been identified and obtained by TIAX. These Hexcel materials were HexWeb CRIII 1/4-5052-.004 and HexWeb CRIII 3/8-5052-.005. HexWeb CRIII is an aluminum honeycomb coated with a polymer for corrosion resistance. Each of these honeycombs is made from aluminum foil sheets that are bonded together and then expanded to form a cellular honeycomb configuration. CRIII 1/4-5052-.004 is made from 5052 series aluminum foil of thickness 0.004 in that is formed into 0.25-inch cells. CRIII 3/8-5052-.005 consists of 0.005-inch-thick foil formed into 0.375-inch cells. These specific products were chosen because their reported crush strengths (725 and 505 psi, respectively) were in a range that, given expectations of lateral crush strength of approximately 3–5 percent of axial crush strength, would provide the appropriate crush strength for the table. (These expectations are based on experience with this type of material in previous projects.)

The samples were crushed in four different directions: (1) the T direction (axial); (2) the L direction (longitudinal or ribbon—the orientation of the foil sheets before expansion into cells); (3) the W direction; and (4) at a 45-degree angle with respect to the L and W directions. Table 4 summarizes the results of these tests in the estimated average crush strength. As is evident from these results, the CRIII 1/4-5052-.004 is stronger than the CRIII 3/8-5052-.005 material, and the strength in the L direction is greater than that in the W direction or the 45-degree direction.

Given the expectations for the contact area of the colliding ATD, peak force levels, and energy absorption requirements for the workstation table, CRIII 1/4-5052-.004 was selected as the honeycomb, and the L direction was selected as the direction of crush.

Table 4. Average Crush Strength for Aluminum Honeycomb Samples

Sample	Estimated Average Crush Strength (psi)			
	T direction	L direction	W direction	45-degree
CRIII 1/4-5052-.004	1,000*	26	16	21
CRIII 3/8-5052-.005	500*	11	7	Not tested

* A very rough estimate due to small sample size (only a few cells).

Figure 13 shows the plotted results of crush strength versus crush percentage from the crush test of CRIII 1/4-5052-.004. Crush percentage, or crush displacement efficiency, is determined by taking the ratio of crush displacement to initial sample thickness. As the figure illustrates, the load increases and plateaus after crushing approximately 5–7 percent of the initial thickness of the sample. The load remains steady until the crush reaches approximately 60 percent, at which point the load starts to rise as the honeycomb consolidates. The average crush strength over the interval from 5 to 60 percent was calculated to be 26.3 psi. The sample that was crushed was 0.625 in thick (T direction) by 6 in wide (W direction) by 1.5 in deep (L direction). Figure 14 shows a sample of honeycomb before the test (top photograph) and during the test (bottom photograph). Note the high crush efficiency that appears to be attainable with this material.

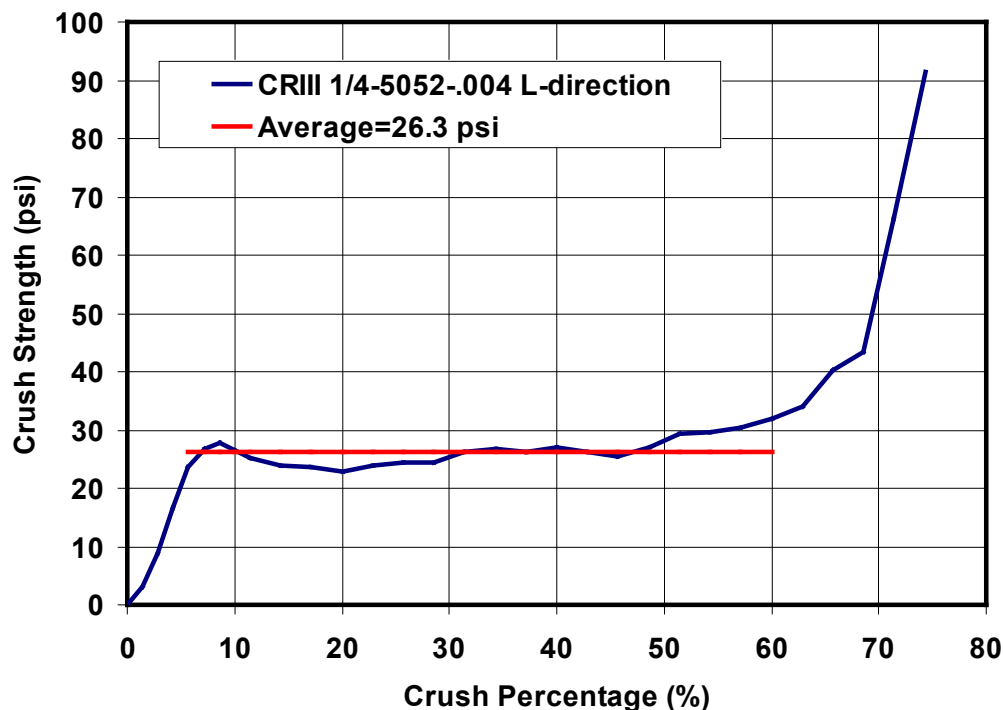


Figure 13. The Load-Crush Curve for Hexcel HexWeb CRIII 1/4-5052-.004 when Crushed in the L Direction

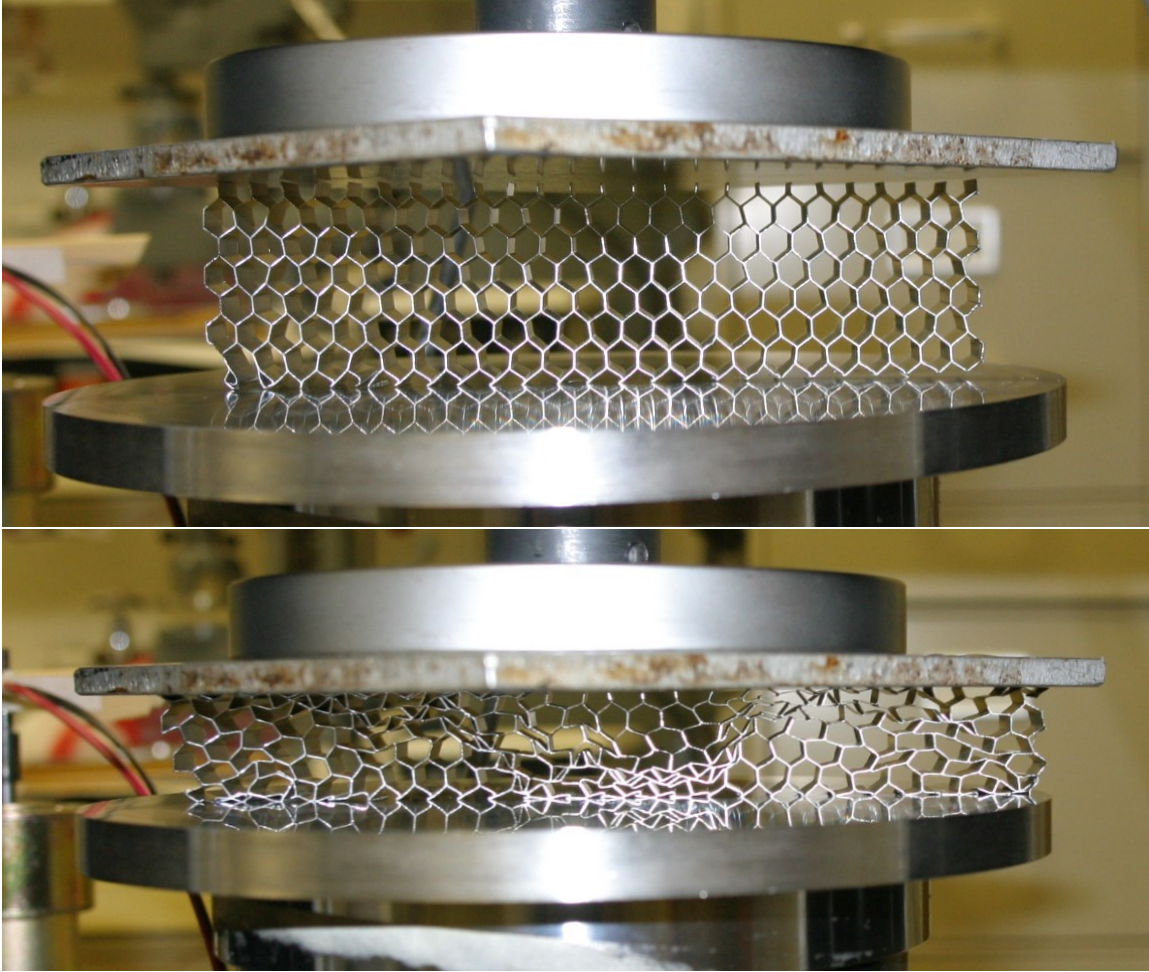


Figure 14. A Hexcel HexWeb CRIII 1/4-5052-.004 Aluminum Honeycomb Specimen before Crush (above) and during Crush (below)

5.1.2 Preliminary Composite Panel Crush Tests

Melamine was selected as the material for the tabletop based partly on its known usage in existing rail workstation tables. The table design called for the melamine sheet to be bonded to the honeycomb. Another set of crush tests was performed to investigate the extent to which the melamine affects the crush performance of the honeycomb.

In this set of experiments, a composite that was formed by bonding two melamine sheets to either side of a 4- by 4-inches-square by 10-inch-tall block of honeycomb was tested in compression. The honeycomb by itself was also tested. Figure 15 shows one of the composite specimens before a compression test. The first test was conducted on a specimen in which the melamine was bonded to the aluminum using epoxy. When tested, this specimen did not crush at all before the load reached the maximum capacity of the load cell (1,000 lbf). Clearly, the epoxy-bonded melamine sheet carries a great deal of load—too much for use in the workstation table—as the honeycomb should crush at approximately 420 lbf (4 in by 4 in \times 26.3 psi).



Figure 15. A 4- by 4- by 10-Inch-Tall Honeycomb/Melamine Sandwich Panel before Crush Testing

The next two tests were performed on panels in which the melamine had been bonded to the honeycomb with contact cement. (Because the melamine appeared to have some surface texture, two separate specimens were constructed with the melamine bonded in two different orientations; however, no texture effects appeared.) As Figure 16 shows, the melamine began to separate from the honeycomb quickly for both specimens and was fully separated after just a few tenths of an inch of crush. The crush strength (i.e., the crush load normalized by the honeycomb cross-sectional area) for this case is compared with that of the honeycomb-only sample in Figure 17. The sharp drop in strength at the beginning of the curve is associated with the buckling of the melamine sheets. Thereafter, the strength is essentially that of the crushing honeycomb. The small difference between the two crush strength curves, and in particular the difference in crush efficiency, is likely the result of the very different shapes of the two specimens.

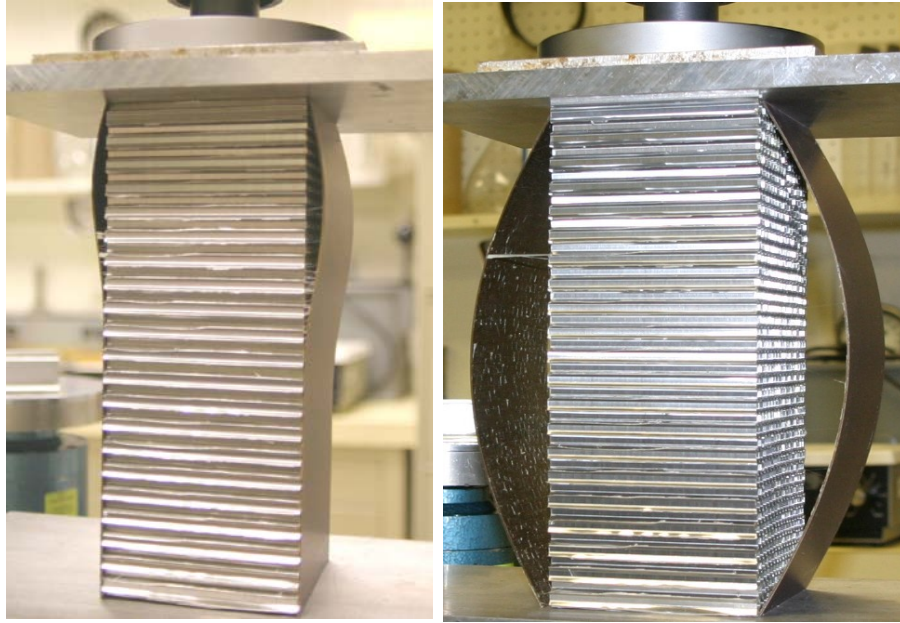


Figure 16. A 4- by 4-Inch by 10-Inch-Tall Composite Panel with the Melamine Bonded to the Honeycomb with Contact Cement (left: just after the melamine has begun to separate from the honeycomb; right: the melamine has separated fully from the honeycomb)

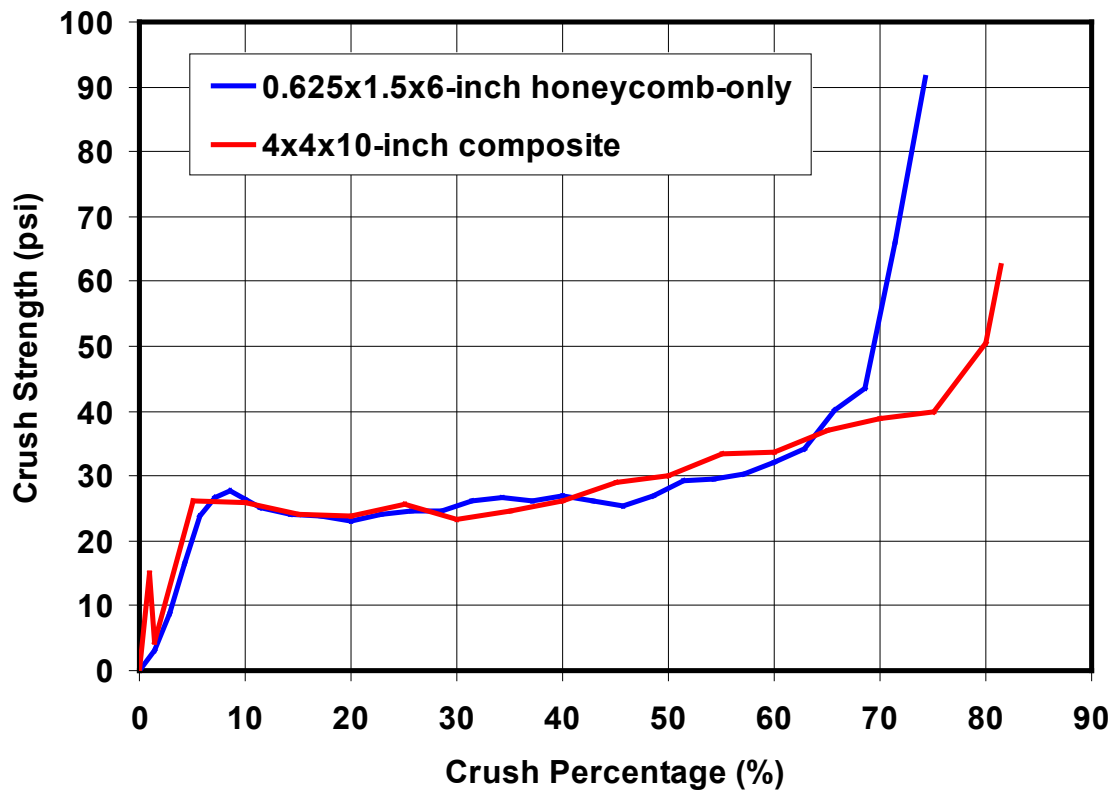


Figure 17. A Comparison of the Crush Strengths of the 0.625- by 1.5- by 6-Inch Honeycomb-Only Specimen and the 4- by 4- by 10-Inch Composite Specimen

5.2 Vertical Strength Tests

Three tests were performed in TIAX laboratories to assess the performance of the aluminum honeycomb/melamine composite table construction with respect to the vertical service load requirement.

5.2.1 *Single Panel Attached with Screws to C-Channel*

The performance of a panel formed from a single 20-inch-wide by 10-inch-deep by 4-inch-thick block of honeycomb bonded with contact cement between two 0.050-inch-thick melamine sheets was examined in the first test. With eight 6-32 flathead screws, this panel was mounted to a C-channel that represented half of the I-beam that serves as the backbone of the table frame. The eight screws were inserted into 1-inch-long, 0.25-inch-diameter standoffs, four along the top and four along the bottom of the C-channel. The standoffs were inserted into individual honeycomb cells and were spaced approximately 6 in apart along the axis of the C-channel. To provide support for the table in a manner that allowed the table to bend downward under the action of a vertical load, the C-channel was welded to two 2- by 2-inch tubes, spaced approximately 23 in apart, so that the panel was cantilevered off of the C-channel and free to move between the support tubes. Figure 18 shows the panel specimen mounted in the Instron machine before the test. The load was applied in compression. A 4-inch-diameter plate was used to distribute the load over the surface of the melamine. The plate was centered over the edge of the specimen, near the center of the 20-inch-wide panel; however, because of the size of the specimen and limitations on placement of the load by the Instron equipment, the load could not be applied at the very edge of the panel. Instead, the load was applied approximately 2 in away from the edge as evident in Figure 18. (Relative to the impact edge of the table, the location of the applied load was similar to that in the quasi-static vertical test.) The load was ramped slowly to a maximum of 400 lbf.

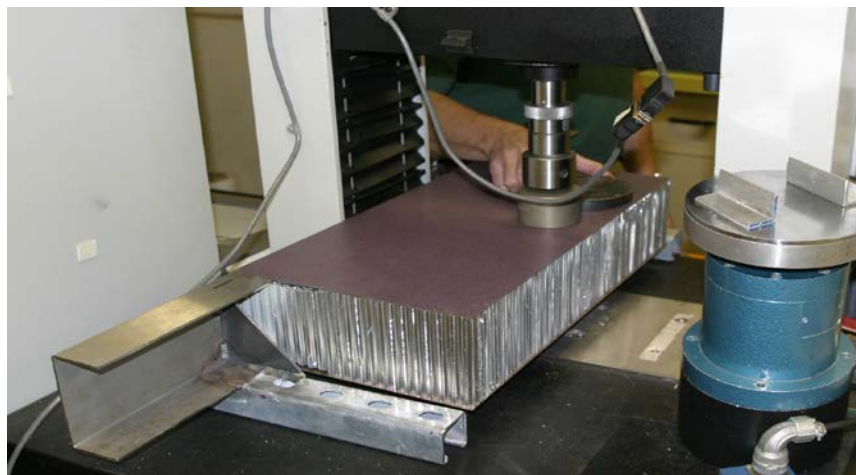


Figure 18. The Table Specimen Mounted in the Instron before the First Vertical Load Test

Table 5 summarizes the results of the test and indicates that the table moves downward significantly because of the applied vertical load. Some of this displacement, however, appears to be the result of rotation of the C-channel about the support tubes. The lateral displacement, as shown in Table 5, reaches as much as 0.054 in for the 400-pound-force load. Given the

geometry of the panel, this corresponds to approximately 0.13 in of vertical displacement. Table 5 lists the vertical deformation of the tabletop panel corrected for the C-channel deformation.

Table 5. Results of the First Vertical Load Test

Load (lbf)	Measured Tabletop Vertical Displacement (in)	Measured C-channel Lateral Displacement (in)	Corrected Vertical Deformation of the Panel (in)
200	0.35	0.022	0.30
300	0.57	0.043	0.46
400	0.85	0.054	0.72

Even after it has been corrected to remove test fixture displacement, the magnitude of vertical deformation is much more than desired. Posttest inspection of the table specimen indicated that the screws connecting the honeycomb to the C-channel had pulled out. For this reason, a new attachment method was devised.

5.2.2 Single Panel Bonded to C-Channel

For the second test, the 20-inch-wide by 10-inch-deep by 4-inch-thick block of honeycomb was bonded with epoxy to the web of the C-channel. Two sheets of melamine were again attached to the honeycomb/C-channel assembly. For this test, the honeycomb block was machined per the design drawings to allow it to fit inside the C-channel and to create space to place the plastic spacers between the honeycomb and the melamine. The honeycomb was bonded to the melamine with contact cement. The plastic spacer and the C-channel were bonded to the melamine with epoxy. No screws were used in the construction of this table. To reduce twisting, two gussets were welded to the C-channel just outside of the support tubes.

The applied load for this test was ramped slowly to 350 lbf (the vertical service load specified in the requirements document). Figure 19 shows a photograph from the test with the 350-pound-force load applied to the table. Table 6 summarizes the results of the test. The displacements under load are much smaller for this test than they were in the first test; the posttest deformation is also very small. Clearly, the bonding of the honeycomb to the web of the C-channel significantly improved the performance of the table with respect to this test. The lateral displacement of the C-channel is much smaller than it was in the first test. This is directly attributable to the stiffening gussets that were added to the C-channels.

Table 6. Results of the Second Vertical Load Test

Load (lbf)	Measured Tabletop Vertical Displacement (in)	Measured C-Channel Lateral Displacement (in)	Corrected Vertical Deformation of the Panel (in)
175	0.10	0.01	0.08
350	0.22	0.02	0.17
0 (posttest)	0.01	0.00	0.01

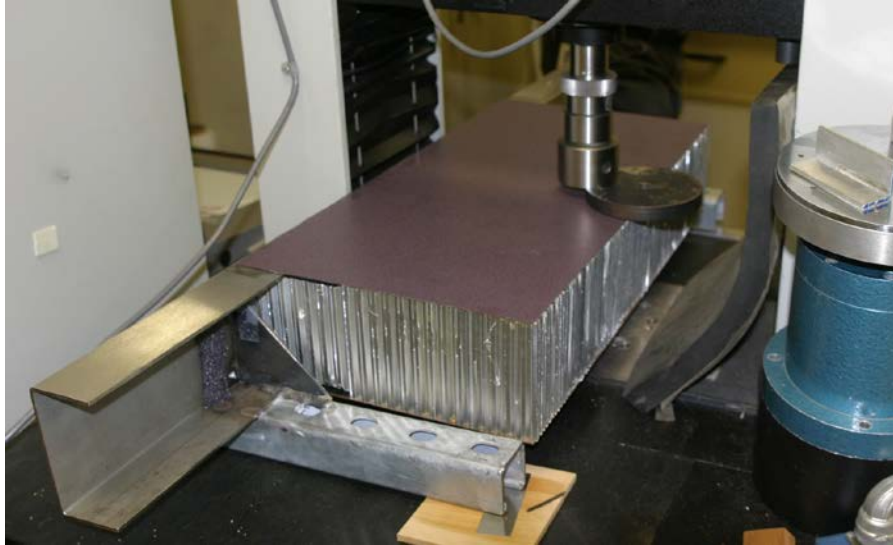


Figure 19. A 350-Pound-Force (1.56 kN) Load Is Applied to a Single-Block Panel that Has Been Bonded to the C-Channel

5.2.3 Five-Block Panel

The third and final vertical load test investigated the performance of a panel consisting of five blocks of honeycomb instead of one. Each block was 4 in wide by 10 in deep by 4 in thick. The blocks are bonded to the C-channel and to the melamine but not to each other. This configuration was examined because of the likelihood that it would improve the crush performance of the table in the longitudinal direction.

The results of this test, however, suggest that such a configuration cannot withstand the 350-pound-force vertical service load. Figure 20 shows the five-block table specimen loaded to 350 lbf. The blocks appear to undergo significant shearing with respect to one another. For this reason, the deformation of the block under the load is considerable. The results of the test indicate that the table specimen is only able to withstand a load of 165 lbf (displacing downward by 0.25 in) before failing. These results suggest that the multiblock approach would not work for the workstation table without considerable engineering to address its deficiencies.

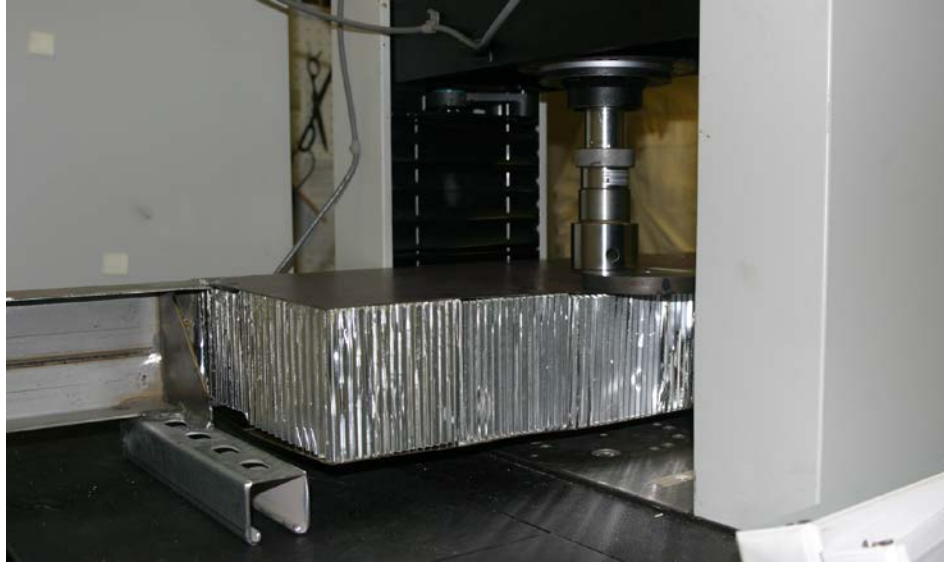


Figure 20. The Five-Block Panel under a Load of 350 lbf (note: the shearing of the blocks with respect to one another)

5.3 Composite Panel Crush Tests

5.3.1 Four-Inch Honeycomb/Melamine Panels

Crush testing of the honeycomb/melamine table panels was conducted at MMR on October 28, 2005. The use of an outside testing laboratory was mandated because the expected loads exceeded the 1000-pound-force load capacity of the Instron at TIAX. Two panels were tested: one 20-inch-wide by 10-inch-deep by 4-inch-thick block panel and one five-block panel where each block measured 4 in wide by 10 in deep by 4 in thick. The panels were crushed using a steel indenter sized to represent the abdomen of an ATD. The 12-inch-wide by 10-inch-deep steel plate has 2-inch-diameter pipes welded to either end to give it rounded edges. The tests were performed at a displacement rate of approximately 1 in/minute (min) to a displacement of about 7 in.

The results of the test indicated that:

- Measured loads were approximately 500 lbf higher than expected,
- The melamine panels did not buckle out of the way completely but instead adhered to the honeycomb to some extent and exhibited much cracking,
- The melamine appeared to be carrying a significant amount of load. At one point during the single-block test, a loud pop was followed by significant drop in load,
- The plastic spacers, used to maintain a relatively smooth and stiff surface for the tabletop in the region where the honeycomb was recessed, appeared to behave as intended,
- The 2-inch region in which the honeycomb material was recessed in front of an I-beam flange appeared to behave as intended, and

- The load response stiffened sharply at a displacement of approximately 6.5 in, as expected.

Figure 21 shows a sequence of images from the five-panel crush test. As the figure shows, the melamine sheet on the visible side of the honeycomb bent out of the way as was intended. The panel on the other side did not behave in a controlled fashion as intended and exhibited significant cracking. The 12-inch-wide indenter crushed the three central panels (also 12 in wide) with little deformation of the two outer panels.

Figure 22 shows a similar sequence for the single-block test panel. For this case, the failure of the melamine was much less elegant—cracking instead of buckling out of the way. A comparison of the load-crush curve in Figure 23 indicates that the effect of both the cracking and the number of honeycomb blocks was significant. For the single-block panel, the point at which the loud “pop” was heard during this test is indicated. Because this sound was associated with the fracture of a piece of melamine, the nearly 1,500-pound-force drop in load indicated that the melamine was carrying much more load than intended. This issue led to some design changes for the melamine surfaces.

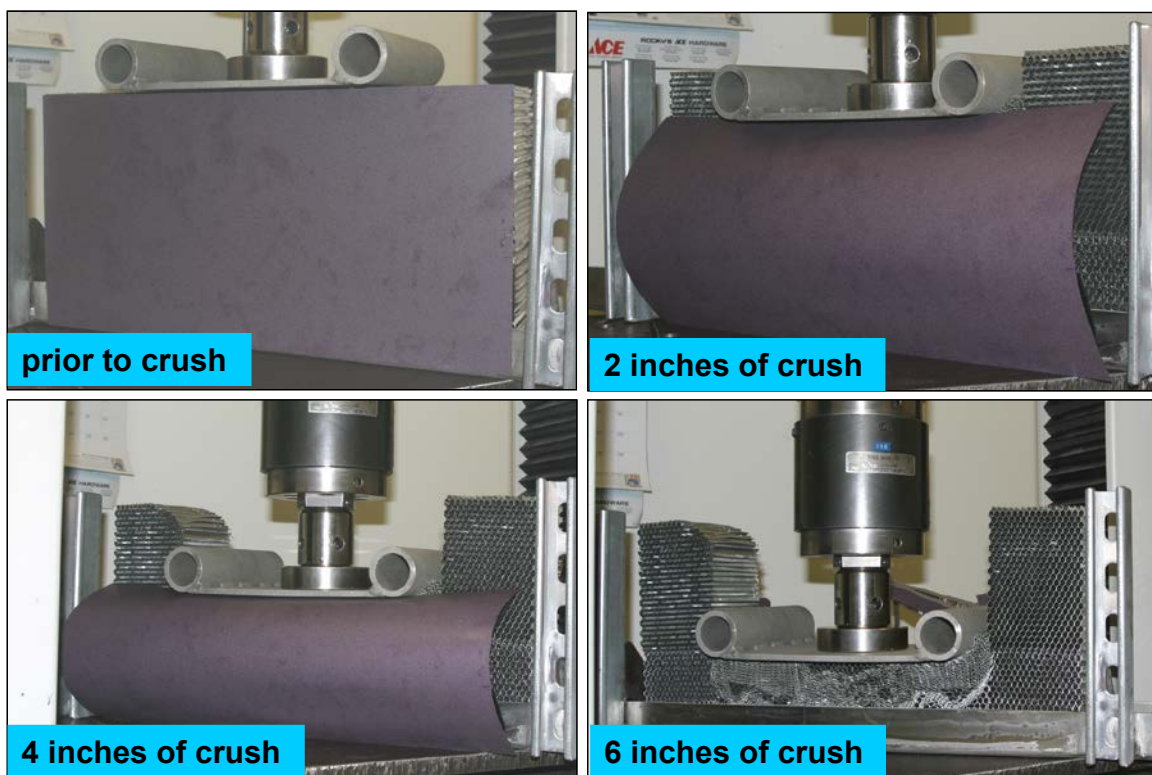


Figure 21. A Series of Images from the Five-Panel Crush Test

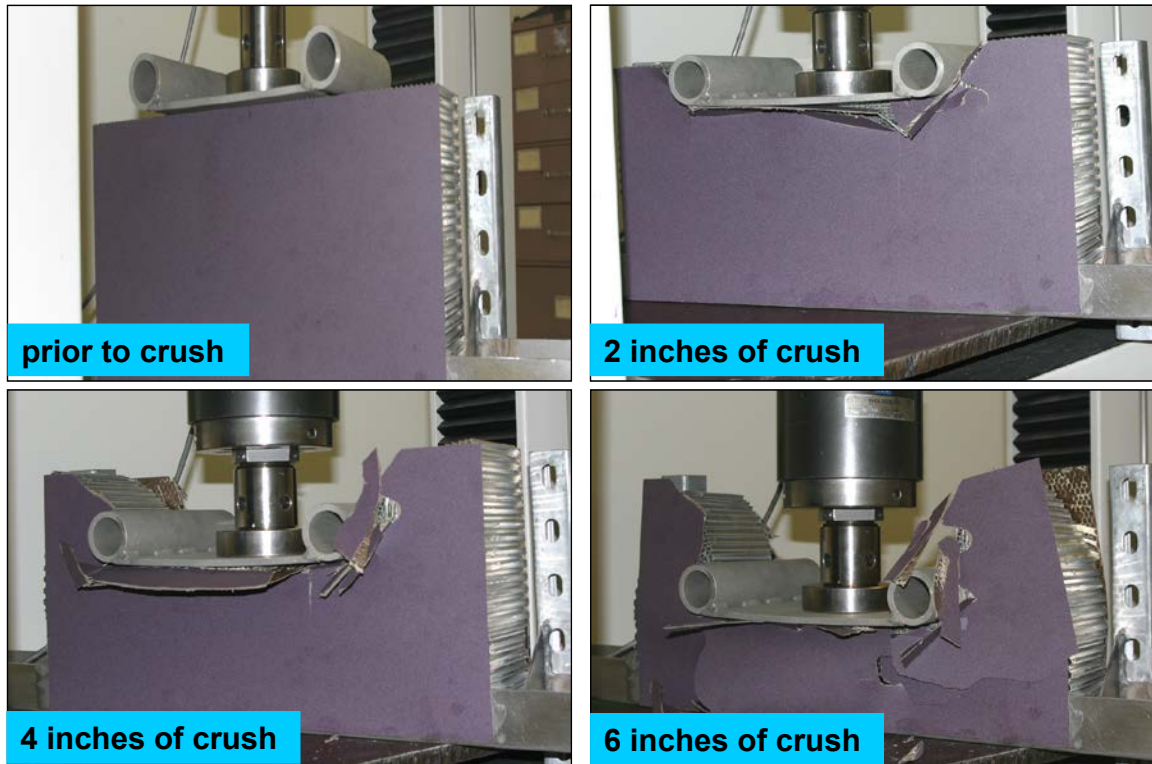


Figure 22. A Sequence of Images Showing Crush of Single-Block Panel

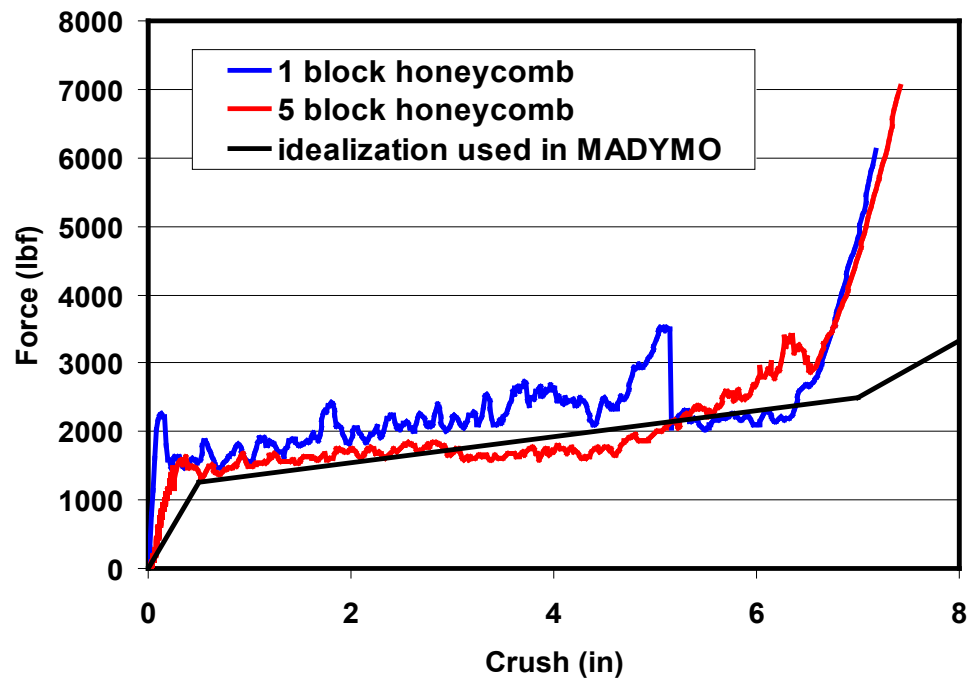


Figure 23. A Comparison of the Measured Load-Crush Curves for the Two Honeycomb Panels

5.3.2 Two-Inch Honeycomb/Melamine Panels

To address the issues related to the manner in which the melamine fails during crush and the associated additional load that the melamine carries, a second set of panel crush experiments were performed. These tests were performed in TIAX laboratories to save time. Because of the noted limitation of the Instron testing machine, the 4-inch-thick honeycomb blocks were cut in half to limit the load. As Figure 24 shows, melamine sheets were bonded with contact cement to either side of the 2-inch-thick honeycomb blocks to form composite panels that were held in place with angle irons and clamps during the test. The angle irons were approximately 2 in high and so were representative of the flange of the I-beam.



Figure 24. A 2-Inch-Wide Honeycomb/Melamine Composite Test Panel Clamped to Supporting Angle Irons, Shown in the Instron before Testing

To eliminate the contribution of the melamine to the crush resistance of the panels, the melamine sheets were scored at two locations: (1) four in from the forward edge of the panels; and (2) eight in from the forward edge of the panels, just in front of the clamped angle irons representing the I-beam. These scores were made with the expectation that the melamine panels would fracture across the thin ligament formed by the scoring and fold away with little or no contribution to the load.

Two composite panels were crushed with the 12-inch-wide indenter. For comparison, two blocks of honeycomb without any melamine were crushed as well. Note that the second honeycomb block was cut to a width of 1.5 in so that it could experience additional crush before reaching the 1,000–pound-force load limit of the Instron.

Figure 25 shows one of the test panels being crushed. As shown in the figure, the scored melamine appears to fold away as intended. Figure 26 compares the measured load-crush curves for the four tests. Note that these curves have been normalized so that they are representative of a 3.5-inch-thick panel. As can be seen in the figure, very little difference exists between the three curves. The crush begins at a load of approximately 1,100 lbf and increases to approximately 1,700–1,800 lbf at a crush of approximately 4–5 in. This is the point at which the load reached the limit of the Instron for the three 2.0-inch-wide panels. The 1.5-inch-side honeycomb-only sample was crushed a distance of 7.0 in.

On the basis of the results of this test, the tabletop design was modified to include machined grooves on the backside of the melamine surfaces. An idealized load-crush curve was identified, based on the consistency of load-crush curves and the absence of any significant difference between the honeycomb-only panels and the composite panels. This curve (refer to Figure 26) rises to 1,100 lbf at a crush of 0.4 in and then increases more gradually to a load of 2,100 lbf at a crush of 7.0 in. As the crush increases beyond 7.0 in, the load is assumed to increase dramatically, consistent with other test results (see Figure 23). The idealized curve was used to characterize the table assembly in subsequent computer modeling.

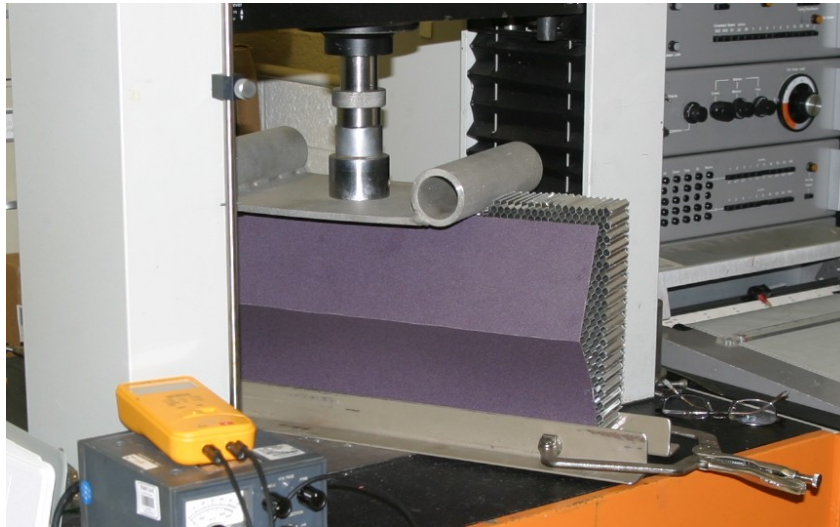


Figure 25. A 2-Inch-Wide Honeycomb/Melamine Composite Test Panel Shown during Crush

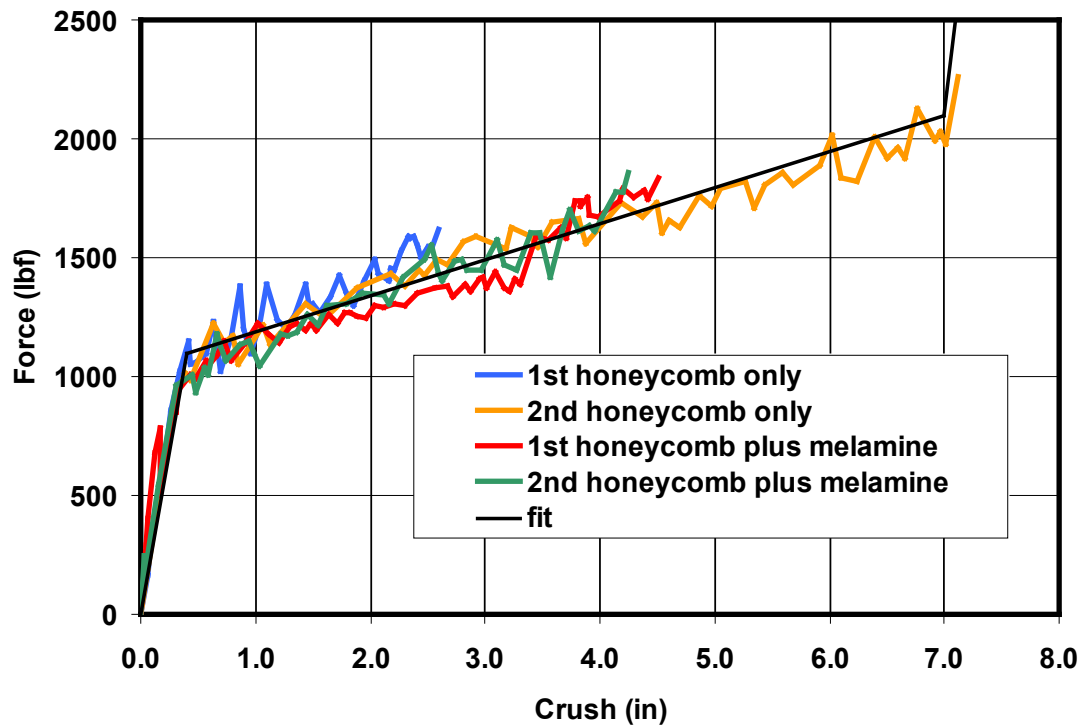


Figure 26. A Comparison of the Load-Crush Curves for Two 2-Inch-Wide Honeycomb/Melamine Panels and Two Honeycomb-Only Blocks (note: loads are scaled to represent a 3.5-inch-wide sample)

6. Table Model Development and Analyses

This section describes the models used to help guide the design of the crushable workstation table. Two types of numerical models were developed. ABAQUS finite element models were developed by TIAX and used to determine the crush response and structural integrity of the crushable table. MATHematical DYnamic MOdel (MADYMO) occupant interaction models were refined by Altair and used to determine the risk of injury to an occupant seated at the crushable table for two collision scenarios. The two collision scenarios included:

- The standard 8g, 250-millisecond triangular acceleration test pulse
- A predicted acceleration pulse derived from the CEM full-scale train-to-train test (the CEM pulse)

The finite element models used in this project were developed at both the component level and the system level. First, simplistic component models of various crushable concepts were developed to help understand which of the material concepts was viable. Next, a detailed model of the aluminum honeycomb elements was made and refined, based on the component testing of the honeycomb.

A detailed model of the table structure was developed by using Altair Hypermesh software on the basis of the Pro-Engineer computer-aided design (CAD) models generated for the table design. The refined model of the honeycomb crush elements was added to the table model, which was used to determine the expected force/crush response as well as to verify that the design could withstand the operational loads.

In parallel with the finite element modeling, Altair developed a MADYMO model to represent the crushable table by using rigid elements connected to the table structure by spring and damper elements. MADYMO includes predeveloped occupants in the form of models that represent ATDs and can predict the risk of injury (e.g., from a head or abdomen impact). For this work, the THOR ATD model was used because the physical THOR dummy was to be used in an onboard experiment involving a crushable table in the full-scale CEM train-to-train test, held in March 2006. The approach was to take the performance characteristics from the detailed design as predicted by the finite element results and implement them in the MADYMO model of the table to predict the injury risk to a 50th-percentile male occupant seated at the table. Specifically, the predicted force/crush response of the table, together with some key dimensional characteristics, was used as input to the MADYMO model.

6.1 Finite Element Models and Analyses

Three types of finite element models were constructed to support the development of the workstation table:

- Models of a block of honeycomb to characterize the crush performance of the honeycomb material,
- Models of the full table crushed by rigid impactors to determine the crush characteristics of the table and to ensure that the table structure was able to withstand the peak collision loads without excessive deformation, and

- Application of the service loads to the table to verify that it met these requirements.

The results of these models guided the development of the design and verified that the final design met its performance requirements. Some details of each of these models are described in the next subsection. Numerous modifications to these models were developed as the design evolved.

6.1.1 Honeycomb Crush

A geometrically detailed model was developed to simulate the crush of a block of honeycomb sized to be representative of the honeycomb blocks that were ultimately used in the table design. A block of aluminum honeycomb is known to exhibit a very uniform crush at a level of strength that is well documented. However, because the abdomen of the ATD is crushing only part of the honeycomb block, the force/crush characteristics of the honeycomb under such a loading are less certain. Figure 27 shows the mesh for the crush analyses. Approximately 70,000 shell elements are used to represent a block that is approximately 3.7 in deep by 8.3 in wide by 1.0 in thick. On the basis of the results of preliminary tests, the honeycomb is oriented in the workstation table so that it crushes along its longitudinal, or L direction. This is the stronger of the two lateral directions, with a crush strength that is approximately 4 percent of the crush strength in the axial (T direction).

Note that the shape of the cells matches the honeycomb material (CRIII 1/4-5052-0.004), which was procured from Hexcel. Each cell is 0.25 in wide in the weaker W direction; however, the cells do not form perfectly symmetric hexagons but instead are elongated in the L direction, as indicated. Each element that is oriented in the L direction (indicated in orange in Figure 27) has been given a double-thickness, because in each of these sections, two sheets of aluminum have been bonded together.

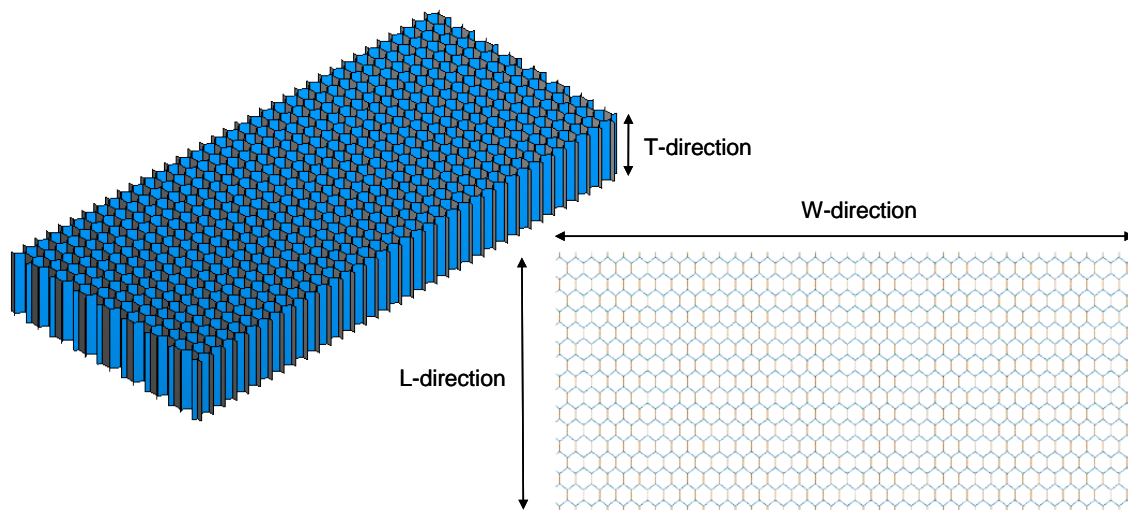


Figure 27. The Mesh Developed to Simulate Crush of a Honeycomb Block along Its L Direction

In the first analysis, the honeycomb block was crushed between two flat rigid plates. Figure 28 shows the results of the analysis, which indicates that the model predicts the crush strength of the honeycomb quite well. The efficiency of the honeycomb appears to be overpredicted by approximately 8–10 percent. This difference may be due to the difference in width between the actual block and the model block. It may also be attributable to differences in friction coefficient between the rigid plates and the block or between the cells of the block. (Note the lateral expansion of the block following crush.)

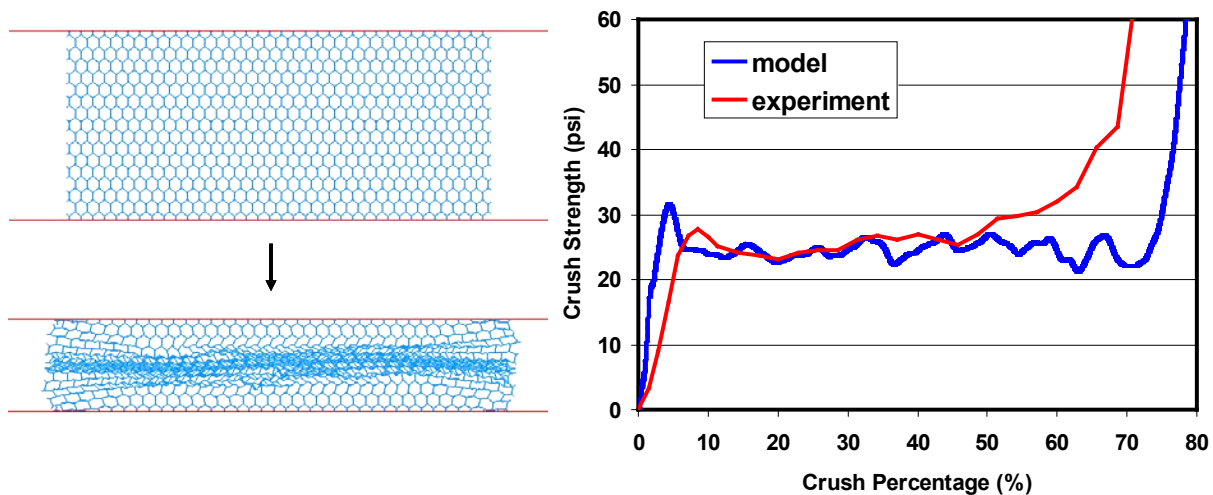


Figure 28. Uniform Crush of the Honeycomb Block between Two Flat Plates (left: the undeformed and deformed blocks are shown; right: the predicted crush strength curve is compared with the measured curve)

A second crush simulation was performed to assess the effect of crushing only a central portion of the honeycomb block. Figure 29 summarizes the results of this simulation. Note that the crush strength for this case was determined by dividing the total crush force by the area of the

indenter. The results indicate that the added resistance attributable to pull-in of the material outside of the indenter significantly increases the effective strength of the honeycomb.

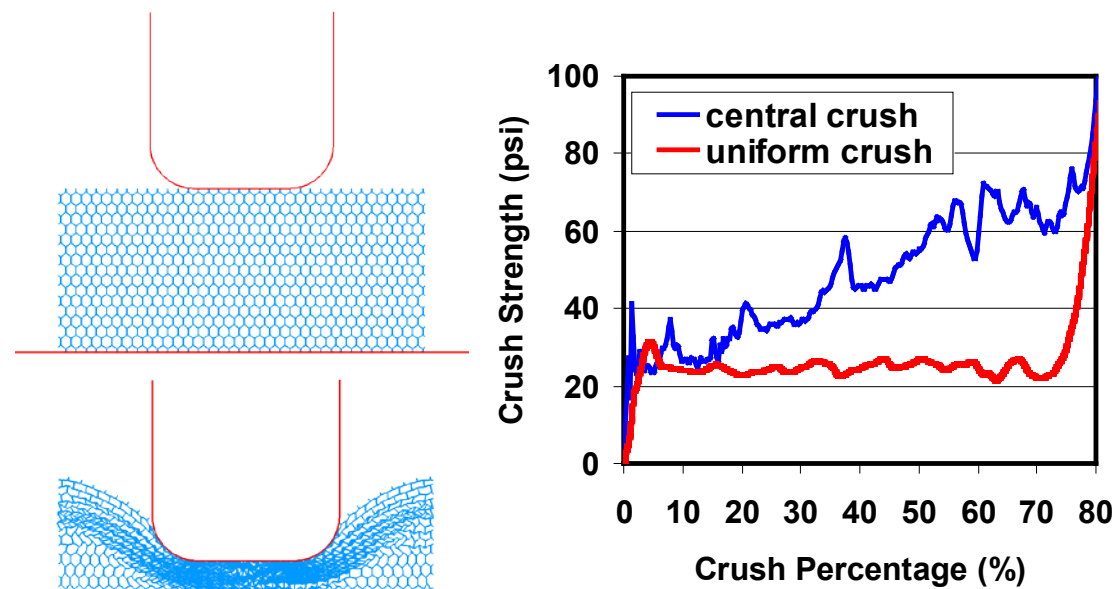


Figure 29. Crush of the Honeycomb Block with a Centrally Located, Rigid Indenter (left: the undeformed and deformed blocks are shown; right: the predicted load crush curve is compared with the prediction for crush by a rigid flat plate)

Finally, a third simulation is presented in which the honeycomb is crushed by the centrally located rigid indenter, but it has been split into three pieces so that not as much material on either side of the indenter participates in the crush. The results of this analysis are presented in Figure 30, and they indicate that the cutting of the honeycomb block serves to alleviate much of the resistance to crush provided by the material away from the indenter. The resulting crush strength curve closely follows the uniform crush curve.

The results of these studies influenced the final design of the table, which uses two honeycomb blocks per side of the table. They also helped to define additional tests that were performed to characterize the behavior of the honeycomb panels (see Section 5) and to define the characteristics of the more simplified material model for the honeycomb that was used in the finite element models for simulating the crush of the table.

The model for simulating the crush of the full workstation table (see Section 6.1.2) relies on a continuum description of the honeycomb by using ABAQUS solid elements (C3D8R) rather than a geometrically explicit description of the honeycomb. The material law for these solid elements is based on a metal foam plasticity model that is available in ABAQUS. On the basis of the results of the crush tests using the centrally located indenter, the material model was defined to include hardening with the strength of the honeycomb increasing from 26 to 46 psi at a crush level of 70 percent. Figure 31 shows a result from a simulation similar to those already described but using a simplified, continuum model for the honeycomb. The honeycomb block in this case is 19.3 in wide by 10 in deep by 3.5 in thick—about the same dimensions as the honeycomb blocks used in the table. Like the models above, it is crushed by the 12-inch-wide

indenter. The deformation pattern exhibited by this model is reasonably consistent with that shown in Figure 29. Figure 32 shows the load crush response from this model compared with the idealized curve developed for the honeycomb based upon test results.

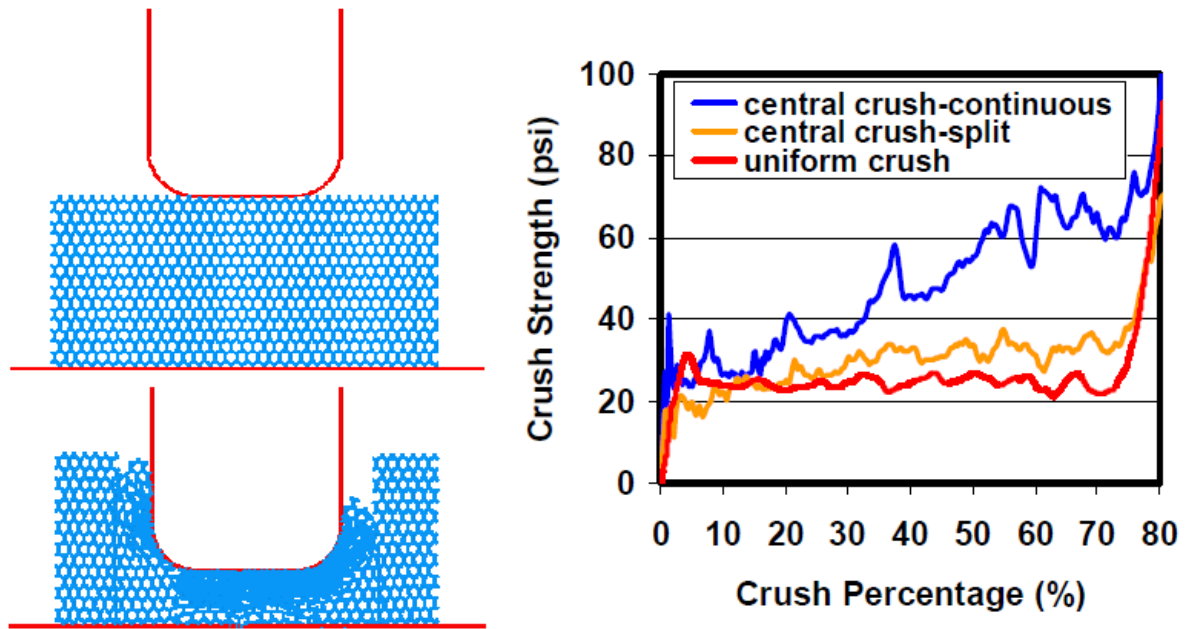


Figure 30. Crush of the Split Honeycomb Block with a Centrally Located, Rigid Indenter (left: the undeformed and deformed blocks are shown; right: the predicted load crush curve is compared with the predictions of the other models)

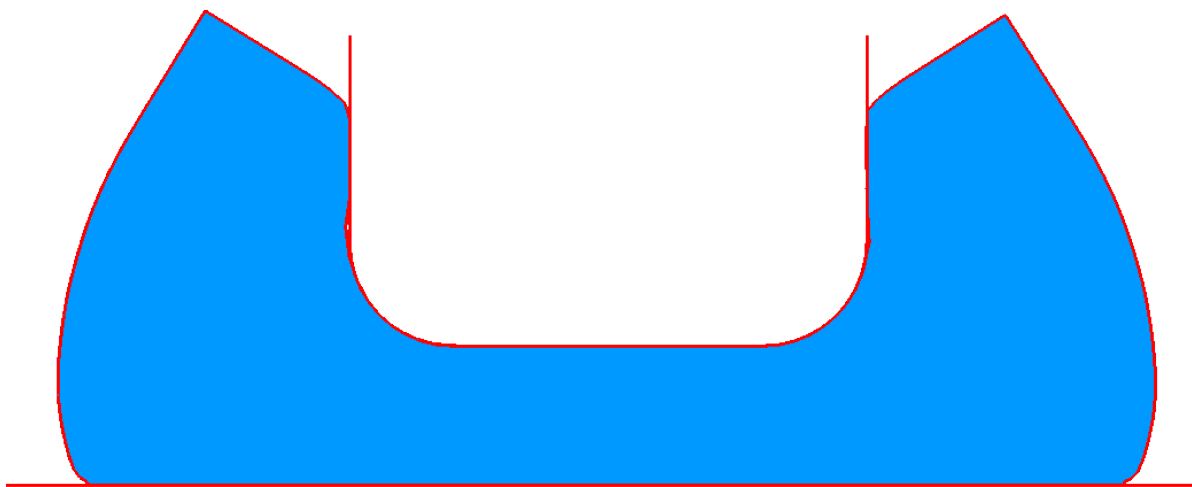


Figure 31. The Deformed Honeycomb Block for a Crush of 7 in

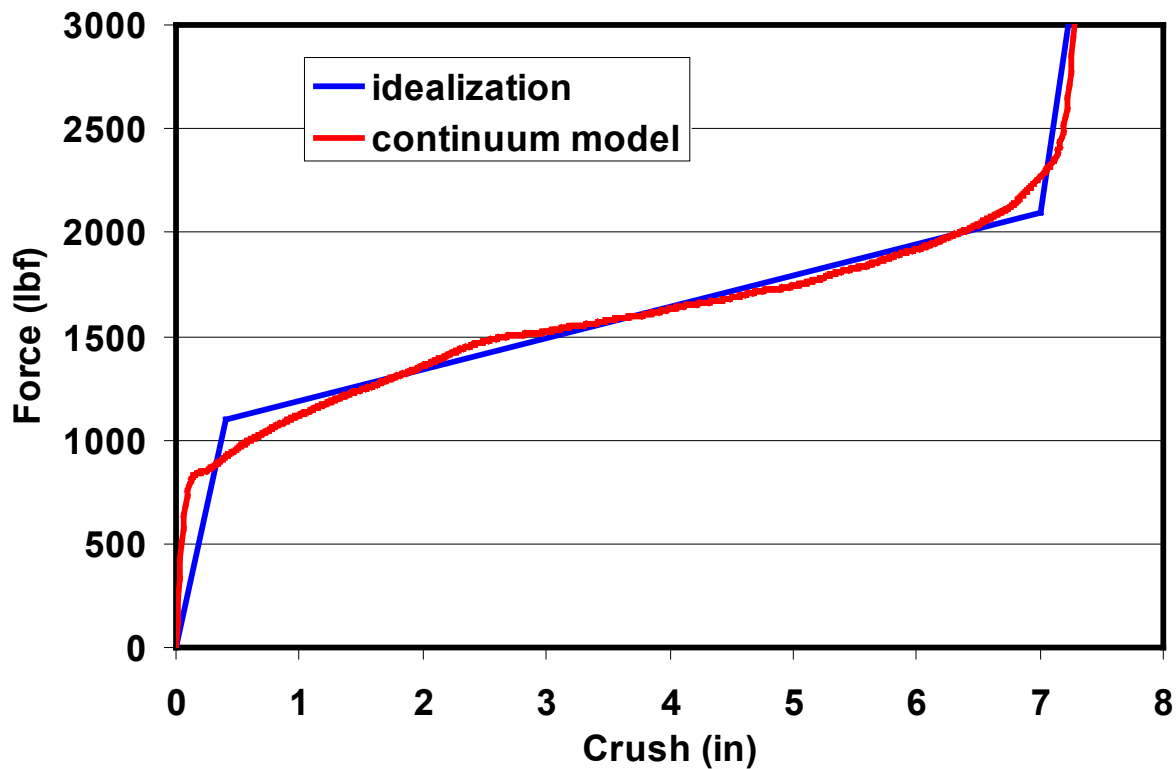


Figure 32. A Comparison of the Load-Crush Response Predicted by the Continuum Honeycomb Model with the Idealized Curve Determined from Tests

6.1.2 Table Crush Models

Finite element models were developed to simulate the crush of the table in support of the development of the table design. The modeling results indicate that the table support structure is able to withstand the collision loads and to verify that the deformation model of the table is consistent with expectations.

Figure 33 shows the finite element mesh for the workstation table. The graphic at the top of this figure shows the steel frame of the table: the I-beam assembly is shown in blue, the table and leg supports in orange, and the top and bottom wall-mounting brackets in red. In graphic (b), the four honeycomb blocks, shown in yellow, have been added as have the plastic spacers shown in dark gray. The graphic at the bottom of the figure shows the melamine tabletop and the rigid indenters representing an ATD abdomen. Although an ATD abdomen is not actually rigid, it is modeled as such for simplicity in evaluating the force-crush behavior of the table. Note that the rubber edge was not included in the model and that the melamine has not been scored.

Not shown in Figure 33 is a series of springs that connect the nodes of the honeycomb to the nodes of the melamine and the nodes of the I-beam to the nodes of the melamine. The force-deflection characteristics of these nonlinear springs were defined to represent the strength of the contact cement and the epoxy, respectively. On the basis of estimates from laboratory work, the

contact cement was defined to have a very small strength of approximately 0.8 psi; the epoxy was assumed to have a much greater strength of the 80 psi. The strength of the contact cement

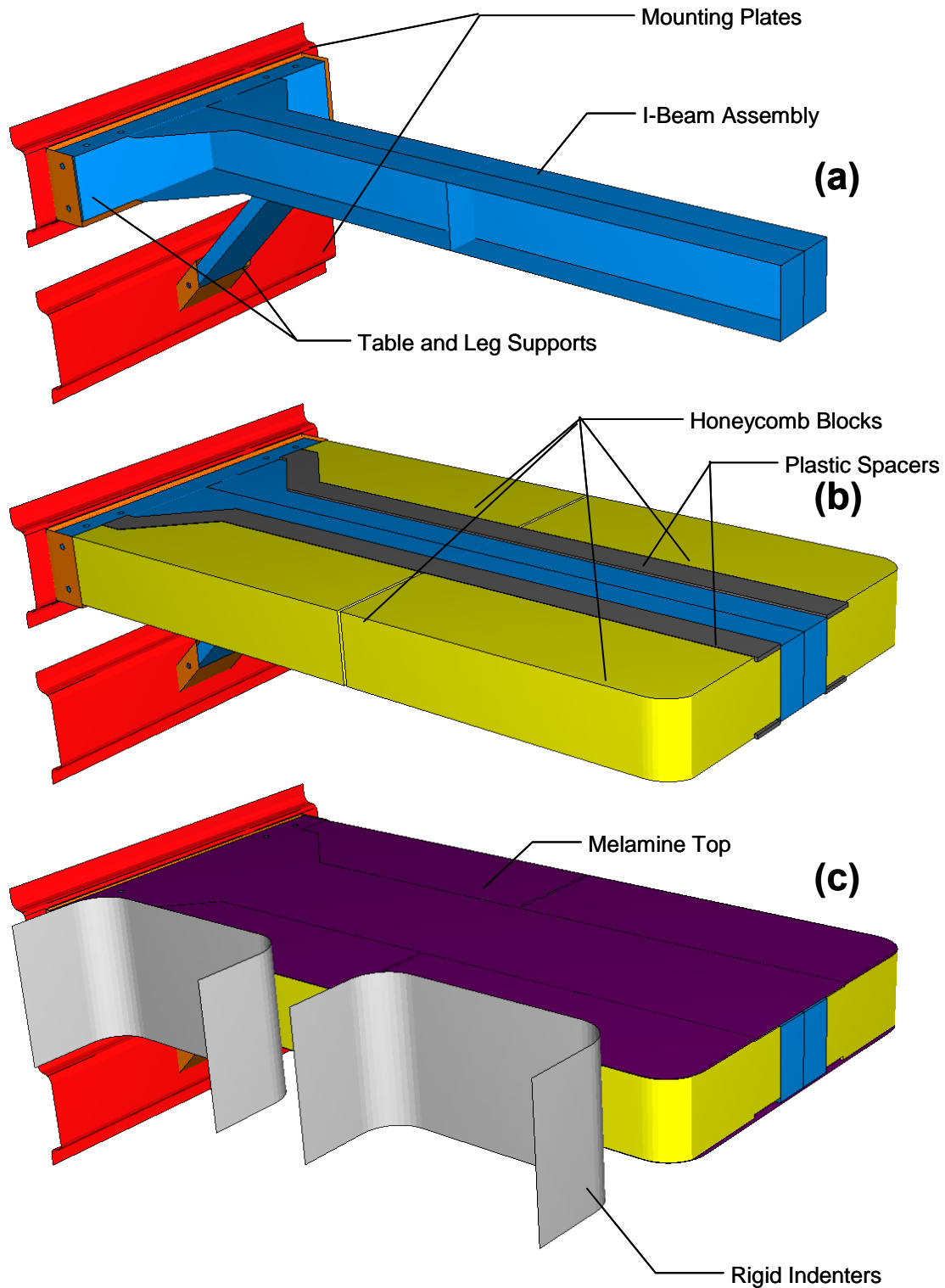


Figure 33. The Finite Element Model for the Workstation Table: (a) Table Frame Only; (b) Honeycomb Blocks and Spacers Added; (c) Melamine and Rigid Indenters Added

was assumed to peak when the separation of the honeycomb and the melamine reached 0.1 in and then decrease after the separation reached 0.2 in as shown in Figure 34. (This strength was distributed to the nonlinear springs, with 16 springs per square inch assigned a maximum strength of 0.05 lbf each.)

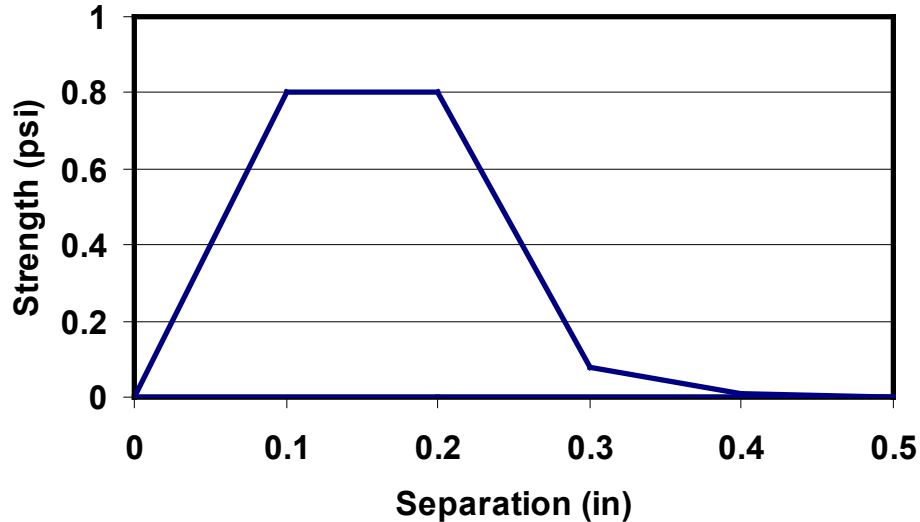


Figure 34. The Separation-Strength Curve Assumed for the Contact Cement

The collision loads were applied to the table by two rigid indenters, 12 in wide with 2-inch radii at either side. Each indenter was centered on one of the honeycomb blocks, constrained to move only in the longitudinal direction, and given an effectively uniform velocity of 50 in/s (2.8 mph or 1.3 m/s). This small velocity was selected so that the analysis was essentially quasi-static—the effect of inertia on the outcome of the analysis was minimal.

The nodes along the top and bottom rims of the mounting brackets were fixed. In addition, the groups of nodes on either side of the bolts connecting the I-beam assembly to the table and leg supports were constrained to move together using ABAQUS multiple-point constraints.

The analysis simulated 7 in of motion of the rigid indenters. The results of the analysis, described below, indicate that the frame of the table should be able to withstand the collision forces. In addition, the results of the analysis indicate that no unexpected modes of deformation should be associated with the collision.

Figure 35 shows the deformation of the table after 6 in of crush. The honeycomb in front of the indenters was crushed completely. As was seen in the honeycomb-only crush models and in the panel tests, the honeycomb on either side of the indenters was pulled in. The two honeycomb blocks separated by a few inches near the impacted side of the table. Note that because the scoring of the melamine was not modeled, the melamine did not fold, but rather bent out of the way on both the top and bottom of the table. In either case, its contribution to the resistance of the table was minimal. No substantial twisting of the frame or other modes of deformation appears that might compromise the crush performance of the table.

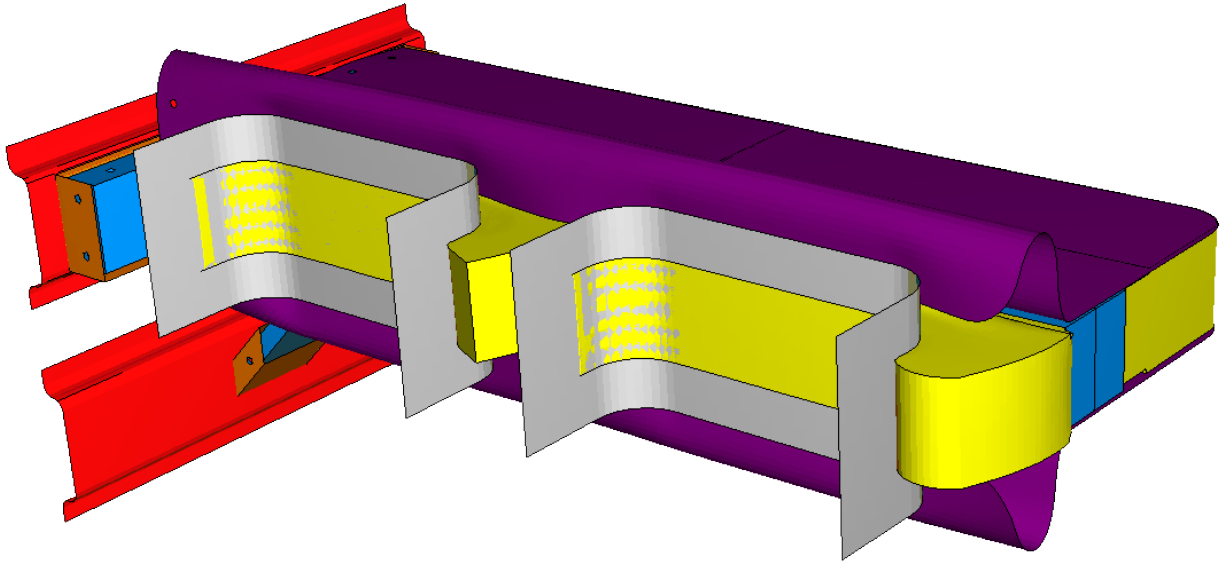


Figure 35. The Predicted Deformation of the Workstation Table after 6 in of Indenter Motion

Figure 36 shows a top view of the deformation after 6 in of indenter motion. The outline of the undeformed mesh is shown for comparison (and the melamine has been removed). The I-beam bent approximately 0.5 in as a result of the applied load (which, after 6 in of indenter motion, is approximately 2,600 lbf on the window side and 2,400 lbf on the aisle side).

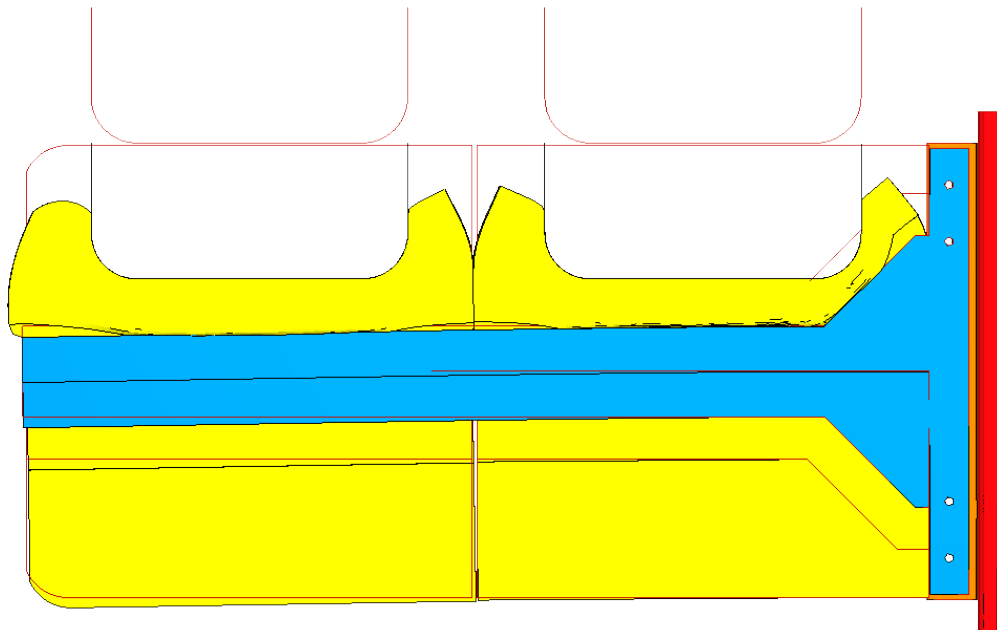


Figure 36. The Predicted Deformation of the Workstation Table after 6 in of Indenter Motion (top view showing outline of undeformed mesh; melamine not shown)

Figure 37 shows the stresses that arise in the steel frame of the table. The frame stresses are dominated by bending of the I-beam. The stress exceeds the minimum yield strength for A572-

65 (65 ksi) in only a very small region at the edge of the I-beam web where it meets the angled piece. Figure 38 shows the resulting plastic strain, which is small (a maximum of less

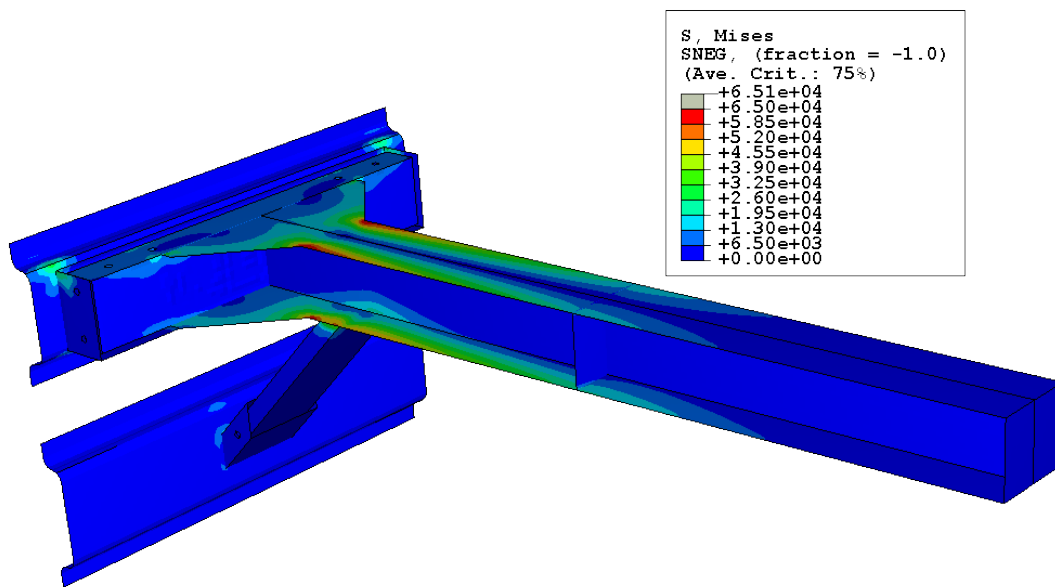


Figure 37. The Distribution of Mises Stress at an Indenter Displacement of approximately 6 in (a total load of about 5,000 lbf)

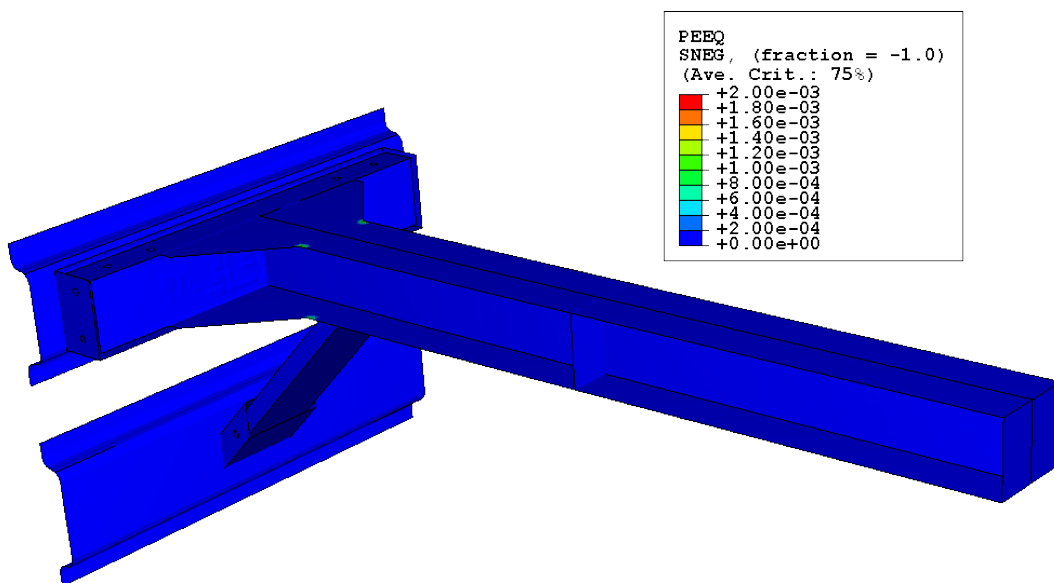


Figure 38. The Distribution of Equivalent Plastic Strain at an Indenter Displacement of approximately 6 in (a total load of about 5,000 lbf)

than 0.002 in/in) and arises within a very small region. Given that the measured yield strengths for A572-65 exceed the 65 ksi minimum by 20–40 percent, it is probable that no plastic deformation would occur.

Figure 39 shows the load-displacement response for the aisle-side and window-side indenters. The displacement, or crush, in the graph includes both plastic and elastic deformation. This is particularly true for the aisle-side indenter because of the deformation of the I-beam, which is almost entirely elastic. As is evident from these curves, the strength at which the table crushes is greater on the window-side than on the aisle-side. More significantly, the window-side response stiffens at least one-half inch sooner than the aisle-side response. This is consistent with the extent of bending (refer to Figures 35 or 36).

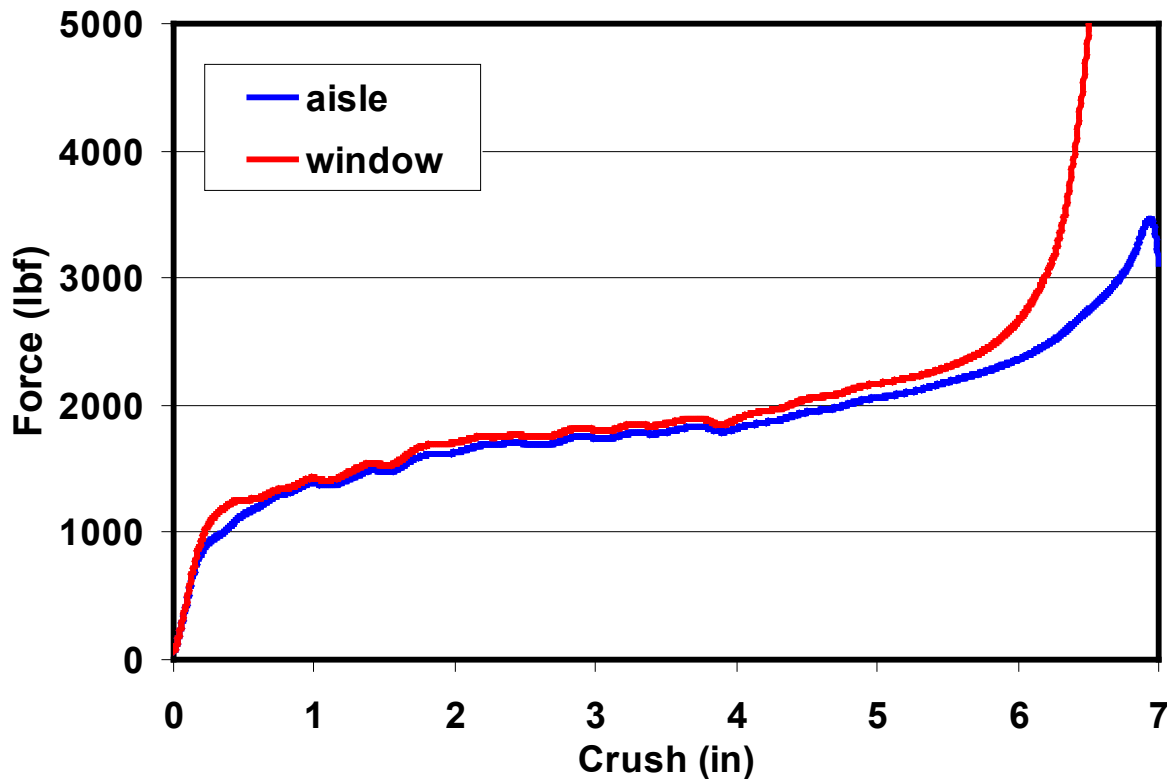


Figure 39. Load-Displacement Curves for the Window-Side and Aisle-Side Indenters

6.1.3 Vertical Service Load Model

A honeycomb model was also used to establish that the workstation table is able to support the required 350-pound-force vertical load. The table crush models presented in Section 6.1.2 were deemed unnecessarily complex for modeling a quasi-static load. Instead, an assumption was made that the table will be at least as strong as a single honeycomb block cantilevered from one end (where it is bonded to the I-beam). In other words, the contribution of the melamine to vertical strength is neglected.

Figure 40 shows the mesh used for the analysis of a block of 1/4-5052-0.004 honeycomb, 19.3 in wide by 10.2 in deep by 3.5 in thick. The model uses 177,000 ABAQUS-type S4R shell elements. The 350-pound-force load is distributed over a 4- by 4-inch patch of nodes at the top corner of the block, as highlighted in the figure. The nodes at the back end of the mesh are encastre. The analysis was performed by using ABAQUS/Standard, with the 350-pound-force load applied incrementally using the nonlinear geometry option, and then removed.

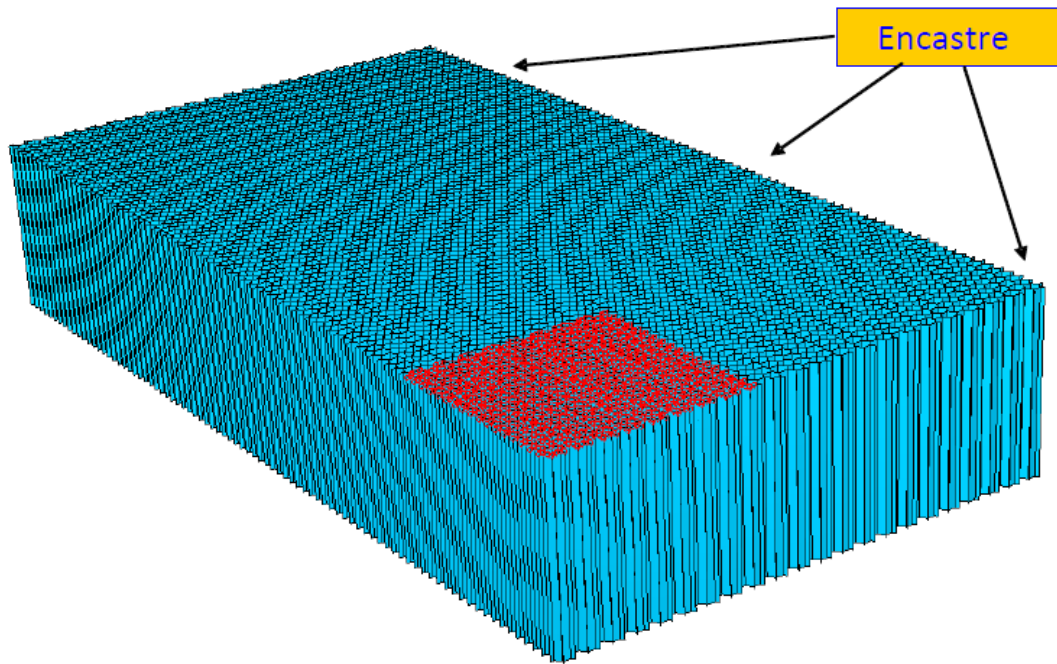


Figure 40. The Mesh for the Vertical Service Load Model (the load is applied to the region highlighted in red)

Figure 41 shows the predicted distribution of vertical displacement. The results of the analysis indicated that the total downward displacement was approximately 0.32 in. Figure 42 shows the associated distribution of stress. The stress exceeded the yield strength of the 5052 aluminum (37 ksi) in a very small region, causing plastic strain of less than 1 percent. Upon removal of the load, the residual vertical displacement is only 0.001 in. Given the likely contribution of the melamine to the stiffness of the panel and the additional support that might be provided by the flange of the I-beam, both of which have been neglected in this analysis, these results suggest that the table will likely satisfy the vertical load service requirement.

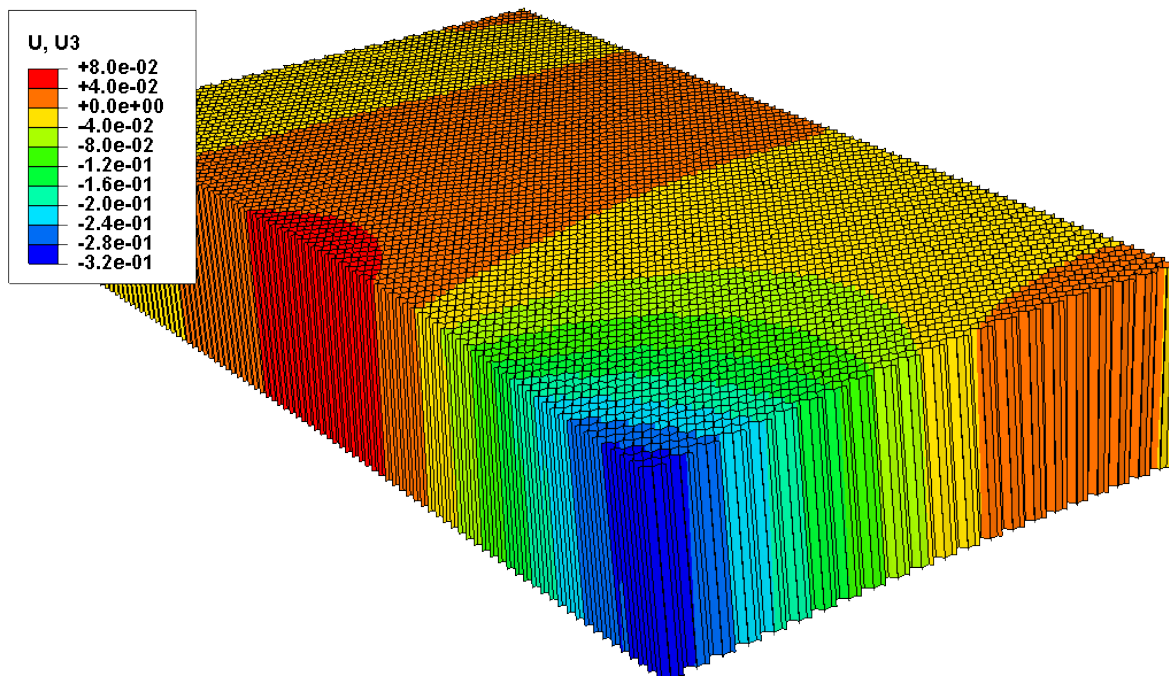


Figure 41. The Distribution of Vertical Displacement for a 350–Pound-Force Vertical Load

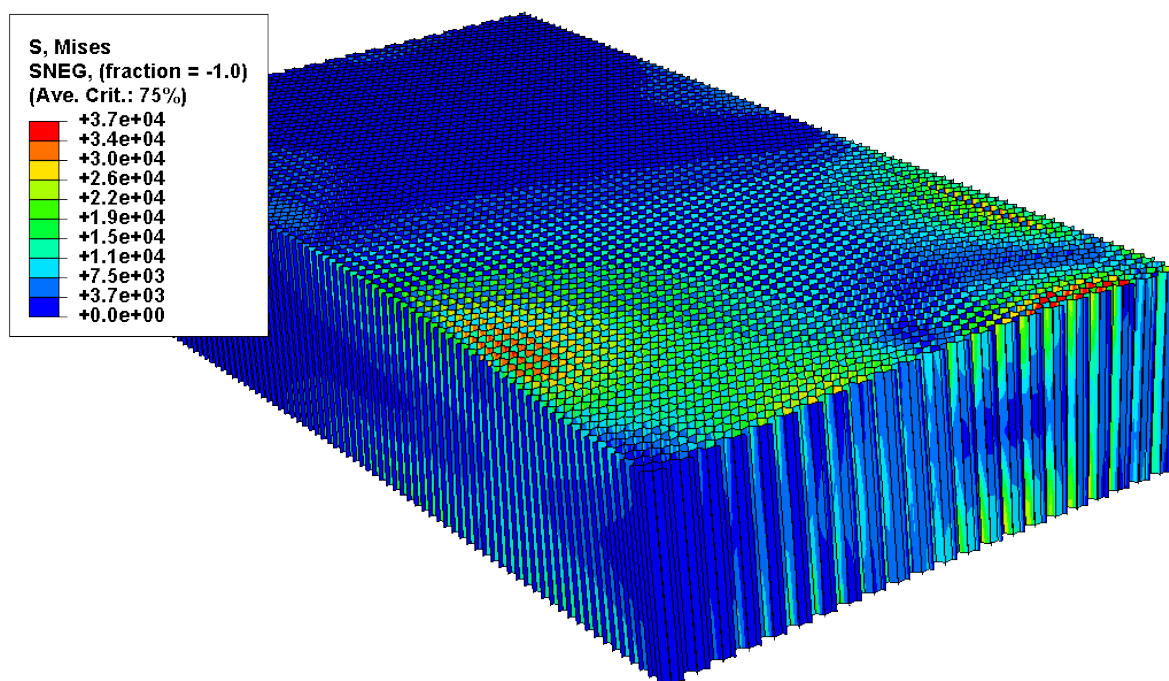


Figure 42. The Distribution of Mises Stress for a 350–Pound-Force Vertical Load

6.2 MADYMO Model and Analyses

The finite element results were used to guide the design of the crushable table. The table crush performance results from those analyses were used in the MADYMO occupant response model to predict the injury risk to an occupant seated at the crushable table during a collision.

MADYMO is a software package developed by TASS to analyze occupant safety systems. The Volpe Center supplied an existing MADYMO model of a conventional table struck by a 50th-percentile occupant. This model was developed for a previous test and refined on the basis of the results of that test [7]. Several modifications were made to this model as follows:

- A second 50th-percentile THOR test dummy was added and placed in the aisle seat. The original file and test used a single test dummy.
- The wall support of the table was modified to include the angled strut to verify that the occupant's knees would not impact it.
- The table thickness, length, and height above the floor were modified according to the new table design.
- Two crush elements were added to the impacted side of the table. They were represented by spring/dampers with the force/crush response defined by the finite element analysis results.
- Knee interactions with the seat on the opposite side of the table were included. A contact characteristic was added to represent the stiffness of the knee-bolster padding.

Figure 43 shows an image of the MADYMO model developed for this project.

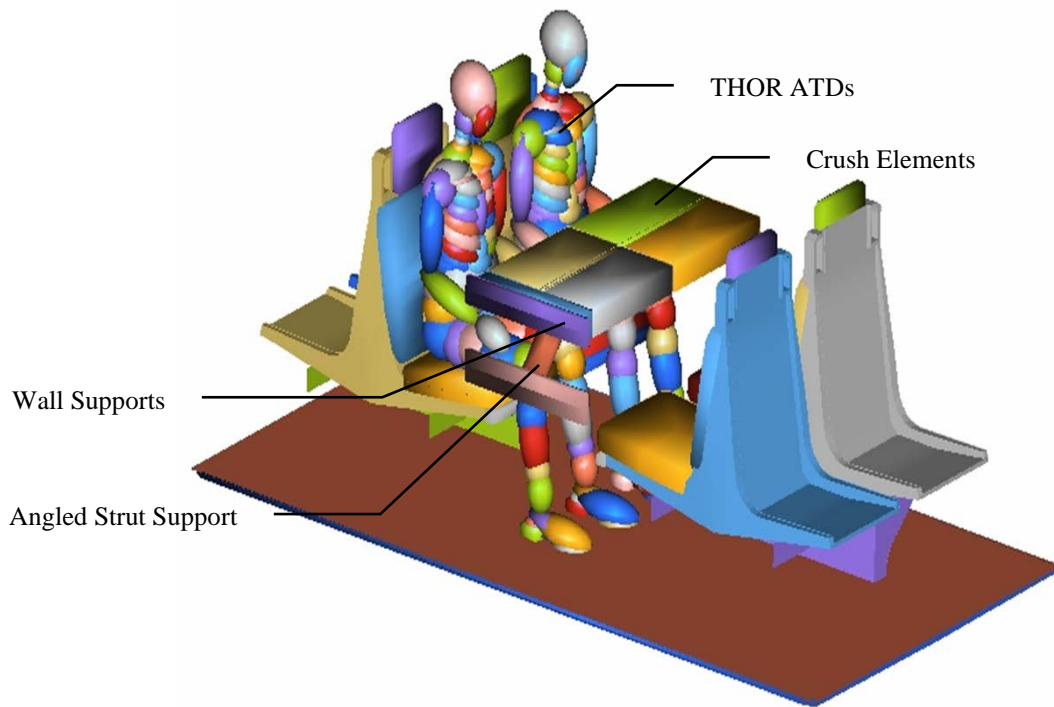


Figure 43. An Image of the MADYMO Model of the Crushable Table with Two 50th-Percentile THOR ATDs Seated at the Table

The table shown in Figure 43 is mounted to the rail car wall with stiff springs (19,000 lbf/in, 3,300,000 N/m) to predict the forces at the mounting locations. The table is positioned with the top surface 32 in above the floor. This allows the 3.5-inch-table thickness to interact with the lower rib cage and the upper abdomen. The four crush elements that make up the table are each connected to the center support I-beam of the table by a spring-damper element. The spring has a nonlinear force/crush characteristic consistent with the curve shown in Figure 44. A damping coefficient of 0.0571 lbf-s/in (10 N-s/m) was applied to the crush element connection. Two THOR 50th-percentile ATDs were seated at the table with their hands resting on their knees. They were seated upright with their feet flat on the ground. A friction coefficient of 0.3 was used between the bottom of the foot and the floor surface. Contact was defined between the abdomen and chest of the ATDs and the table edge as well as between the arms and the table edge. In case it occurred, contact was also defined between the head and the tabletop. In previous testing, it was noted that the knees of the ATD could strike the front of the seat of the facing seat, and this contact was included in the model. Contact between the back surfaces of the ATDs and the launch seat surfaces were also modeled to realistically simulate the rebound of the occupant back into the seat.



Figure 44. The Table Crush Response Used in the MADYMO Occupant Interaction Model

Two acceleration pulses were used. The industry standard 8g, 250-millisecond triangular pulse is shown in Figure 45. The 8g pulse simulation results were used to determine whether the table design met its requirements. The predicted acceleration pulse derived from the CEM train-to-train test is shown in Figure 46. The CEM pulse was used to predict how the table would perform in this more severe environment in preparation for the CEM train-to-train test. The pulses were applied to the models, and the occupant response and loads at the mounting points were predicted.

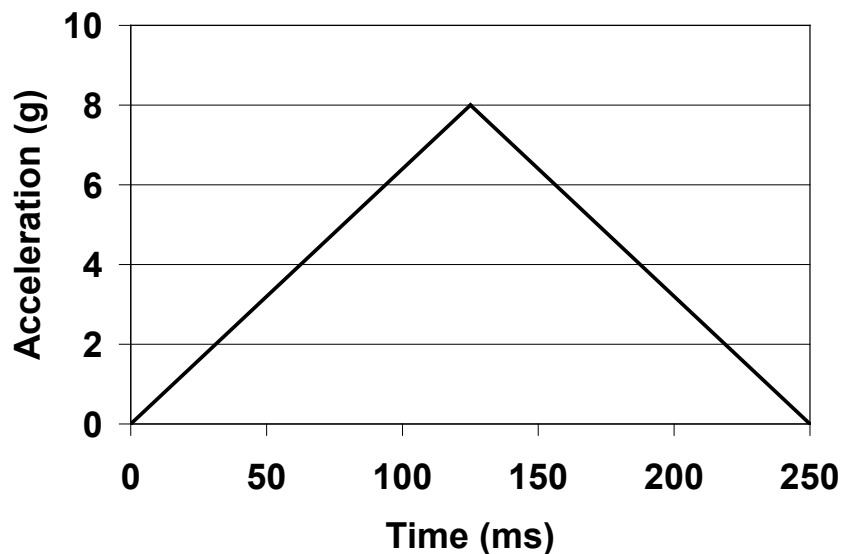


Figure 45. The 8g Peak, 250-Millisecond Triangular Acceleration Pulse Used in the MADYMO Analyses

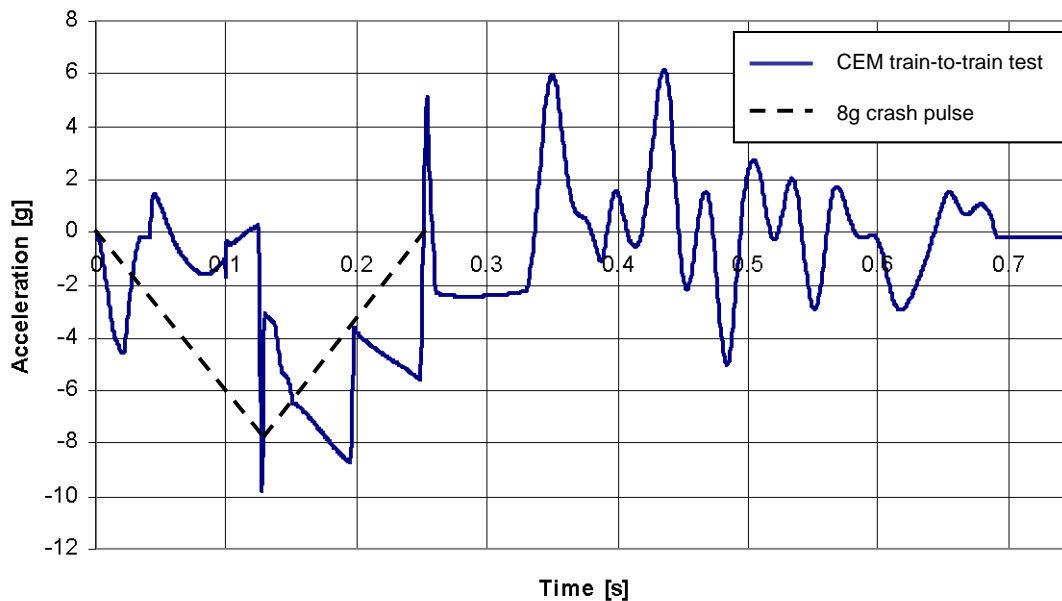


Figure 46. The Predicted CEM Train-to-Train Acceleration Pulse Used in the MADYMO Analyses

6.2.1 Eight-G Acceleration Pulse Results

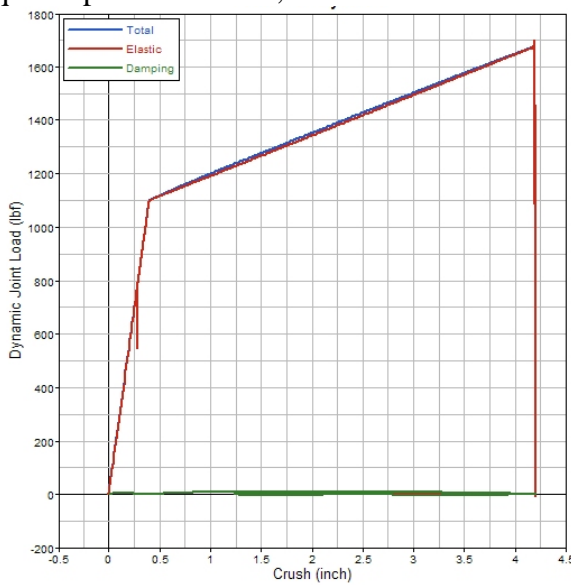
In the first MADYMO analysis, the industry standard 8g, 250-millisecond triangular acceleration pulse was applied to the model (see Figure 45). The two occupants slid forward on their seats, and the chest and upper abdomen struck the 3.5-inch-thick edge of the table, causing it to crush. The crush response and peak force of the table and the occupant response measurements and their respective requirements for comparison are provided in Table 7. Each of the occupant response measurements is below the IARVs defined by the design requirements. In addition, the predicted crush and peak force levels of the table are less than the required limit.

Table 7. Table Crush and Occupant Response Measurements for the 8g Acceleration Scenario

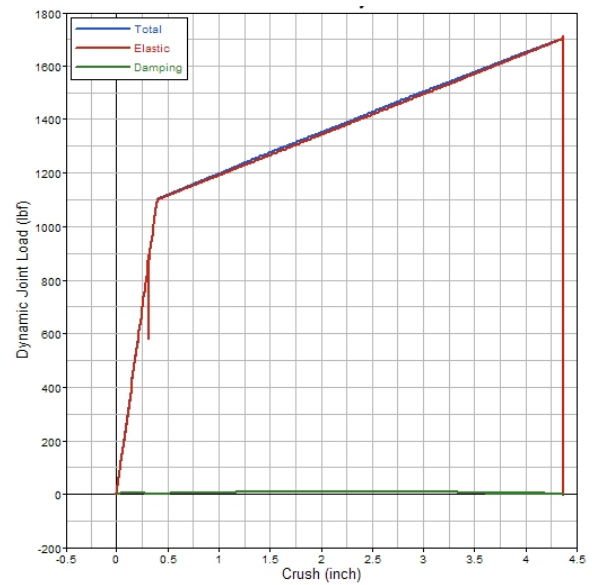
Category	IARV	Aisle Occupant	Window Occupant
HIC15	700	18	20
Nij	1.0	0.22 NTE	0.26 NTE
Neck tension	940 lbf (4,170 N)	150 lbf (665 N)	190 lbf (844 N)
Chest 3 ms	30g	21g	24g
Chest compression	2.4 in (60 mm)	1.8 in (45.7 mm)	1.9 in (48.3 mm)
Chest viscous criterion	31.5 in/s (0.8 m/s)	4.0 in/s (0.1 m/s)	8.7 in/s (0.2 m/s)
Upper abdomen compression	2.75 in (70 mm)	2.4 in (61 mm)	2.2 in (56 mm)
Upper abdomen viscous criterion	50 in/s (1.25 m/s)	21.1 in/s (0.54 m/s)	25.5 in/s (0.65 m/s)
Table Crush	10 in (0.25 m)	4.2 in (0.11 m)	4.4 in (0.11 m)
Peak force (measured at the table edge)	2,200 lbf (10,000 N)	1,690 lbf (7,500 N)	1,700 lbf (7,550 N)

The predicted HIC15 was far below the limit because the head never impacted the table. The Nij and neck tension levels were also low. The 3-millisecond chest acceleration levels approach the limit but are comfortably below the required 30g. The chest and abdomen compressions are comfortably below the limit as are the chest and abdomen viscous criteria.

Figure 47 shows the predicted force/crush response of the table for the aisle and window occupants. Note that the peak forces predicted for each of the table positions are below the required peak force of 2,200 lbf.



(a)



(b)

Figure 47. The Predicted Force vs. Crush Response of the Table for the 8g Acceleration Pulse Scenario for (a) the Aisle Occupant and (b) the Window Occupant

These predicted results suggest that the improved table design can meet the occupant protection requirements and table performance requirements for the 8g, 250-millisecond triangular acceleration pulse.

6.2.2 CEM Acceleration Pulse Results

In the second MADYMO analysis, the acceleration pulse predicted for the CEM full-scale train-to-train test was applied to the model (see Figure 46). This acceleration pulse was more severe than the industry standard 8g acceleration pulse. This scenario was run to predict how the table would perform in this more severe environment in preparation for the CEM train-to-train test. The results from this analysis were not directly used to guide the design of the table but provide a basis from which to compare the results of the test.

In the simulation, the two occupants slid forward on their seats, and their chest and upper abdomen struck the 3.5-inch-thick edge of the table, causing it to crush. Table 8 provides the crush response of the table and the occupant response measurements, together with their respective requirements. Values that exceeded the criteria are printed in bold text.

Table 8. Table Crush and Occupant Response Measurements for the CEM Acceleration Scenario

Category	IARV	Aisle Occupant	Window Occupant
HIC15	700	183	149
Nij	1.0	0.35 NTE	0.33 NTE
Neck tension	940 lbf (4,170 N)	280 lbf (1,245 N)	255 lbf (1,130 N)
Chest 3 ms	30g	33g	29g
Chest compression	2.4 in (60 mm)	1.9 in (47.5 mm)	2.2 in (55.9 mm)
Chest V*C	31.5 in/s (0.8 m/s)	9.3 in/s (0.24 m/s)	11.9 in/s (0.3 m/s)
Upper abdomen compression	2.75 in (70 mm)	3.25 in (82.6 mm)	3.10 in (78.7 mm)
Upper abdomen V*C	50 in/s (1.25 m/s)	28.2 in/s (0.72 m/s)	31.6 in/s (0.8 m/s)
Table crush	10 in (0.25 m)	6.3 in (0.16 m)	6.2 in (0.16 m)
Peak force	2,200 lbf (10,000 N)	1,950 lbf (8,670 N)	2,000 lbf (8,890 N)

As Table 8 shows, most of the response measurements predicted for the occupants of the workstation are below the required injury assessment reference values. The chest acceleration for the aisle occupant and the abdominal compression for both occupants are slightly above the requirements. The predicted crush and peak force levels of the table are less than the required limit. The predicted HIC15 is well below the limit because the head never impacts the table. The Nij and neck tension levels are also low. The chest compression is comfortably below the limit as are the chest and abdomen V*C. Keep in mind that these requirements are based on an impact severity of an 8g, 250-millisecond triangular acceleration pulse.

Figure 48 shows the predicted force/crush response of the table for the aisle and window occupants. Note that the peak forces predicted for each of the table positions are below the required peak force of 2,200 lbf.

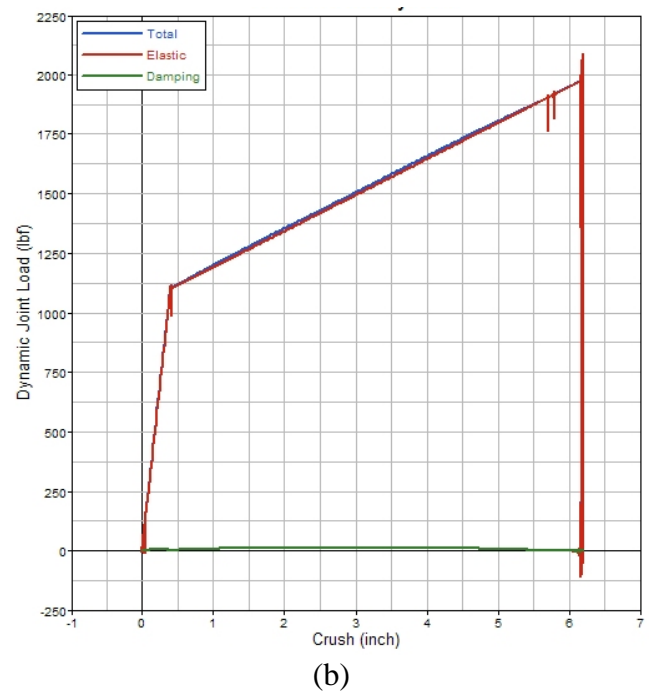
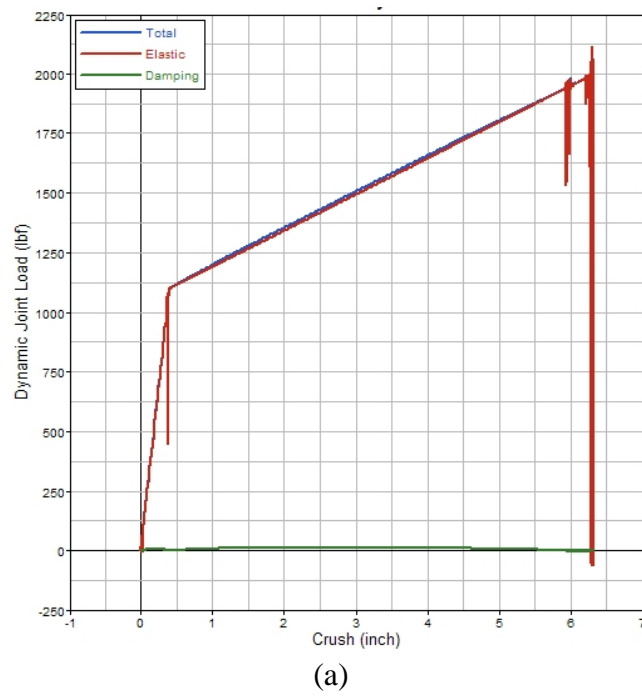


Figure 48. The Predicted Force vs. Crush Response of the Table for the CEM Acceleration Pulse Scenario for (a) the Aisle Occupant and (b) the Window Occupant

7. Quasi-Static Tests

7.1 Introduction

Quasi-static testing on the workstation table was conducted at Simula's facilities in Phoenix, AZ, on February 15 and 16, 2006. The testing had three objectives:

1. To demonstrate that the table satisfies its service load requirements,
2. To establish the workstation table longitudinal force/crush characteristic, and
3. To determine the longitudinal force levels required to ensure that the table remains attached under impact loads.

A single prototype table was used for all of the quasi-static tests. Two service load tests and one crush test were performed as follows:

- A horizontal service load of 500 lbf applied against the facing edge of the table near the aisle side,
- A downward vertical service load of 350 lbf applied to the tabletop near the aisle side corner, and
- A horizontal collision load applied by two application load plates, each representing the width of a 50th-percentile male upper abdomen, of sufficient magnitude to crush the honeycomb core on one side of the table.

Note that the vertical service load test was repeated to verify the downward displacement of the table and that the collision test was repeated (i.e., the crush was continued) after the load had reached a limit level during the initial test. These tests were conducted to demonstrate compliance with specific performance requirements listed in Appendix A.

The results of the two service load tests indicated that the table was able to withstand the applied load and experienced an extent of permanent set that was within allowed tolerances following removal of the load. The results of the crush test, however, indicated that there was a flaw in the assembly of the table that limited the honeycomb from crushing to its full design potential of 7 in. This finding led to a change in the manner in which the table was assembled.

Individuals who were onsite with Simula and CVID personnel to witness the test were Mr. Daniel Parent (Volpe Center), Dr. Tom Tsai (FRA), Mr. Telis Kakaris (Metrolink), Mr. Ralph Dolinger (LTK), and Dr. Richard Stringfellow (TIAX).

7.2 Test Facilities and Setup

Simula's test facilities are located in a 33,000-square-foot building at 10016 South 51st Street in Phoenix, AZ. This indoor quasi-static and dynamic facility houses a 10-foot-wide, 9-foot-high, and 2-foot-deep rigid quasi-static loading frame system for conducting testing. The quasi-static loading frame is capable of conducting single and simultaneous multiaxis loading up to 25,000 lbf.

This test facility is environmentally conditioned to maintain temperatures of 66–78 °F and 10- to 70-percent relative humidity. A provision for high-speed filming of dynamic tests is in place in the facility. State-of-the-art signal conditioning and data recording equipment of all and dynamic tests are also incorporated into this facility to meet a variety of testing requirements.

7.2.1 *Quasi-Static Test Frame*

The quasi-static test frame was constructed of 10-inch structural steel I-beams to provide a mounting structure with sufficient rigidity for component deflection measurements to be taken without the need to correct for loading frame deformation (see Figure 49). The mounting points for the test articles, the load cylinders, and the string potentiometers (displacement transducers) were positioned in a manner that most closely represents installation in the field.

7.2.2 *Quasi-Static Test Setup*

A single table was required for quasi-static testing and was designed and provided to Simula by TIAX. Simula designed and built a structure to mimic the side of a rail car along with the interface plates needed to attach the table to the fixture with load cells.

Individual 3-inch-diameter hydraulic cylinders were used to apply the loads. The hydraulic cylinders are manually controlled from a remote console. The console, which is fed by a single, electrically driven hydraulic pump, provides for directional control, pressure regulation, and flow rate control. The electronic load transducers were located between the cylinders and the test component to provide the primary loading indicators. All the tests were conducted with the hydraulic cylinders operating in a compressive mode. For the crush test, one supply circuit was used with a manifold that split the supply equally and independently between the two cylinders. This allowed each load applicator to apply an equal load to the table.

A 10,000–pound-force strain gage load transducer (load cell) was used to record the input loads produced by the hydraulic actuator for each test. It was set to quarter-scale for the service load tests and half-scale for the collision strength test. The readings were electronically recorded as well as monitored visually by Simula personnel.

A dial gage was used in the two service load tests to measure the maximum displacement of the table during loading, and any residual displacement after each test was completed. One revolution of the dial gage represents a 0.1-inch displacement. Figure 50 shows how the dial gage was set up in the two service load tests.



Figure 49. The Quasi-Static Test Frame with the Table Setup for Testing

A potentiometric displacement transducer (string pot) was used in the collision strength test to measure the displacement of the table caused by crushing (and table distortion). Two string pots were installed between the test frame and the test article, and another was installed to measure the displacement of the hydraulic cylinder (see Figure 51).



Figure 50. A Dial Gage Was Used to Measure Table Displacement in the Horizontal Service Load Test (left) and the Vertical Service Load Test (right)



Figure 51. Two String Pots Were Used to Measure Table Displacement in the Crush Strength Test (note: the white box attached to the fixture is one such string pot)

Three 10,000–pound-force triaxial load cells were installed onto the test fixture to monitor the interface loads between the table and the fixture (Figure 52). These load cells were filtered according to SAE CFC 60. The load cells, string pots, and dial gages were all zeroed out before the test. Table 9 lists the variety and ranges of the instrumentation that Simula used to conduct the quasi-static tests.



Figure 52. Three 10,000–Pound-Force Triaxial Load Cells Were Used to Measure the Wall Attachment Loads, Shown Here from a Side View of the Table-to-Wall Attachment

Table 9. Quasi-Static Test Instrumentation

Instrumentation	Manufacturer	Model	Range	Response Limit
Triaxial attachment load cell	Denton	2177A	10,000 lbf	DC-1,250 Hz frequency response
Uniaxial load cell (to measure input load)	Interface	1210	5,000 lbf and 10,000 lbf	DC-1,250 Hz frequency response
Horizontal string potentiometers	Celesco	PT-101-20C	Various ranges	100g max retraction rate
Vertical string potentiometers	Celesco	PT-101-20C	Various ranges	100g max retraction rate
Digital camera	HP	945	5.3 MP	N/A
Video camera	Panasonic	S1	Real time	N/A

A Pacific Instruments data acquisition system and a Validyne load measurement system were used to collect, filter, and process the data in the tests. The Pacific Instruments Model 5600A was used to collect the table attachment loads. The Validyne system was used to manage and monitor the input loads through the load cell on the hydraulic ram and manage the string potentiometer data. All data from these systems was collected, filtered, and processed in accordance with SAE J211 and SAE AS 8049.

Several digital still photographs were taken before and after each test. These photographs showed an overall view of the test article and its orientation on the test frame and some of the significant details of the test article before and after each test. One real-time video camera was used to capture the overhead view of the test article during testing. A second video camera was used to capture the side view of each test.

7.3 Quasi-Static Test Procedures

Table 10 summarizes the three tests that were performed to satisfy the four quasi-static test requirements pertaining to the ability of the table to withstand service loads and to absorb energy during a collision. Figure 53 identifies the load application sites for each one of the tests.

Table 10. Quasi-Static Test Series Requirements

Test	Requirement	Applied Load	Transducers	Passing Requirements
Horizontal Service Load	Attachment strength	500 lbf longitudinal load on table edge near aisle-side	Three wall attachment load cells (3-axis): 142 = top right (TR); 95 = top left (TL); 144 = center (CTR); dial gage (max. reading of 0.5 in.)	No deformation at attachments
	Table edge strength (horizontal)			<0.050 in residual deformation to tabletop
Vertical Service Load	Table edge strength (vertical)	350 lbf downward vertical load on tabletop	Three wall attachment load cells (3-axis); 142 = top right (TR); 95 = top left (TL); 144 = center (CTR); dial gage (max. reading of 0.75 in.)	<0.050 in residual deformation to tabletop
Collision Strength	Table edge collision strength	Steadily increasing displacement of actuators	Three wall attachment load cells (3-axis); 142 = top right (TR); 95 = top left (TL); 144 = center (CTR); string potentiometer	Crush initiation must occur at or above 750 lbf; peak crush force of 2,200 lbf

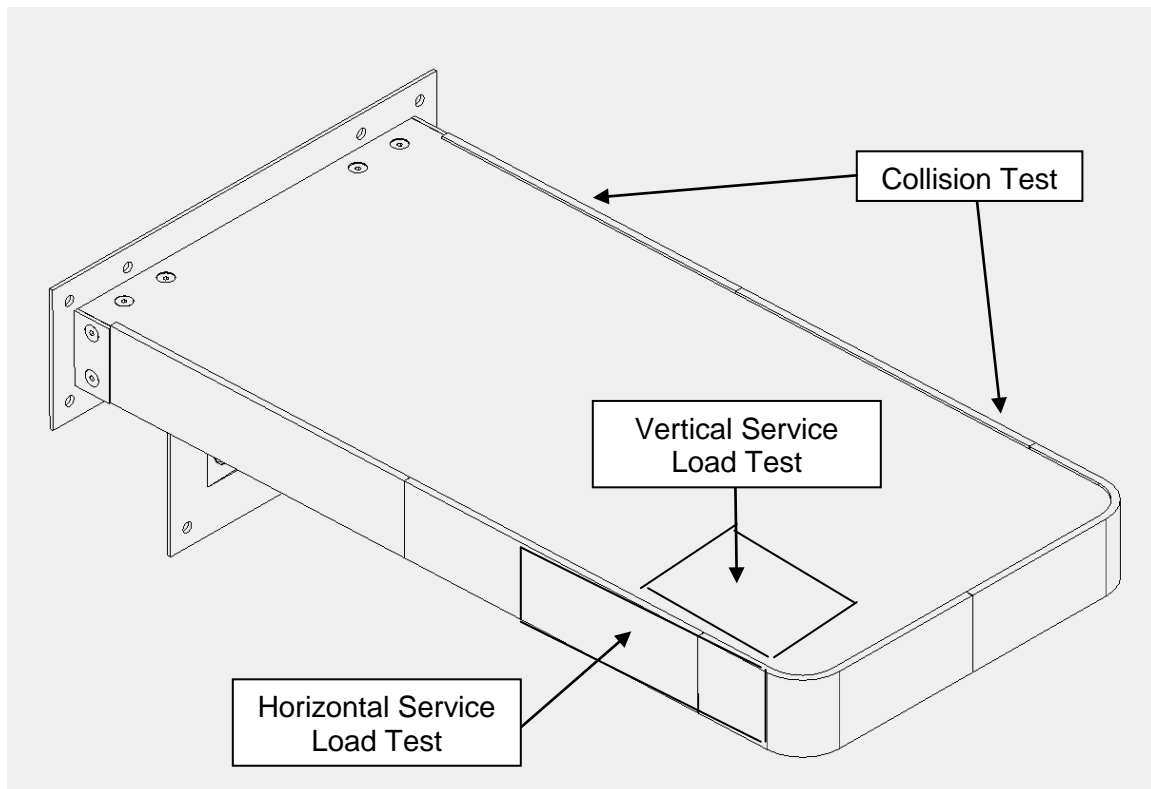


Figure 53. Load Application Sites for the Three Tests

7.3.1 Service Load Tests

The table was first tested under a horizontal load to meet the “Table Attachment Requirements” (Section 4.1.3 of the Workstation Table Requirements Document—refer to Appendix A) and one of the “Table Edge Requirements” (Section 4.2.2-b, Appendix A), and then, it was tested under a vertical load to meet the other of the “Table Edge Requirements” (Section 4.2.2-a, Appendix A).

The location and area of each load application site was specified as shown in Figure 53. For each test, the area under the distributed load was limited to the surface of the table. To keep the load applicator flush with the table and to eliminate any voids or spaces between it and the table, the 5- by 5-inch load area did not include the neoprene table edge. The 8- by 3.5-inch area defined for the horizontal load was limited to the side surface of the table, precluding it from extending beyond the rounded edge.

For both service load tests, the load was increased at a rate of approximately 1 in/min until the desired maximum load was reached (500 lbf for the horizontal test and 350 lbf for the vertical test). The maximum applied load was held for approximately 10 s before the load was released.

The table position was measured pre- and posttest. A dial gage was used to measure the maximum displacement of the table as well as the residual displacement after each test was completed. A hydraulic cylinder was actuated in compressive mode to apply the load to the table through a load application plate sized to fit the required table surface area. A piece of foam was positioned between the table surface and the metal plate to ensure complete contact (see Figure 54).

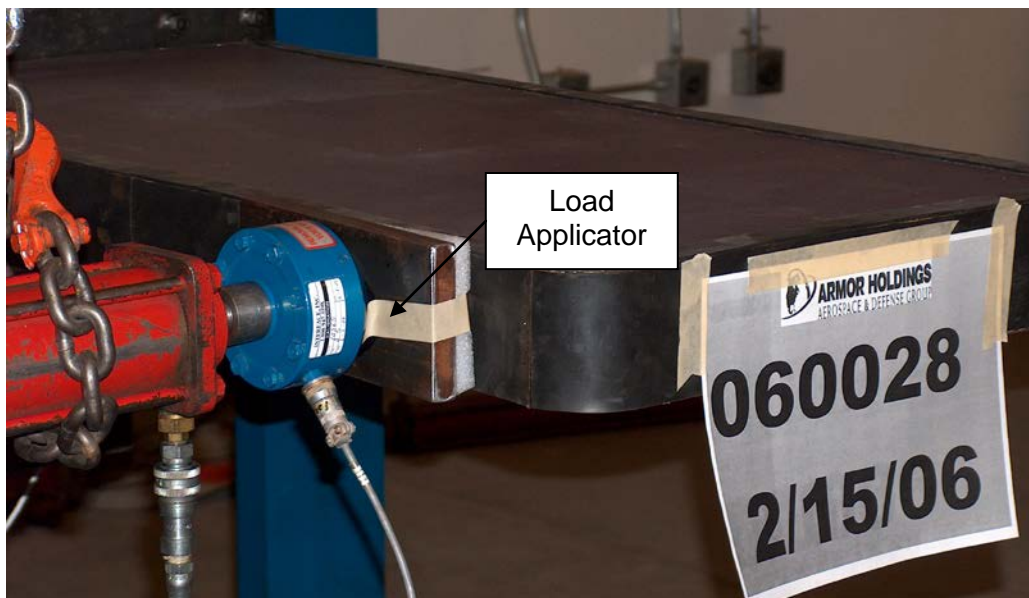


Figure 54. The 10,000–Pound-Force Load Cell, the Load Application Plate, and the Foam Piece Used to Distribute the Compressive Force on the Edge of the Table

These tests were conducted before the collision strength test and in a sequence intended to minimize the risk of any damage to the test specimen so that it could be used again for testing. Figure 55 shows the pretest set up with two hydraulic cylinders positioned to apply load to the

table; the horizontally oriented cylinder was set up to apply a compressive force to the facing edge of the table and the vertically oriented cylinder was set up to apply a compressive force to the top surface of the table.



Figure 55. Two Hydraulic Cylinders Are Prepositioned to Separately Apply Load to the Table in Service Load Test

7.3.2 Longitudinal Crush Test

The crush test was conducted to evaluate the longitudinal crush strength of the table edge and provided force versus crush data to support and refine the crush analysis modeling. The table was tested to meet the table edge collision strength requirements listed in Section 4.2.3 of the Workstation Table Requirements Document (refer to Appendix A). This was a destructive test to validate the deformation behavior of the tabletop and any other deformable components in the table design.

The hydraulic cylinders, used to apply the load, were actuated in a compressive mode. Because these cylinders tend to be less stable when used in compression, they had to be secured in their positions during the compressive load application. As Figure 56 shows, chains were used above to hang the cylinders in place, and a turn buckle was used to secure each cylinder from below.

A compressive load was applied to the table edge individually through each of the two steel load applicators (Figure 57) at a rate of approximately 1 in/min and released after the honeycomb crushed to its maximum capability or when the load in each actuator reached 3,500 lbf. After a period of observation following the first test, some of the melamine tabletop was removed, and the load was reapplied in an attempt to increase the extent of crush.



Figure 56. Two Hydraulic Cylinders Prepositioned to Apply Horizontal Load to the Table through Two Load Applicators Representing 50th-Percentile Male Abdomens in Test 3

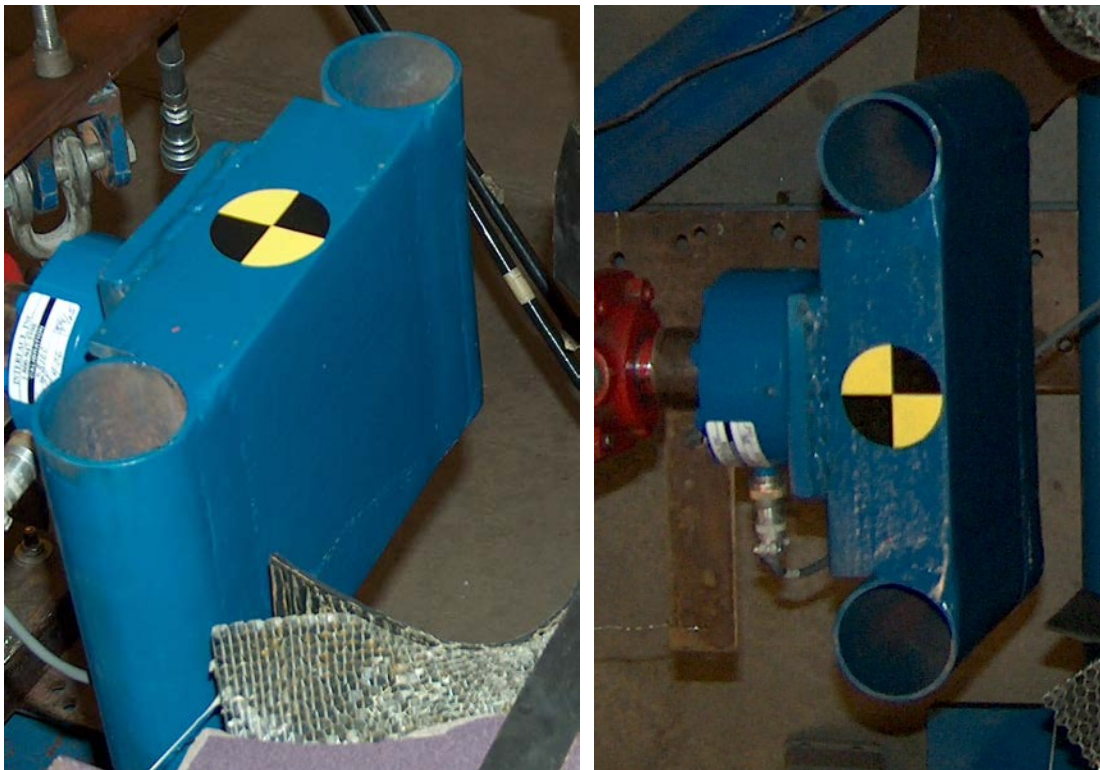


Figure 57. The Load Applicator Was Sized to Represent a 50th-Percentile Male Abdomen

7.4 Test Results

Five tests were conducted to evaluate the structural integrity of the test table. Two of these were repeat tests to confirm additional information. Table 11 summarizes the results of each test.

Table 11. Quasi-Static Test Results

Test	Requirement	Test No.	Required Loads	Actual Recordings	
				Maximum Load (lbf)	Maximum Displacement (in)
Horizontal Service Load	Attachment strength <i>and</i> table edge strength (horizontal)	060028 (2/15/06)	500 lbf horizontal load on table edge near aisle-side	527	0.20
Vertical Service Load	Table edge strength (vertical)	060029 (2/15/06)	350 lbf vertical load on tabletop	369	0.43
		060030 (2/15/06)		369	0.42
Collision Strength Testing	Table edge collision strength	060031 (2/16/06)	Crush initiation must occur at or above 750 lbf and peak crush force of 2,200 lbf	3,585 (InBd) 3,747 (OutBd)	6.92 (InBd) 7.76 (OutBd)
		060032 (2/16/06)		3,272 (InBd) 3,414 (OutBd)	7.60 (InBd) 8.81 (OutBd)

The attachment load cells provided the force versus time characteristics that were recorded at the wall attachments. The peak loads and corresponding times recorded at each of the attachment points are listed in Table 12 for each test. The orientations of the positive x, y, and z components of the peak force are noted in Figure 58. The orientation of the load cells is such that load cell TR is shown to the left of load cell TL when viewed from the aisle-side edge of the table. The y-component of force is positive moving from the wall toward the aisle.

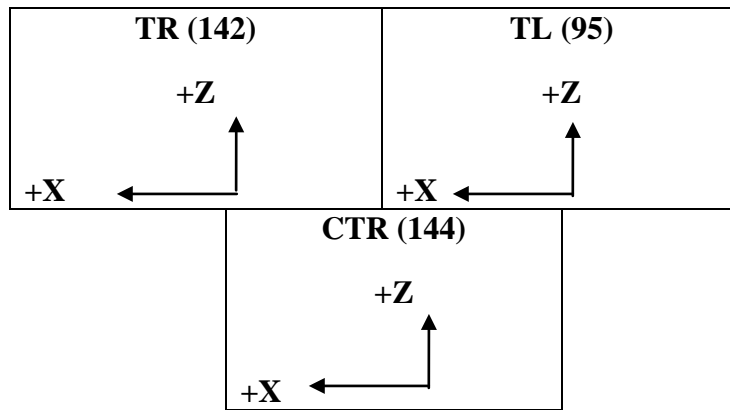


Figure 58. The Orientation of the Wall Attachment Load Cells When Viewed from Inside the Rail Car, Standing at the Aisle-Side Edge of the Table

Table 12. Peak Loads Recorded at the Three Wall Attachment Points for Each Test

Test No.	Comp.	142 = top right (TR)		95 = top left (TL)		TR144 = center (CTR)	
		Peak Force (lbf)	Time (s)	Peak Force (lbf)	Time (s)	Peak Force (lbf)	Time (s)
060028 (2/15/06)	X	-185	136	-227	136	-118	136
	Y	911	136	-903	136	-15	166
	Z	291	136	-302	136	-15	136
060029 (2/15/06)	X	-404	90	494	90	-63	90
	Y	486	90	564	90	-1018	90
	Z	86	90	388	90	-849	90
060030 (2/15/06)	X	Not recorded (data malfunction)					
	Y	Not recorded (data malfunction)					
	Z	Not recorded (data malfunction)					
060031 (2/16/06)	X	3,717	235.5	1,467	236	2,151	236
	Y	-7,710	235.5	7,930	236	666	236
	Z	-1,674	235.5	2,011	236	201	217
060032 (2/16/06)	X	7,193	304.5	1,612	81	2,165	81
	Y	6,888	264	7,593	81	-326	84
	Z	-1,925	78	2,531	81	-422	84

7.4.1 Horizontal Service Load Test

In Test No. 060028, a horizontal load was applied at a rate of approximately 1 in/min to the edge of the table near the aisle side. The load reached 528 lbf, exceeding the required limit by 28 lbf. The dial gage indicated a peak longitudinal table deflection of 0.200 in. Upon removal of the load, the displacement returned to approximately 0.004 in. No visible damage to the table was observed after the test. Figure 59 shows pre- and posttest photographs of the table.



Figure 59. Pre- and Posttest Photographs of the Horizontal Service Load Test (Test No. 060028)

7.4.2 Vertical Service Load Tests

In Test No. 060029, a downward vertical load was applied at a rate of approximately 1 in/min to the top surface of the table, near the aisle side. The applied load peaked at 370 lbf, exceeding the 350-pound-force limit by 20 lbf. The dial gage indicated that the table deflected downward by 0.43 in. Upon removal of the load, the displacement returned immediately to approximately 0.03 in. The displacement then gradually decreased over the next few minutes to approximately 0.02 in.

A question was raised about the total downward displacement under load during this test. The dial indicator had two hands: one larger hand that records in thousandths of an inch, with one full revolution of the hand measuring 0.100 in; and a much smaller dial that records tenths of an inch. During the test, the large dial made one complete revolution very quickly (i.e., with the load less than 100 lbf) and then proceeded much more slowly. At the end of the test, discussion occurred as to whether the large hand swept three, four, or five complete revolutions. For this reason, the test was repeated.

During the second application of the load (Test No. 060030), the displacement under load was measured to be approximately 0.42 in. Upon removal of the load, the displacement returned immediately to 0.02 in and then after a couple of minutes reduced to 0.01 in. Note that the dial indicator was reset between tests. Figure 60 shows photographs of the table before Test No. 060029 and after Test No. 060030.

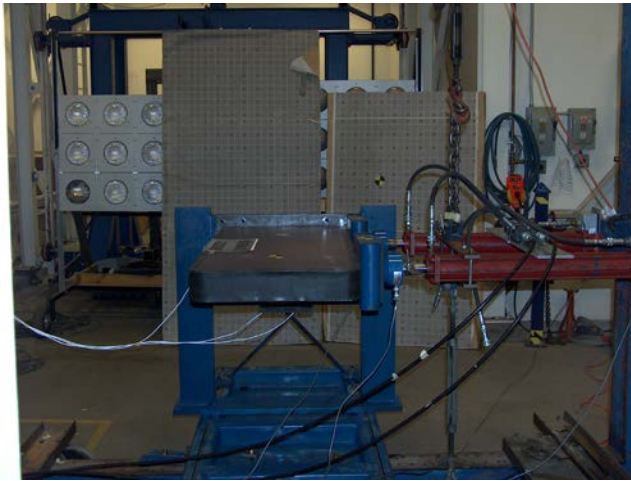


**Figure 60. Pre- and Posttest Photographs of the Vertical Service Loading Tests
(No. 060029 and No. 060030)**

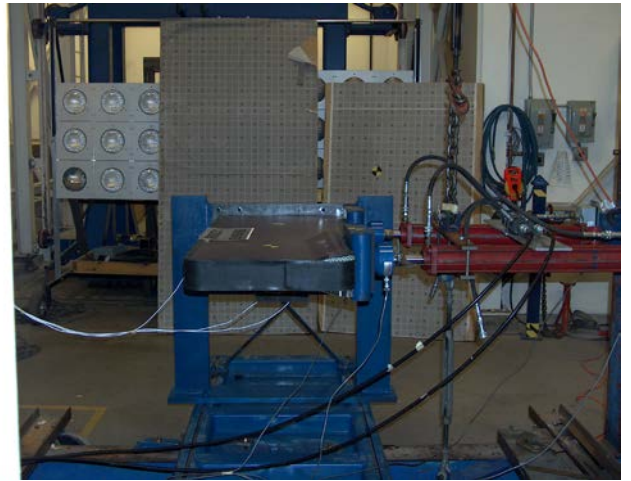
7.4.3 Collision Strength under Horizontal Loading

The load for this test (No. 060031) was applied to the side of the table opposite from where the loads were applied during the horizontal service load test. Two load applicators were used to apply loads at the outboard (window) and the inboard (aisle) sides of the table.

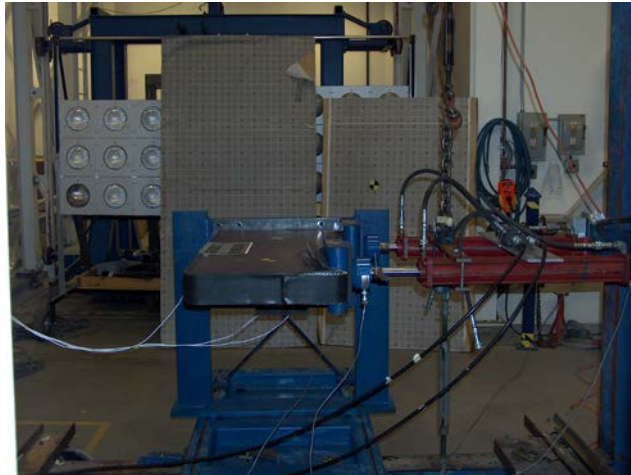
Figure 61 shows a series of photos (1–6) indicating the progression of table crush during Test No. 060031. As shown in these photographs, in addition to crushing, the table deforms significantly. The far corner of the table appeared to move at least 2 in. This is consistent with a posttest measurement of approximately 0.75-inch difference in crush between the outside and the inside of the 12-inch-wide aisle-side indenter. (If the sine of the angle is equal to $(0.75/12)$, the angle is approximately 3.6 degrees, so the total displacement is approximately 40 in (the length of the table) multiplied by $\sin(3.6 \text{ degrees})$ or approximately 2.5 in.)



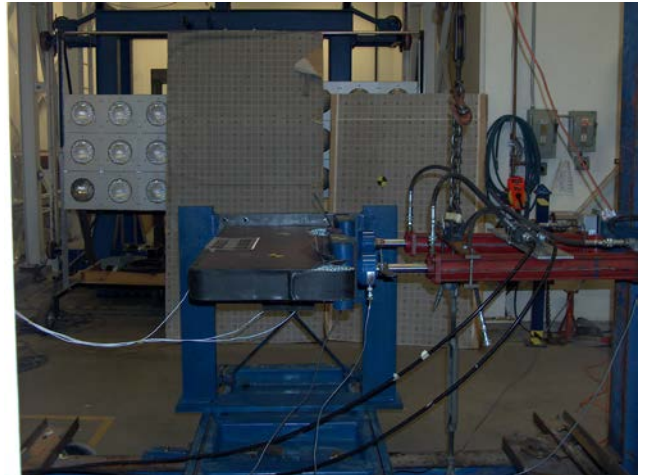
1



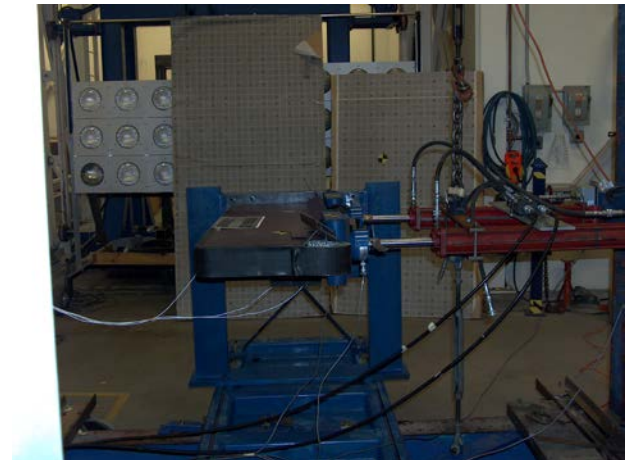
2



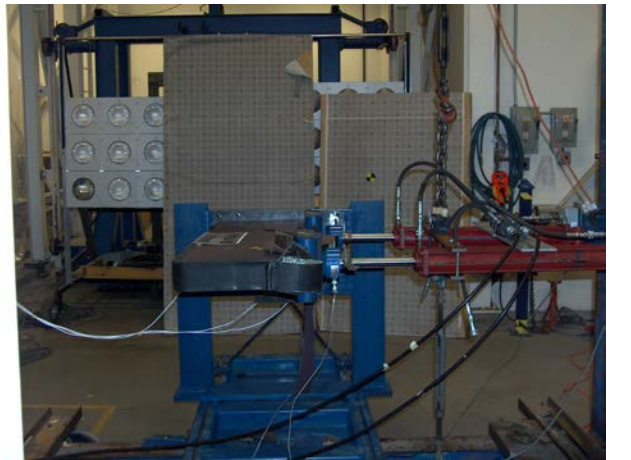
3



4



5



6

Figure 61. A Series of Photos (1–6) Showing Progression of Table Crush during Test No. 060031

Figure 62 shows the force versus deflection curves for the two load actuators. The results of the test indicate that table crush was initiated at approximately 1,500 lbf (the requirement is

for an initiation load of greater than 750 lbf with a design target of 1,250 lbf). The force increased to 1,600–1,700 lbf as the deflection of the actuators grew to approximately 4.0 in on the inboard side and 5.0 in on the outboard side. From this point onward, the load increased rapidly. The test was stopped when the load reached 3,500 lbf in both actuators for a total load of 7,000 lbf on the table.

Posttest inspection revealed that some of the honeycomb remained uncrushed. After the test, a portion of the melamine surface was removed near the center of the table. Apparently, the epoxy that was intended to bond the melamine to the top surface of the I-beam backbone of the table had leaked around the top flange during fabrication and bonded the honeycomb to the edge of the flange. This reduced the crush efficiency of the table by approximately 2 in (the width of one flange), thereby reducing the extent of crush at the expected force level. The melamine had also bonded to the honeycomb in this region, affecting its ability to bend and lift out of the way as crush progressed. This resulted in the tabletop fracturing in an uncontrolled manner. Figure 63 and Figure 64 show pretest and posttest photographs of the table from this test. Figure 65 records a posttest view of the crushed honeycomb core after the melamine laminate was removed.

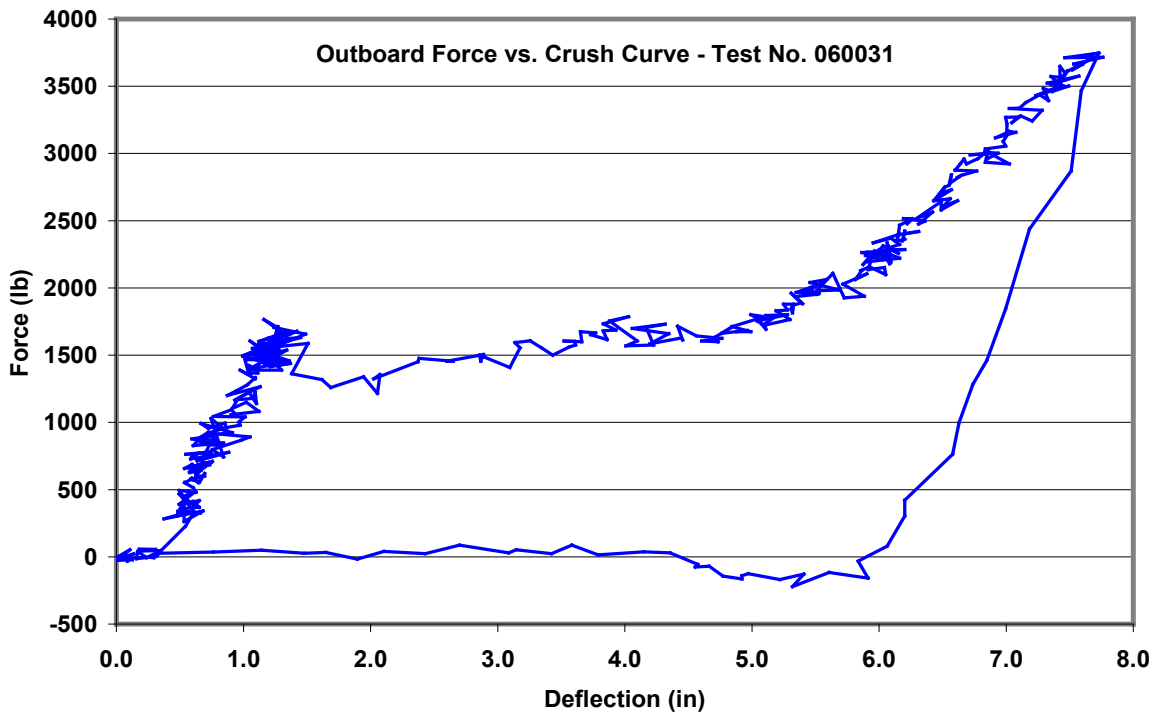
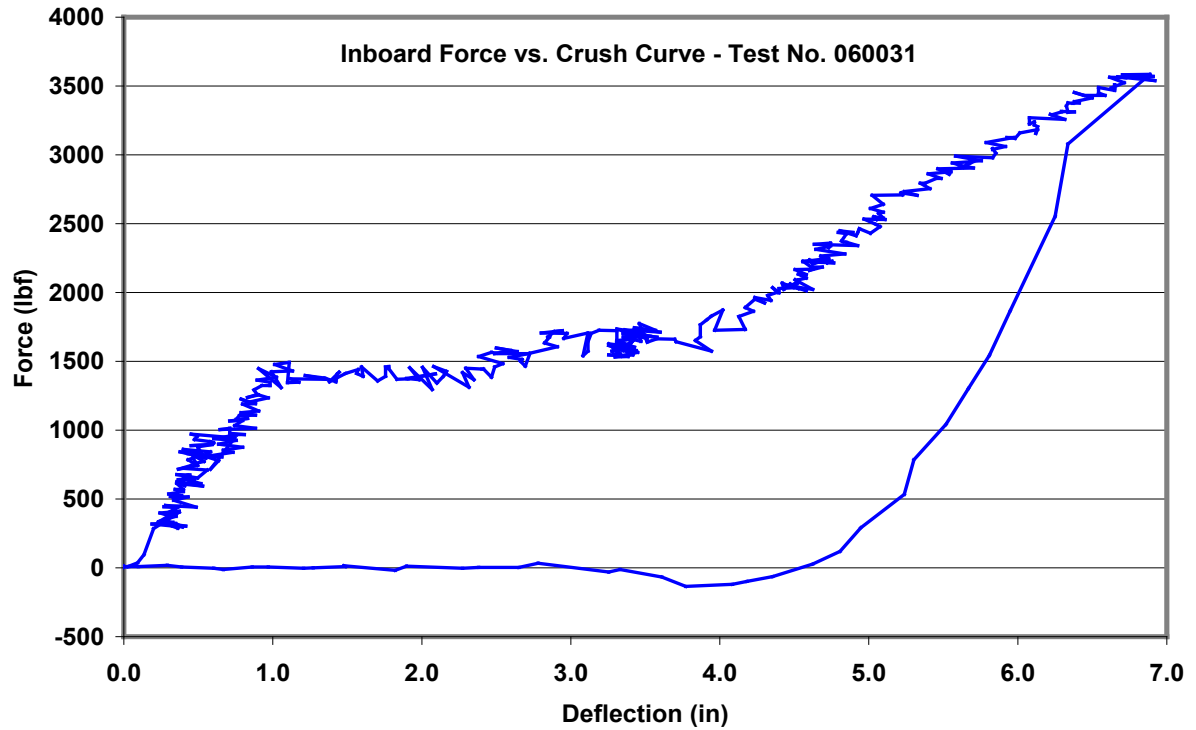


Figure 62. The Measured Table Force vs. Deflection Curves for the Inboard (above) and Outboard (below) Load Applicator Positions for the Horizontal Crush Test (Test No. 060031)

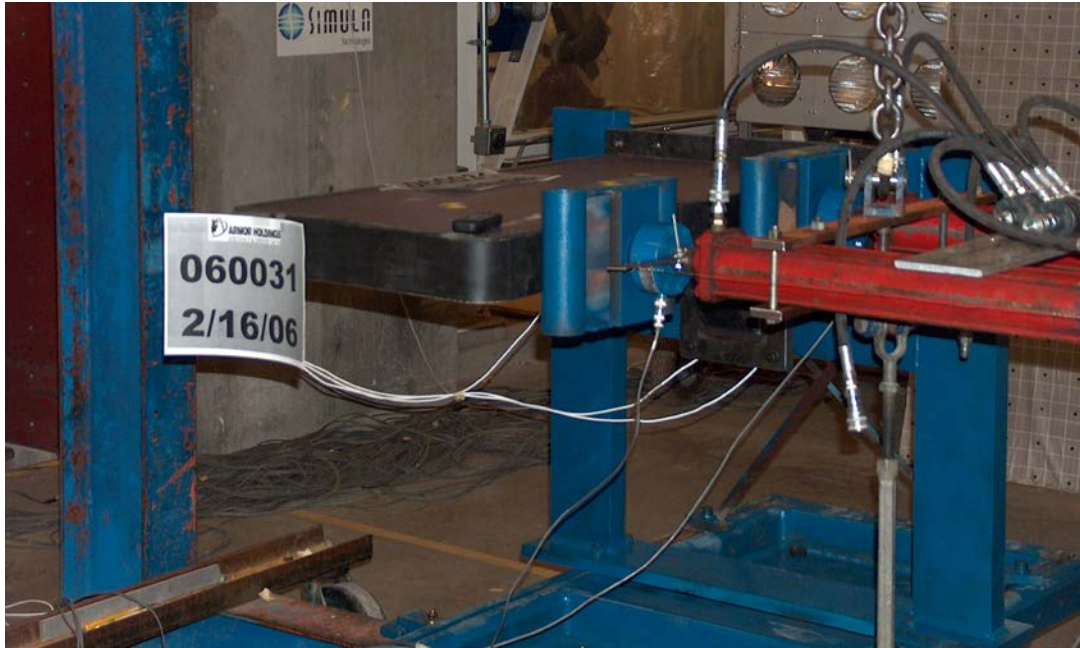


Figure 63. A Pretest Photograph Showing the Experimental Setup for the Horizontal Crush Test (Test No. 060031)



Figure 64. A Posttest Photograph of the Horizontal Crush Test (Test No. 060031)



Figure 65. A Posttest Photograph Showing the Crushed Honeycomb Core after the Horizontal Crush Test (Test No. 060031)

Test No. 060032 was repeated to determine how much more of the uncrushed honeycomb could be crushed once the honeycomb/melamine that had bonded to the I-beam flange had been removed. Before this repeat test was conducted, a portion of the melamine tabletop was removed near the center of the table. During the test, the remaining honeycomb did indeed crush further under the action of a load in each actuator that ramped up to approximately 3,300 lbf. Figure 66 compares the outcome of the crushed honeycomb after Test No. 060031 (before the melamine was removed) and after Test No. 060032 (after the melamine was removed). The inboard side of the table was crushed an additional 0.7 in (an increase in actuator displacement from 6.9 to 7.6 in), and the outboard side of the table was crushed an additional 1 in (an increase in actuator displacement from 7.8 to 8.8 in).

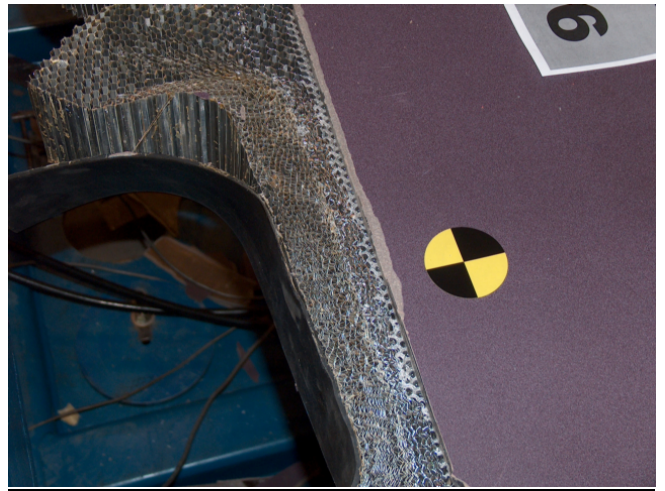


Figure 66. Posttest Photographs of Crushed Honeycomb Core after Test No. 060031 (left) and Test No. 060032 (right)

The results of this test show that some modifications to the procedure for bonding the melamine tabletop to the honeycomb core and the steel frame of the table were required. In fact, such changes were implemented shortly after these tests and, as evidenced by the successful performance of the table during the full-scale test, corrected the problem.

8. Table Design

As the table concept evolved, several important table components were designed, analyzed, and documented in detailed drawings. Some of the important design issues included:

1. The method of attachment to the rail car,
2. The design of the table structure to support the operational and impact loads,
3. The number of crush elements to be used in the table,
4. The method of attaching the honeycomb to the table structure, and
5. The method of attaching the tabletop to the table.

Each of these issues is discussed, in turn, in the following sections.

8.1 Table Attachment Method

As part of the concept generation task, operational discussions were held with rail industry representatives, including rail-car operators. These discussions highlighted the need for the table to minimize any impact on rail-car maintenance and cleaning. The discussions also identified the necessity to minimize any ingress or egress leg obstacles from the seated position as well as to maximize occupant comfort. With these issues in mind, the decision was made to cantilever the table from the wall of the vehicle. Through analyses, it was determined that a short, angled strut could be used to minimize the deflection of the aisle-side table edge when a 350-pound-force (1.56 kN) vertical force is applied near the edge. Care was taken in the design to ensure that the legs of the window-seated occupant would not impact the strut during a collision. Figure 67 shows the assembled crushable table and its mounting support brackets.

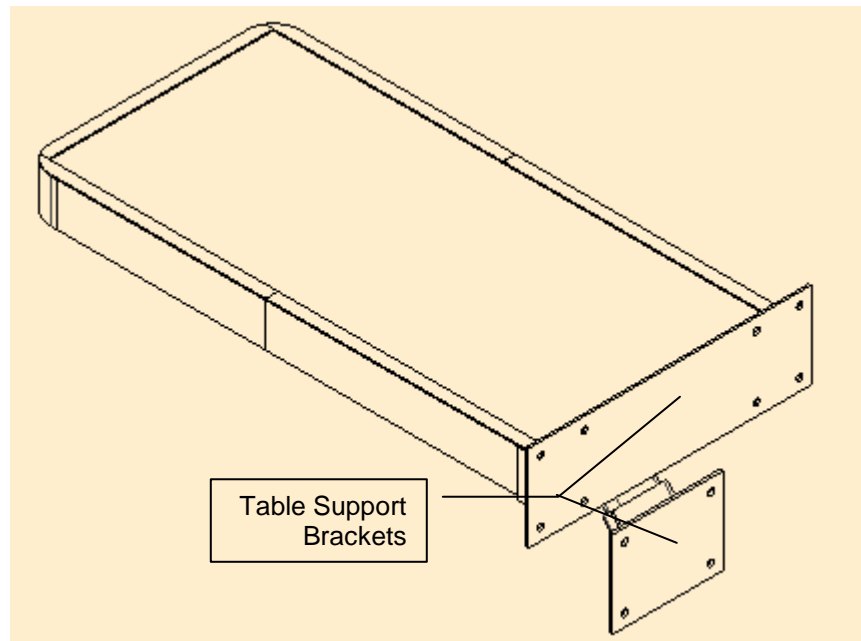


Figure 67. An Isometric View of the Crushable Table with Its Mounting Support Brackets

8.2 Table Frame and Structure

The table frame consists of a built-up I-beam made of A572 material with gussets at the aisle end and its mid-length. Figure 68 shows an exploded view of the components in the table. These gussets help to stabilize the I-beam flanges and provide pockets for the placement of the aluminum honeycomb elements. The I-beam structure is welded to a box beam, which sits in a mounting bracket. The welded structure, indicated as item 1 in Figure 68, was fastened to the mounting bracket by using two bolts on each side of the bracket (item 20) and four vertically oriented bolts (item 19). An angled strut, welded to the bottom of the I-beam, slides into and is bolted to the lower mounting support (item 3).

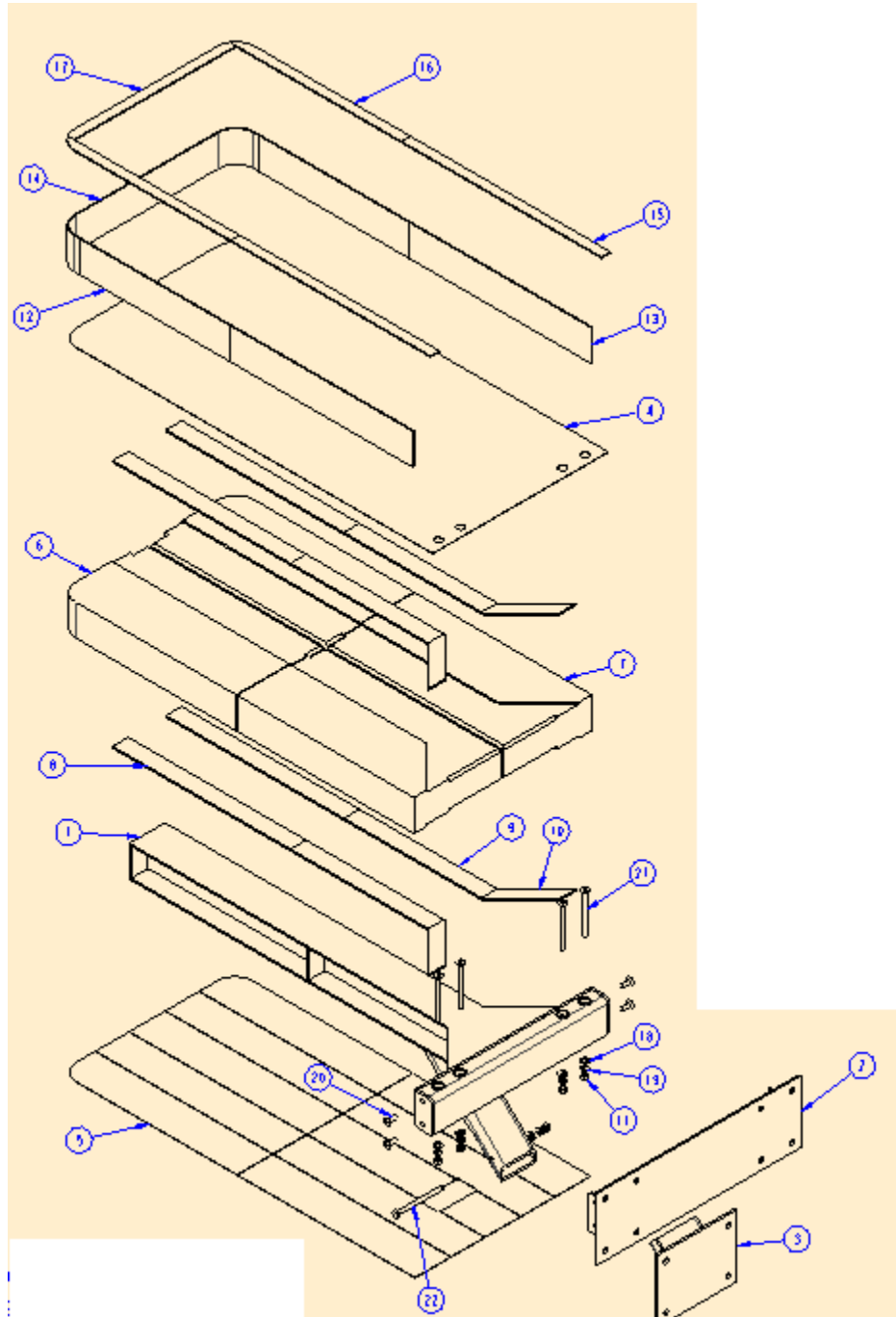


Figure 68. An Exploded View of the Crushable Table Showing all the Table Components

8.3 Table Crush Elements

Four aluminum honeycomb panels (items 6 and 7 in Figure 68) were used. Each honeycomb panel is designed to accommodate a seated 50th-percentile male occupant in a collision represented by an 8g, 250-millisecond triangular acceleration pulse. Component analyses and tests were performed to guide the selection of the number of honeycomb panels to be used on each side of the table. They are summarized in the test and analysis sections above (Sections 5

and 6). The number of panels per side that were investigated included one, two, and five. Results from the tests showed that as the honeycomb is crushed by an indenter that is not as wide as the panel, the material on either side of the impact area provides additional resistance to the crush. This resistance can increase the crush force beyond the desired level. Such behavior raises issues regarding the crush performance of the table when one person is seated. Figure 69 is an image from one of the tests showing the honeycomb material that was pulled in from the sides.



Figure 69. Results from a Crush Test Showing the Honeycomb Pulling in from the Sides during the Crush

To address this issue, a configuration with five panels was investigated. Although the crush results improved, the ability to meet the vertical operational load requirements for a table made up of smaller panels was a concern. Analyses showed that this configuration would not be able to meet the vertical load requirement of no permanent deformation greater than 0.050 in (1.1 mm) when a 350-pound-force load is placed at the edge of the table and removed.

The use of two aluminum honeycomb panels per side was then investigated. Analyses showed that this configuration would provide the required crush response and meet the operational load requirements. Subsequent quasi-static testing of the table showed that the assembled table meets the requirements.

The maximum allowable width of the table is 20 in. The selected design uses a stiff central beam that is not intended to crush. For this reason, the crushable material on each side of the table must be less than 10 in. The 60- to 70-percent crush efficiency of aluminum honeycomb provides 6–7 in of crush stroke.

8.4 Crush Element Attachment

The aluminum honeycomb is attached to the table by potting the honeycomb between the flanges of the I-beam with strong epoxy. The honeycomb surface is recessed by an amount equal to the thickness of the I-beam flange in the region where the honeycomb fits in between the flanges. This recessed area extends outward 2 in (51 mm) beyond the edge of the I-beam (see Figure 68, items 6 and 7). The extension of the recess allows the honeycomb that is just outside of the flanges to crush and not prematurely bottom out on the edge of the flanges. To maintain solid

and flat tabletop and bottom surfaces, hard rubber spacers were placed in the recessed areas next to the I-beam flange (items 9 and 10). The spacers were bonded to the underside of the melamine, and lift out of the way with the melamine as the table crushes. Figure 70 shows a photograph of the crush elements inserted into the I-beam; the recessed areas are evident in this photograph.



Figure 70. A Photograph of the Table Crush Elements Installed in the I-Beam Showing the Recessed Areas

8.5 Tabletop Attachment

The top and bottom surfaces were made of a 0.05-inch (1.2 mm)-thick melamine. Figure 71 shows a melamine table surface, prepared with rounded edges at the aisle end, and ready to be assembled to a table. Melamine is a stiff and fairly brittle material and will not deform in a controlled manner if struck on its edge. To help control its deformation while the table crushes, shallow grooves were placed on the backside of the melamine. Figure 72 shows an example of the grooves that were machined into the melamine. Two grooves were machined on each side of the longitudinal centerline of the table. These grooves are “triggers” that help the melamine to bend in an accordion manner as the table edge is crushed. Additional grooves were machined perpendicular to the existing grooves and on either side of the lateral center of the table. The grooves are used to allow the melamine to fracture in the direction of crush. These additional grooves are necessary to ensure that the table performs as designed if only one person is seated at the table. Figure 73 shows the locations of the final groove layout. The grooves in the photograph have been masked to shield them from the adhesive.



Figure 71. The Finished Surface (top side) of the Melamine Tabletop

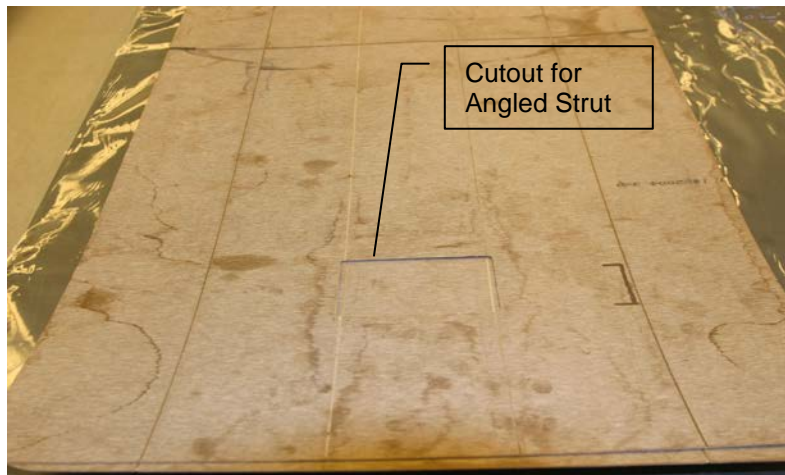


Figure 72. Examples of Grooves Machined into the Backside of the Melamine Sheets (note: the sheet for the bottom surface of the table is shown)

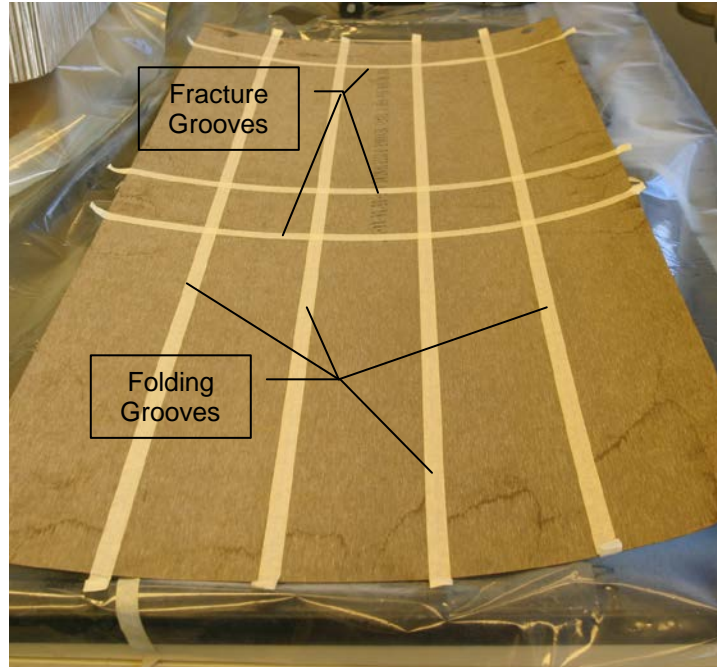


Figure 73. Locations of the Grooves that Are Cut into the Back Side of the Melamine

The melamine is bonded to the top and bottom surfaces of the assembled I-beam and honeycomb panels. A rectangular opening is cut into the bottom surface of the melamine to accommodate the angled strut (see Figure 72). A neoprene surface is bonded to the outside edge of the table to cushion and protect the occupant. Seams in the neoprene are arranged to allow it to deform and move with the outer edge while it crushes to continue to protect the abdomen and chest of the occupant. Neoprene strips bonded to the top surface of the tabletop to complete the marine edge. Figure 74 shows the fully assembled table.



Figure 74. An Assembled Table Showing the Neoprene Edge and Marine Guard

9. Fabrication

This section describes the processes used to fabricate the crushable workstation tables. All of the tables were fabricated at TIAX's facilities. Two tables were fabricated in preparation for the CEM train-to-train full-scale test. The remaining two tables were fabricated to be tested in the planned quasi-tests (discussed in Section 7) and sled test.

9.1 Fabrication Process

Four tables were fabricated as part of this project. The tables were designated A, B, C, and D, based on the order that they were fabricated. TIAX fabricated the tables and shipped one of them (Table A) to Simula in Phoenix, AZ, for quasi-static testing. Tables B and C were sent to TTC in Pueblo, CO, for integration into the CEM cars for full-scale testing, and Table D was sent to Metrolink in Los Angeles, CA, at the request of the Volpe Center. The general sequence of fabrication was as follows:

- 1) Plate and bent steel parts were ordered from the material vendor.
- 2) Honeycomb, melamine, fasteners, and other fabrication materials were ordered from various vendors.
- 3) The steel parts were then machined as required and welded together into an I-beam structure.
- 4) All of the welds were examined by a certified welding inspector.
- 5) The honeycomb was potted into the I-beam structure and the finishing surfaces were added.
- 6) Periodic inspections were made throughout the fabrication process.

A572-65 steel was chosen as the primary material of construction for the I-beam and other structural elements. It is commonly used in the construction of rail vehicles for operation in North America. The material was obtained in 0.188-inch (4.8 mm) and 0.25-inch (6.4 mm) thicknesses. Table 13 lists the average values for the measured material properties for the A572-65 material used to construct the table frames. These averages are based on data from material certifications that were obtained for all structural materials used in the table.

Table 13. Average Mechanical Properties for the A572-65 Steel Used to Fabricate the Table Frame Structure

Property	Average Value
Yield strength	76,500 psi (527 MPa)
Tensile strength	91,400 psi (630 MPa)
Elongation (in 2 in)	24%

The minimum required yield strength for this material is 65,000 psi (448 MPa). As is typical, the properties of the actual material are significantly greater than the minimum material specification.

All required welding was carried out by using the tungsten inert gas process following the requirements of AWS D1.1. The welds were inspected by a certified welding inspector from Artisan Industries, Inc., in Waltham, MA. Figure 75 shows one of the table I-beams during welding.

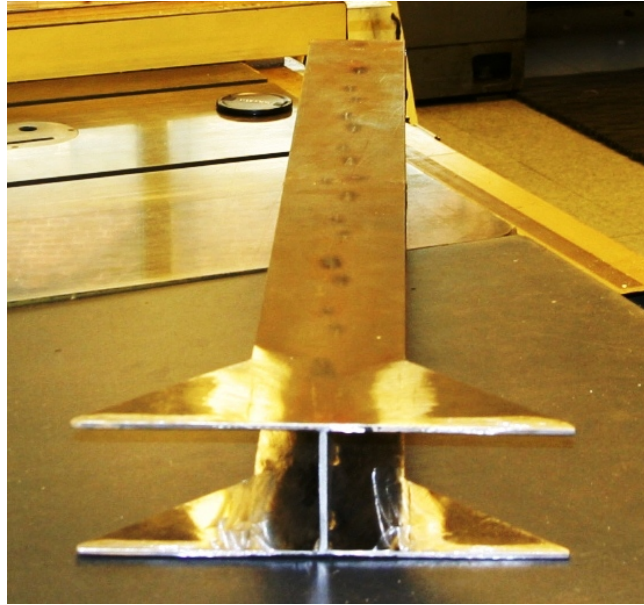


Figure 75. A Welded I-Beam before Being Welded to the Box Beam

9.1.1 Honeycomb Panel Preparation and Installation

The aluminum honeycomb material was manufactured by Hexcel. It was 3.5-inch (89 mm) thick and designated as DC 7.9-1/4-.004-N 5052 H39. Four honeycomb panels were cut to size and machined with recessed regions for insertion into the I-beam. The two panels on the aisle end were shaped differently than the two at the window end of the table. The panels at the window end of the table were rectangular. The aisle-side panels had rounded corners at the aisle end of the table so that no sharp corners could cause injuries. A check-fit of the honeycomb into the I-beam was made to verify that the pieces were compatible. The honeycomb was then removed, and the box beam and angled strut were welded onto the I-beam. Figure 76 shows the final weldment of the structural frame for Table A and its check-fit with the mounting brackets.



Figure 76. The Finished Weldment for Table A Installed in the Mounting Brackets

The honeycomb was inserted into and potted to the I-beam using a two-part epoxy of Epon Resin 815C and Epicure Curing Agent 3282. Each side of the table was installed and cured separately. The honeycomb panels were clamped to flat boards and cured overnight to ensure flatness and uniformity of the table. Figure 77 shows the second side of Table A prepared for curing. Note the small sample cure cup in the foreground, which was used to help verify that the cure process was complete.

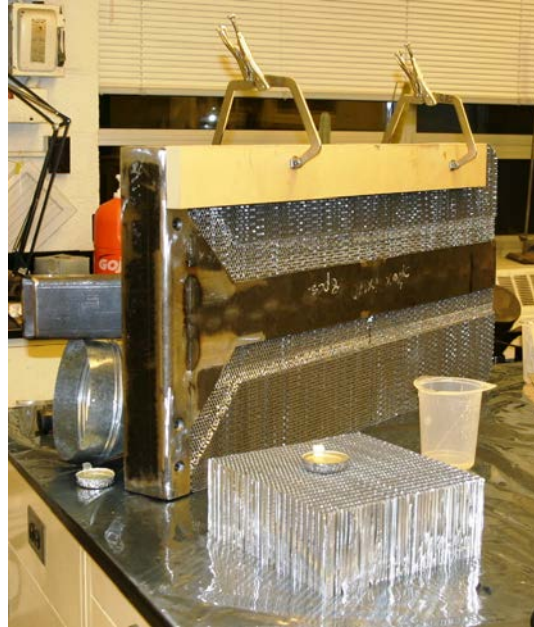


Figure 77. The Second Side of Table A Is Prepared for Curing

9.1.2 *Tabletop Attachment*

After the honeycomb panels were inserted, the melamine tabletop was attached. The melamine sheet was prepared with grooves to promote fracture at specific locations. The preliminary design called for the melamine to be epoxied to the table frame and to several polycarbonate spacers and only contact-cemented to the honeycomb. The contact cement used was Wilsonart 600. Figure 78 shows the melamine and table prepared for bonding.



Figure 78. A Melamine Sheet Prepared for Bonding to the Frame and Honeycomb Inserts for Table A

9.1.3 Tabletop Attachment Modifications

A quasi-static crush test of Table A was conducted to evaluate its force/crush performance (see Section 7). During the test, it was discovered that epoxy had seeped around the I-beam flange and had bonded the honeycomb and the spacer to the edge of the flange. This had the effect of reducing the effective crush distance of the honeycomb, because none of the honeycomb inside the I-beam could crush. Because of these results, the method for bonding the melamine to the top and bottom surfaces of the table was modified. The epoxy and contact cement were replaced by 3M™ Super 77, a spray-on contact cement. The groove locations were masked on both the melamine (Figure 79) and the honeycomb during lamination (Figure 80).

The quasi-static test showed that the melamine surfaces did not perform as expected, based on the component testing. Four grooves had been placed in the backside of the melamine surface in the long direction of the table (window to aisle direction), two on each side of the table (refer to Figure 79). These grooves are intended to allow the melamine to bend in an accordion fashion while the table edge crushes. The original groove depth was 0.015 in (0.4 mm). The quasi-static results suggested that the bend points needed to be weaker. The depth of the grooves was increased to approximately 0.020 in (0.5 mm), about half the thickness of the melamine, following some additional component testing. The depth of the grooves was limited because melamine is brittle and can break easily during handling and assembly if the grooves were too deep. Deeper grooves could also be seen from the top surface, which was generally undesirable. Figure 79 shows the revised groove pattern on the melamine.



Figure 79. The Underside of the Melamine Top with the Revised Groove Pattern Masked in Preparation of Spraying the Contact Cement

The design included two transverse grooves to help control the fracture of the melamine in the crush direction. These grooves had the same depth as the previously mentioned grooves. One groove was located at the window side of the table at the interface between the box beam and the honeycomb. The second groove was placed midway between the seated locations. During the quasi-static test, it became apparent that the groove pattern located between the occupants needed to be revised to ensure that the melamine would fracture in a controlled manner. Two

grooves replaced the single center groove (see Figure 79), moving the break line closer to the impact region for each seated occupant.

During the quasi-static test, the plastic spacer used to support the top surface in the area of the recessed honeycomb, near the I-beam, became trapped between the impactor and the I-beam flange (see Figure 80 for spacer location). It appears that this entrapment was caused by the epoxy issue mentioned above, not the plastic spacer itself. As a precaution, the plastic spacer was replaced by a neoprene rubber spacer in case it should become trapped in a similar manner. The neoprene rubber spacer is strong enough to support the melamine above during normal operation while flexible enough to bend and move out of the way during crush of the table edge. Figure 80 shows the neoprene spacers in place before the attachment of the melamine.

Revising the bonding method, depth and location of the grooves, and the spacer material helps ensure that the honeycomb will be free to crush inside the I-beam, and the melamine will fracture and bend at the prescribed locations. Tables B, C, and D were fabricated with the modifications to the grooves and the revised bonding method.



Figure 80. The Tabletop following the Spraying of the Contact Cement in the Revised Lamination Process—the Neoprene Spacers Are in Place

While the adhesive between the melamine tabletop and the honeycomb cured, the flatness of the table was maintained by weighing it down on a foam slab (see background of Figure 80). This method allowed for a constant and uniform pressure to be applied on the table surface while the adhesives set.

9.1.4 Tabletop Edges

The table edges were finished with sections of neoprene cut to fit and contact-cemented to the honeycomb edges. The rough honeycomb edges were prepared by bending the loose edges of the partial honeycomb cells at the surface of the honeycomb blocks to make the surface as flat as possible for good contact. Neoprene pieces were cemented to the tabletop to form a marine edge. Figure 81 shows a finished prototype crushable workstation table.



Figure 81. A Finished Prototype Crushable Workstation Table

9.2 Shipping

Shipping crates were fabricated to specification by Horn International Packaging to protect the tables and ensure safe delivery. These crates were made of wood with foam interior supports, which protected the tables from being damaged during shipping.

10. Summary and Conclusions

This project focused on the design, analysis, fabrication, and testing of a crushable workstation table for rail passenger cars to reduce the injury risk to occupants seated at the table during an inline collision. The workstation table design was required to reduce the forces and accelerations imparted on the occupants while ensuring that compartmentalization is maintained for an 8g collision scenario, thus reducing the likelihood of severe injury. This effort included the analysis of several design concepts; the method most likely to achieve these requirements was chosen to be a table that dissipates energy by plastically deforming or crushing. In addition to the crashworthiness requirements of the table, the design was also required to meet typical table operational loads.

A requirements document was drafted, based on the information included in the request for proposal. It was based on Federal regulations and industry standards. The requirements document was extended and refined during the project. The document covers operational, collision-specific, test, and manufacturing requirements.

A review of existing and planned table designs that incorporate energy absorbing strategies was performed. Industry contacts were surveyed to obtain information about existing and planned tables in rail passenger cars. None of the information received included tables with the ability to crush and absorb energy.

A crushable table was designed that could absorb the secondary impact energy of seated occupants and compartmentalize those occupants to reduce injury risk compared with existing table designs. Several table concepts were generated, evaluated, and screened. This resulted in three concepts suggested for further evaluation, and the crushable edge concept was selected for development. Large deformation finite element analyses were performed to help guide the selection of the concept as well as to inform the design. Component analyses of the crushable table elements were performed to define the crush response in the honeycomb used for the table. Component testing was performed to help refine the model and verify the analysis results. The analyses also helped to establish that the overall strength of the table design, including the I-beam backbone that runs down its center and the mounting arrangement, would meet the requirements that were placed upon it. Component testing was also performed on the tabletop material to define bonding arrangements and methods to make the material fold at specified locations so that it would not hinder the crush of the table. The response of the table, characterized by a force/crush curve, was extracted from the finite element analyses and used in occupant simulation analyses.

MADYMO was used to predict the injury risk to occupants seated at the table during a collision. The force/crush response of the table was used in the model to simulate the crushing of the table edge during occupant impact as a result of an applied acceleration pulse. Two acceleration scenarios were analyzed. One scenario involved the industry standard 8g, 250-millisecond triangular pulse. The second involved applying the acceleration from a previously conducted collision dynamics simulation of the upcoming full-scale CEM train-to-train test. The results from the simulation of the 8g acceleration pulse condition were used to determine whether the table design would yield results below the required injury assessment reference values before table fabrication and testing in the CEM full-scale train-to-train test.

The first prototype table was fabricated and prepared for quasi-static testing. Tests were performed to show that the table design met the operational requirements. In addition, destructive crush tests were performed to obtain the actual force/crush response of the table and to show the mounting arrangement met the requirements. During the crush test, it was determined that the fabrication process had allowed the honeycomb to bond to the flange of the I-beam. This inadvertently limited the amount of crush of the table as well as the amount of energy absorbed. These results highlighted a needed change in the fabrication process, which was implemented during the construction of the subsequent three tables. These changes enabled the two tables that were included in experiments on the March 23, 2006, CEM train-to-train test to perform as designed. Evaluation of the results of the table experiments in the CEM train-to-train test showed that the table met the IARV requirements set for the improved table design. Detailed results from the CEM train-to-train test and table experiments can be found in References 8, 9, and 10. Because the table met the IARV requirements in the severe occupant environment in the CEM full-scale test, it was assumed that the IARV requirements would also be met in the less severe occupant environment represented by the 8g, 250-millisecond triangular acceleration pulse. Therefore, it was determined that the sled test was not necessary.

11. References

1. National Transportation Safety Board. (2002). *Collision of Burlington Northern Santa Fe freight train with Metrolink passenger train, Placentia, California, April 23, 2002* (Railroad Accident Report NTSB/RAR-03-04) (adopted on October 7, 2003). Washington, DC: National Transportation Safety Board.
2. Parent, D., Tyrell, D., and Perlman, A.B. (2004). Crashworthiness analysis of the Placentia, CA, rail collision. *International Journal of Crashworthiness*, 9(5), 527–534.
3. Code of Federal Regulations, Title 49, Part 238, Passenger Equipment Safety Standards, Section 233: Interior Fittings and Surfaces (2005).
4. United Kingdom Association of Train Operating Companies Vehicles Standard: AV/ST9001.10: Fixed Tables.
5. Code of Federal Regulations, Title 49, Part 571, TBD, Section 208: Occupant Crash Protection.
6. Martinez, E., Tyrell, D., Perlman, and A. B. (2004 Nov.). *Development of crash energy management designs for existing passenger rail vehicles* (Paper No. IMECE2004-61601). New York: American Society of Mechanical Engineers.
7. Parent, D., Tyrell, D., Perlman, A. B., and Matthews, P. (2005). Evaluating Abdominal Injuries in Workstation Table Impacts,” Transportation Research Board 84th Annual Meeting, Paper No. 05-1348, Washington, D.C., January 9–13, 2005.
8. Rancatore, B., Llana, P., Van Ingen-Dunn, C., and Bradney, C. (2009 July). *Occupant protection experiments in support of a full-scale train-to-train crash energy management equipment collision test* (U.S. Department of Transportation Report No. DOT/FRA/ORD-09/14). Washington, DC: Federal Railroad Administration, Office of Research and Development.
9. Severson, K., and Parent, D. (2006 Nov.). *Train-to-train impact test of crash energy management passenger rail equipment: Occupant experiments* (Paper No. IMECE2006-14420). New York: American Society of Mechanical Engineers.
10. Tyrell, D., Jacobsen, K., and Martinez, E. (2006 Nov.). *A train-to-train impact test of crash energy management passenger rail equipment: Structural results* (Paper No. IMECE2006-13597). New York: American Society of Mechanical Engineers.

Appendix A

Workstation Table Design Requirements

A.1. Introduction

The workstation table described in this report was developed in accordance with the requirements described in Appendix A.

A.1.1 Purpose

The purpose of this specification is to define the requirements for a fixed workstation table to be installed between facing seats on a rail passenger vehicle.

A.1.2 Definitions

- a) **Facing seats**—passenger rail seats that occur in pairs where two passengers are facing forward and two passengers are facing backward. These are often referred to as “open bay seats” when a workstation table is not present.
- b) **Workstation table**—the interior fixture that is installed between facing-seat configurations in rail passenger cars. Current workstation tables feature a rigid tabletop that is attached to the wall with an L-bracket and a rigid leg that is attached by screws to the tabletop and bolted to the floor seat rail.
- c) **Longitudinal**—the direction in a horizontal plane parallel to the tracks and/or seat rails.
- d) **Lateral**—the direction in a horizontal plane perpendicular to the tracks and/or seat rails.
- e) **Compartmentalization**—a seat design strategy that can be adapted for workstation table design in which the table provides a means to absorb all or a substantial portion of the kinetic energy of a passenger, thus preventing a tertiary impact. An occupant is compartmentalized when the torso is confined within the perimeter defined by the front edge of the workstation table, the full width of the seat, and the seat back surface of the launch seat.
- f) **Ingress/egress space**—space available for passengers to enter or leave an occupant space. This has importance for both normal passenger seating and also for emergency exit considerations.
- g) **Secondary impact**—during a crash, secondary impact refers to the impact of passengers with fixtures in the car or other passengers.
- h) **Tertiary impact**—passengers who have undergone a secondary impact and continue to move, impacting another object in the car.

A.2. Reference Documents/Drawings

A.2.1 Standards

A.2.1.1 Code of Federal Regulations, Title 49, Part 238, Section 233: Interior Fittings and Surfaces

A.2.1.2 Code of Federal Regulations, Title 49, Part 571, Section 208: Occupant Crash Protection

A.2.1.3 UK ATOC Vehicles Standard AV/ST9001.10: Fixed Tables

A.3. General Description

Workstation tables have been identified as a safety concern in passenger rail collisions. This document specifies the requirements for an improved workstation table that mitigates the risk of thoracic and abdominal injury. Four tables will be fabricated to these requirements. One table will be destructively tested in a quasi-static load case, another will be included on a dynamic sled test, and two will be included in the CEM train-to-train full-scale impact test. Each dynamic test will include ATDs capable of measuring the displacement-time history of the abdomen at the location of the table impact. The table will be instrumented to measure the load-time history of the table-abdomen interaction. The measured abdominal compression and load will form the basis for evaluating the crashworthiness performance of the improved workstation table.

The requirements listed here are derived from industry and Federal requirements. These requirements are contained in the 49 CFR 49, Part 238, Section 233 and the UK ATOC Vehicles Standard AV/ST9001.10. Maximum injury criteria values are derived from 49 CFR Part 571, Section 208.

A.4. Specific Requirements

The requirements are divided into three major sections:

1. Requirements specific to the attachment of the table to the carbody,
2. Requirements specific to the table edge impact response, and
3. Performance requirements for dynamic sled testing.

A.4.1 Table Attachment Requirements

A.4.1.1 Attachment Points

The table shall be attached to an existing passenger car by way of seat rails on the floor and/or wall of the carbody. These attachments shall be located so that occupant ingress or egress is not impacted.

A.4.1.2 Mounting Hardware

The hardware used to attach the table to the carbody shall not require modification of the seat rails. This mounting hardware shall conform to 49 CFR Part 238, Section 233, Article (d): “To the extent possible, all interior fittings in a passenger car, except seats, shall be recessed or flush-mounted.”

A.4.1.3 Strength under Service Loads

The table attachments to the floor and/or wall must not experience significant permanent deformation under a quasi-static horizontal load of 500 lbf (2,225 N) applied on a minimum 8-inch (+0.5/-0.0 in) by 3.5-inch area in a longitudinal direction at the aisle-side edge of the tabletop. The test for this load can be combined with the test described in A.4.2.2 (b).

A.4.1.4 Collision Strength

The table attachments to the floor and/or wall must not experience permanent deformation under loading imparted from two 50th-percentile male occupants subjected to an 8g peak, 250-millisecond duration triangular acceleration pulse.

A.4.2 Table Edge Requirements

A.4.2.1 Geometry

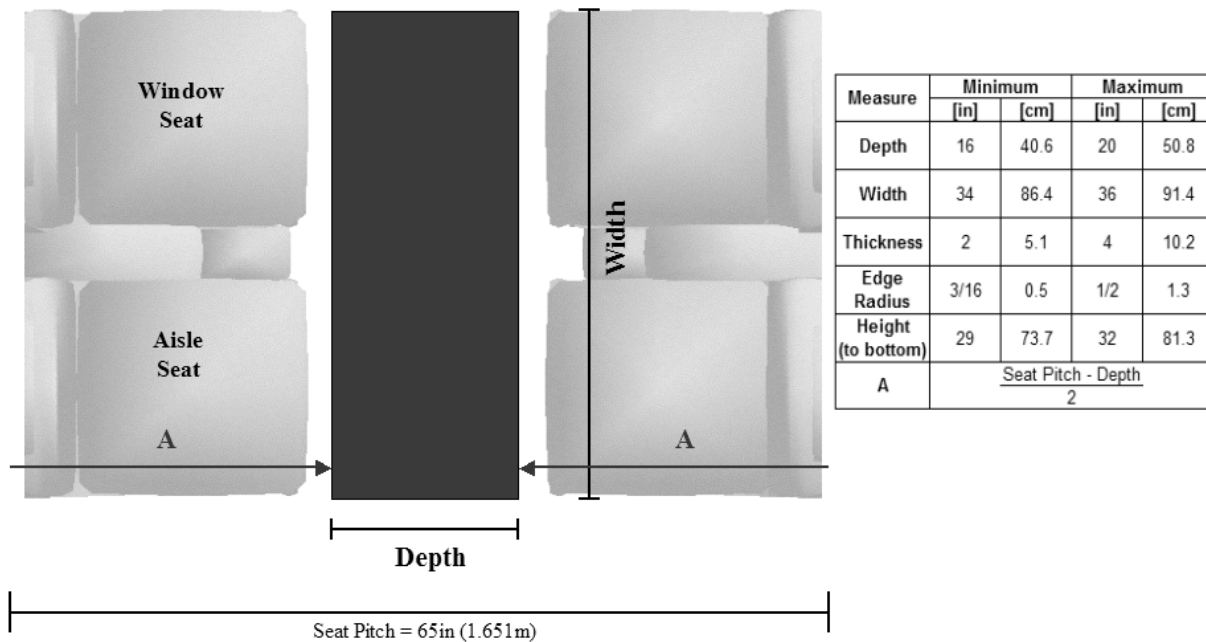


Figure A1. Requirements for Various Geometric Features of the Workstation Table

The table edge shall be a minimum of 2 in (5 cm) in thickness. The corners of the table edge shall be rounded to a minimum radius of 3/16 in (0.5 cm). The table shall be at least 16 in (40.5 cm) but no more than 20 in (51 cm) in depth. The bottom of the table shall be more than 28 in (73.7 cm) but no more than 32 in (81.3 cm) from the floor. The table shall be centered between the facing seats and shall span the entire width of both the aisle and window seats. The top of the table shall be level and continuous.

No part of the table shall occupy the space necessary for an occupant to be seated at any of the seats surrounding the table. The diagram below shows the specific areas that the table may not occupy.

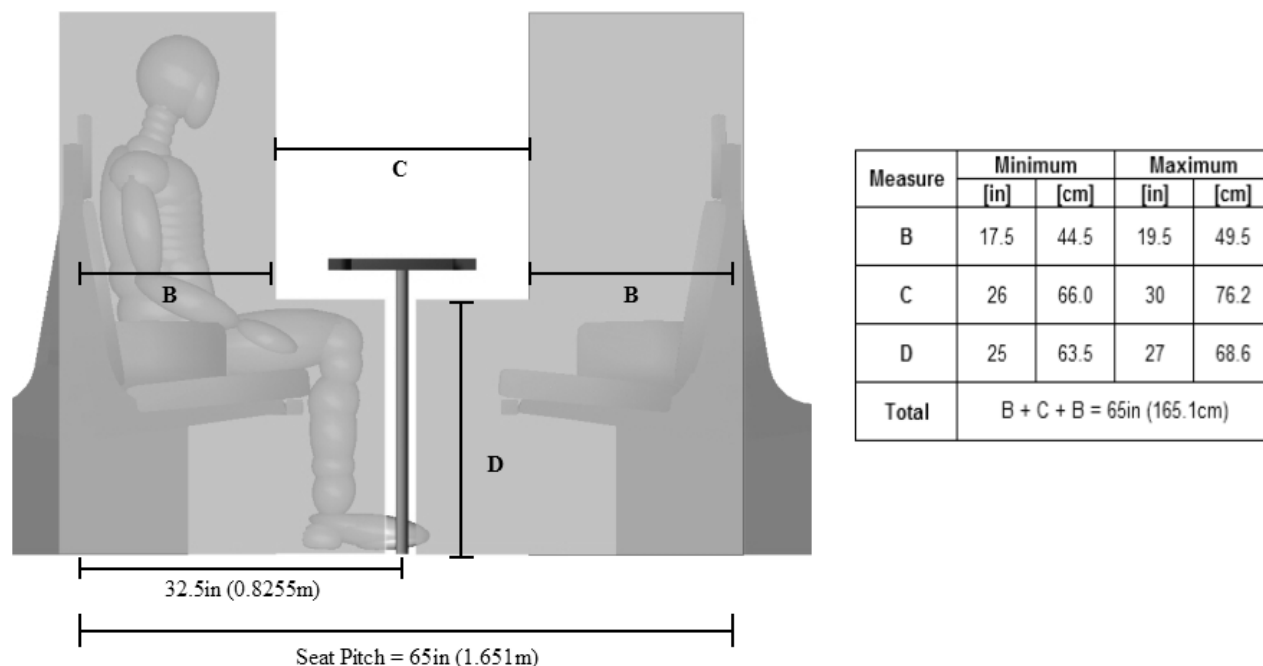


Figure A2. Space Required for Occupant Seating Surrounding the Workstation Table

(The table shall not interfere with the highlighted areas, for which the dimensions are shown in the adjacent table.)

A.4.2.2 Strength under Service Loads

The table edge shall not experience permanent deformation under the following individually applied load conditions:

- a) Minimum 350 lbf (1,555 N) applied on a 5- by 5-inch area (± 0.5 in, in either direction) in a vertical direction at any point on the top of the table.
- b) Minimum 500 lbf (2,225 N) applied on a minimum 8-inch ($+0.5/-0.0$ in) by 3.5-inch area loaded in a longitudinal direction at any point on the table edge.

A.4.2.3 Collision Strength

The edge of the table shall crush no more than half the depth of the table. Upon collision, the table shall not intrude upon the space of the facing occupant so as to prevent the facing occupants' egress. The peak force at the table edge during this crush shall not exceed 2,200 lbf (9,700 N). The minimum force at which crush is initiated shall be 750 lbf (4,400 N). During and upon the completion of crush, the table shall compartmentalize the seated occupants facing the direction of the collision.

A.4.3 Table Performance Requirements

A.4.3.1 Collision Conditions

The improved workstation table shall meet the Table Performance (A.4.3.2) and Occupant Response (A.4.3.3) requirements for both ideal and nonideal collision cases.

A.4.3.1.1 Ideal Collision Case

The ideal collision conditions are defined by the following specifications. These specifications apply to the dynamic sled testing of the improved workstation table.

- a. Facing seats shall match the seats tested in the CEM two-car full-scale test [1].
- b. The seat pitch shall be 65 in (1.651 m).
- c. A prototype workstation table will be installed between the facing seats as intended by its design.
- d. The acceleration applied to the sled shall be an 8g peak, 250-millisecond duration triangular pulse.
- e. Two ATDs shall be seated behind the workstation table, facing the collision. At least one of these ATDs shall be capable of measuring the abdominal displacement-time history (i.e. Hybrid 3RS or THOR). If only one ATD is capable of measuring the displacement-time history, the second ATD shall be a 50th-percentile Hybrid III ATD, placed in the seat nearest the side wall. Both ATDs shall be seated so that their feet are flat on the floor, their lower and upper legs are parallel to each other and the knee joints are oriented at as close to a 90-degree angle as the seat geometry allows, and their back is resting against the back of the seat.
- f. The time history of the force applied to the table by the ATD shall be recorded.
- g. 49 CFR Part 238, Section 233, Article (g): "...the seat structure and seat attachment to the sled that is used in such testing must be representative of the actual seat structure in, and seat attachment to, the rail vehicle subject to the requirements of this section. If the attachment strength of any other interior fitting is to be demonstrated through sled testing, for purposes of showing compliance with the requirements of this section, such testing shall be conducted in a similar manner."

A.4.3.1.2 Nonideal Cases

The nonideal collision conditions are defined below by how they differ from the ideal collision specifications. These test cases are to be evaluated individually.

A.4.3.1.2.1 One Occupant, Center

One THOR ATD shall be seated behind the table directly between the window and the aisle seats, facing the collision. If an armrest is present, it is to be removed for the test.

A.4.3.2 Table Performance

The crush/displacement of the table edge shall occur in a controlled fashion in the longitudinal direction. The table shall conform to ATOC AV/ST9001.10.2: "...the table shall display post-yield plasticity and fail in a manner which is not likely to cause injury." The crush of the table edge shall not present any sharp edges or pinch space that the occupant is at risk of coming into contact with. The crushing of the table edge shall not impart lateral motion to the occupants and shall only impart vertical motion that is beneficial to the occupants (i.e., preventing head impacts with the top of the table). No part of the table shall enter the space of the facing occupant as shown in section A.4.2.1, so as to allow the facing occupant the ability to egress.

A.4.3.3 Occupant Response

In a dynamic sled test conducted to the specifications of Section A.4.3.1, both of the ATDs shall be compartmentalized. Successful compartmentalization requires that the resting position of the ATD after the impact be between the initial seating position and the workstation table. The head, torso, or arms of either ATD shall not impact the seats opposite the table. The injury measurements taken by both of the ATDs must meet the following criteria:

- a) HIC15 must not exceed 700;
- b) N_{ij} must not exceed 1.0;
- c) Neck tension must not exceed 937.5 lbf (4,170 N);
- d) Chest deceleration must not exceed 30g, except for intervals whose cumulative duration is not more than 3 ms;
- e) Chest compression must not exceed 2.36 in (60 mm);
- f) Chest Viscous Criterion must not exceed 2.62 ft/s (0.8 m/s);
 - 1. (e) and (f) measured at the sternum, and
 - 2. (f) calculated using torso depth of 0.229 m, scale factor of 1.3;
- g) Abdominal compression must not exceed 2.75 in (70 mm);
- h) Upper Abdominal Viscous Criterion must not exceed 4.10 ft/s (1.25 m/s);
 - 1. (g) and (h) measured at the upper abdomen/lower CRUX of the THOR,
 - 2. (g) and (h) measured at the lower CRUX of the Hybrid 3RS, and
 - 3. (f) calculated using torso depth of 0.229m, scale factor of 1.3.

A.4.4 Table Fabrication Requirements

A.4.4.1 General

The design shall utilize materials and fabrication methods that a typical metal fabrication company could use.

A.4.4.2 Materials and Workmanship

The materials shall meet the requirements given in CFR Part 238, Appendix B. The table shall be free of protrusions, sharp edges, or corners that could cause injury or catch or damage the clothing of passengers or crew members. The use of exposed fasteners shall be minimized.

A.4.4.3 Safety Requirements

The materials used to achieve the table performance requirements shall be resistant to smoke and flammability.

Materials shall be nontoxic and shall not off-gas harmful vapor or unpleasant odors.

A.4.4.4 Maintainability Requirements

The service life of the tables shall reflect the average time to rebuild a passenger rail car, which is 8–12 years. Other than cleaning, the tables shall not require periodic inspection, testing, or adjustments during the service life.

Surfaces shall be scratch-resistant and smooth and can be wiped clean with typical cleaning products. Materials that require painting for a finish are undesirable, because they may chip and require touch up or repainting on a scheduled basis.

A.4.4.5 Drawings

To fabricate the tables, best-practice manufacturing techniques shall be used and documented. Drawings shall be provided to describe the parts, assemblies, and processes required. The drawings shall, as a minimum, include the following:

- Overall dimensions and tolerances of the table assembly;
- Mounting requirements, including hole sizes, recommended bolt sizes, torque requirements, and recommended grade of bolts, to be used for mounting; and
- Description of materials.

Appendix B

Review of Existing Workstation Table Designs

Table B1. Industry Contact List

Name	Company	Phone	Email	Notes
Railcar Manufacturers				
Gord Campbell	LDK, Canada (for Bombardier)	(905) 577-1052	gcampbell@ldkeng.com	Described design changes made to Metrolink table to improve structural strength.
Ned Parker	Colorado Railcar, CO	(303) 670-1585 x305	ned.parker@coloradorailcar.com	Colorado Railcar makes two types of tables (visit to facility produced photos).
Neil Harwood, Chief Engineer	Alstom		Neil.harwood@transport.alstom.com	Designer and manufacturer of new high-speed Pendolino trainsets used by Virgin Trains on UK's West Coast Main Line. Referenced SMTC as their table manufacturer.
Ralph Dolinger (Steve Roman)	LTK	(215) 542-0700	rdolinger@ltk.com	Provided general information about workstation tables
Blair Slaughter	Amtrak	(302) 661-6952 (302) 463-6191 (cell)	slaughb@amtrak.com	Described Acela's tables
Pat Malin	Amtrak	(215) 349-3815	malinp@amtrak.com	Details on Acela tables (provided drawings).
Andre Gagne	Bombardier	(802) 479-1021		Details on Acela table
European Leasing Companies (TLC)				
Barrie Cottam, Engineering Manager– Fleet	Metronet BCV, Ltd., UK		Barrie.Cottam@metronetbcv.com	Tables they use are designed and approved to a UK Code of Practice; referenced Compin and Winstanley as table manufacturers.
European Operating Companies (TOC)				
Clive Burrows, Director of Engineering	First Group, UK	011-44-17 9349 9423 011-44-78 6049 4931	Clive.burrows@firstgroup.com	European carrier. Operate trains, buses, etc. Owns number of train companies.
Jim Lupton, Head of Engineering and Research	Rail Safety and Standards Board (RSSB)	011-44-20 7554 4611 011-44-78 7687 8800 (cell)	Jim.lupton@rssb.co.uk	Referenced research program that the RSSB is conducting with AEA Technology and in collaboration with the FRA/Volpe.
Roy Windle	AEA Technology Rail (AEAT)	011-44-870 190 1322	Roy_windle@uk.aeat.com	Consultants contracted by RSSB to design crashworthy workstation tables.
John Benyon	AEAT	011-44-870 190 1293	John.benyon@aeat.co.uk	Contacted via Web site www.aeat.co.uk/rail/ .

Table B1. Industry Contact List (continued)

Name	Company	Phone	Email	Notes
David Sawyer, Engineering Director	South West Trains, UK	011-44-20 7620 5847	d.sawyer@swtrains.co.uk	European carrier; TBD
Interior Fitting Supply Companies				
Terry Soesbee, President	RailPlan International, Baltimore, MD	(410) 947-5900	tsoesbee@railplan.com	Rail car table supplier; offered to peer review table design concept(s).
Emmit Lonergan	Frank Ralphs, Buffalo, NY	(716) 549-7997	Lonergan@frankralphs.com	Rail car table supplier; provided information about table construction and attachment.
Morley Smith	GSM Design	(450) 435-4646		TBD
Gilles Le Masson	SMTc, France		lemasson@smtc.fr	Composite specialists and supplier of Pendolino tables for Alstom; they have designed a table per the UK standard; it does not feature a crushable edge, but rather energy absorption at the attachments.
Ken Ullman, Engineering	Cattco USA	(716) 257-3475 x239	Ken.ullman@cattcousa.com	Manufactured tabletop for Acela.
Claude Martin Engineering Director	Compin	33 (0)2 32 33 92 31	cmartin@compin.com	Compin does not supply tables; they supply commuter seats.

Table B2. Table Characterizations

Geometry	<ul style="list-style-type: none"> ▪ Rectangular in shape with a taper at the aisle side to make passenger ingress/egress easier, shaped “like an ironing board” (RailPlan, Colorado Railcar). ▪ Rectangular in shape with rounded ends at the aisle (SMTC). ▪ Traditional Amtrak—tables were plywood-based laminate with bull-nose edge, 1.5 in thick (used as dining and lounge tables). ▪ Acela table has a folding, hinged leaf along each long side of the table that folds upon itself; table dimensions varied depending on location (four varieties)
Table length	<ul style="list-style-type: none"> ▪ Extends to the middle of the aisle seat (Metrolink). ▪ Extends to the aisle side armrest of the aisle seat (Colorado Railcar).
Construction	<ul style="list-style-type: none"> ▪ Ply-metal table construction: plywood core (BBX grade plywood, top of the line, no voids) planed down or particle board; aluminum (or stainless steel) skins on both sides of the table (top and bottom); encased in phenolic-based “Formica” (manufactured by Nevamar or Wilson Art) (RailPlan) or other solid laminate material (Metrolink) like melamine that meets smoke, flame requirements (Frank Ralphs), or solid material like 0.5-inch-thick Corian or Gibraltor (Colorado Railcar). ▪ Edges: (1) rubber bullnose is rabbeted into (pounded in, press fit) the table edge or (2) wrap perimeter with a stainless steel C-channel or (3) cast an epoxy edge with a marine edge (raised radius around the table)—typical of Virginia Railway Express, Metrolink, Maryland Area Regional Commuter (MARC) trains (RailPlan). ▪ Acela tabletop is constructed of aluminum honeycomb core composite—(1) lightweight, (2) offers local crushability and energy-absorption capacity, and (3) maintains rigidity during operational use. Honeycomb core laminated with aluminum Malumin sheets on both faces (B. Slaughter, Amtrak). ▪ Colorado Railcar has a table that is manufactured with a 0.75-inch plywood substrate, laminated on its bottom surface with a plastic sheet, and bonded on its top surface with a 0.5-inch-thick solid material Corian or Gibraltor.
Manufacturing method	<ul style="list-style-type: none"> ▪ Cattco USA manufactures tabletops for Acela as follows: Sheets of aluminum honeycomb core (1.5 in thick) are cut down by using a computer numerical control (CNC) machine to desired tabletop dimensions. An aluminum strip with about 4- or 5-milled-inch hinges (each about 2.5 in long and 6-8 in apart) is placed along the long edges of the table core, and a sheet of aluminum Malumin (Wilson Art) is bonded over both the aluminum honeycomb core and hinge strip, binding all three components together. A Malumin sheet is bonded to the top and bottom surfaces of the table. The hinged sections are screwed to each other. The table edges are placed into flexible strip molds; epoxy is hand poured into these molds to form a smooth edge with a marine lip. The mold is peeled off the table edges. Approximately two tables per mold are manufactured each day. Holes are bored into the bottom of the table surface, and a threaded insert is bonded in [it?] with epoxy (epoxy provides reinforcement and strength). The table is screwed to a structural member that is bolted to the leg and wall

	attachment (that are bolted to mounting tracks on the floor and wall) (Ken Ullman, Cattco).
--	---

Table B2. Table Characterizations (continued)

Cantilever attachment method	<ul style="list-style-type: none"> ▪ Big C bracket spreads load under the table and below the floor grade (LTK) or triangular bracket connects the table bottom to the heater on the wall (RailPlan) (Colorado Railcar). ▪ Square tube attaches the bottom surface of the table to the heater (forms triangular attachment), plus the angle bracket links the table bottom surface to the wall surface (RailPlan) (Colorado Railcar)
Wall attachment (when there is also a floor attachment)	<ul style="list-style-type: none"> ▪ Table attachments to the wall are made at the lower belt rail; a horizontal structure that runs the length of the car both above and below the window (LTK). ▪ Metal plates are embedded inside the plywood before the metal skin is bonded to it, providing a structural insert for machine screw attachments (RailPlan). ▪ Tap plates (with threaded bolt holes) are bonded and screwed to the table surface; bolts are used to attach the table to the wall surface (Frank Ralphs). ▪ Two aluminum angle brackets [are mounted] along the wall surface and table bottom surface. ▪ Steel plates attach to belt rail (Amtrak)—“very, very rugged attachment” (LTK). ▪ Stainless steel mounting brackets—two separate brackets or one long bracket (Frank Ralphs). ▪ Acela—bracket bolted to a rigid metal stiffener that is attached to the table underside and to an aluminum seat track on the wall, 12 in above the floor (seat tracks have 1-inch spacing for attachments). ▪ Colorado Railcar dining tables have a steel-angle plate that is screwed into the underside of the table where a steel plate has been routed into and bonded to the plywood along the width of the table. The angle plate is bolted into the table and riveted to the wall (Colorado Railcar).
Floor attachment method	<ul style="list-style-type: none"> ▪ Table leg goes to seat track on floor (SCRRA Metrolink). ▪ Floor pedestal (less common) (RailPlan). ▪ Steel tubes attach to steel plates beneath the carpet level (Amtrak)—“very, very rugged attachment” (LTK). ▪ Stainless steel legs—one or two legs on aisle side (Frank Ralphs). ▪ One or two stainless steel columns welded together at the top with a plate that fastens to the bottom surface of the table (Frank Ralphs); screwed to table and bolted to floor. ▪ Stainless steel tube, 3-inch diameter; a flange is welded to the top and bottom of the tube. Four bolt holes in flanges that are used to bolt leg to table underside and floor (Frank Ralphs). ▪ Acela—floor mount bolts to the rigid metal stiffener underneath the table and to the seat track on the floor. ▪ Colorado Railcar dining tables have a leg that is bolted to the underside of the table (where a steel plate is routed into and bonded to the plywood along the width of the table) and inserted at the floor onto a drive-on disk where it is bolted along the edge. The drive-on disk is secured to the floor with deck or wood screws (Colorado Railcar).

Table B2. Table Characterizations (continued)

Crashworthiness features	<ul style="list-style-type: none"> ▪ Ideas: use low-density foam, honeycomb, balsa wood, etc., as the core material designed to collapse; skin is sacrificial; rubber edge (RailPlan). ▪ Table is designed with energy-absorption at the attachment (not a crushable table) (SMTc). ▪ Acela table meets Tier II structural crashworthiness (8g, 250-millisecond triangular pulse). However, the tabletop is a sacrificial component of the table. The structural member that it is attached to provides occupant compartmentalization (Pat Malin, Amtrak).
Efforts to improve safety of tables	<ul style="list-style-type: none"> ▪ Bombardier designed a new pedestal leg that is a double stainless steel tube (~1.25-inch diameter). The pedestal leg comes up from the floor and bends 90 degrees and continues toward the wall. This tube is then mounted securely to the wall as well as to the floor. The tabletop (no change in design) is mounted to the horizontal tube rather than just the edge of the table at the wall. San Diego Coaster has the new design (and possibly also Seattle) (Bombardier). ▪ Soft, rounded table edges (Amtrak).
Special features	<ul style="list-style-type: none"> ▪ Table length is partitioned with hinges allowing the table to be folded into a narrower rectangular shape (easier for egress and ingress) (SMTc). ▪ Some tables pull up and out from a case in the wall (RailPlan).

Table B3. Rail Industry Target Areas

Metrolink Bi-Level Cab and Coach Cars	
a)	Subject [Focus?] of April 2002 collision in Placentia, CA.
b)	Tables were the subject of dynamic sled tests conducted at Simula and full-scale collision testing at TTCL.
c)	Tabletop: width is tapered at aisle side to allow for easier ingress and egress and length extends to the middle of the aisle seat; ply-metal core construction = plywood core (BBX grade plywood, top of the line, no voids) planed down or particle board; aluminum (or stainless steel) skins on both sides of the table (top and bottom); encased in phenolic-based "Formica" (manufactured by Nevamar or Wilson Art) (RailPlan).
d)	Two aluminum angle brackets, screwed into the table and bolted to the belt rail along the wall below the window.
e)	One leg with welded flange at top and bottom that bolts to floor and screws to table.
f)	Improvements made to the table attachment: new pedestal leg is a double stainless steel tube (~ 1.25-inch diameter). The pedestal leg comes up from the floor and bends 90 degrees and continues toward the wall. This tube is then mounted more securely to the wall as well as to the floor. The tabletop (no change in design) is mounted to the horizontal tube rather than just the edge of the table at the wall.
Amtrak's Acela Passenger Cars	
a)	The table meets the Tier II test requirements—dynamic sled testing, 250 ms, 8g.
b)	The Acela tabletop core is aluminum honeycomb with aluminum Malumin on the surfaces. The table is designed with hinged sides that allow passengers to fold the table edge to increase the space for ingress and egress. The tabletop spans the entire width of both seats to the aisle. The tabletop is a sacrificial component of the table; it is not designed to protect the occupant. A marine lip is molded to the edges of the table.
c)	A structural component is bolted to a pedestal at the aisle and to a structural member at the wall, providing the structural integrity that withstands the dynamic loading.
d)	An aisle-side pedestal is bolted to the structural component and to the seat mounting track on the floor; a structural member is bolted to the mounting track along the wall and angles to the table where it is bolted to the structural component.
e)	Metal tap plates are bonded and screwed to the table surface to help distribute attachment loads.
Two Additional U.S. Rail Carriers	
a)	MARC and Virginia Rail Express—tables supplied by RailPlan: ply-metal core construction with aluminum skins.
b)	Georgia Rail—see Figure B1.
c)	Colorado Railcar—Some tables are cantilevered to the wall, others have both wall and floor attachments. Cantilevered tables have a triangular truss attachment underneath the tabletop that is bolted to the side wall. Tables extend to the aisle-side armrest of the aisle seat—see Figure B2. Some tables are merely hooked to the wall when passengers choose to rotate their seats and create a facing seat situation. The "ironing board"-shaped table is riveted to the wall along the entire width of the table by using an angle iron attachment plate. The leg is a peg that clicks into a slot on the underside of the table and rests on the floor with a rubber end. Finally, the high-end dining tables are solid plywood with a Corian solid material finish. They are riveted to the wall through an angle attachment that bolts to the underside of the table; the leg is bolted into the underside of the table. It is also bolted onto a drive-on disk that is screwed into the floor.

Table B3. Rail Industry Target Areas (continued)

Two United Kingdom Rail Carriers	
a)	Pendolino Trainsets—tables are manufactured by SMTC who has designed a crashworthy table by using energy absorption at the attachments. SMTC specializes in a large range of composite panels and finished products by gluing various materials such as rigid cores, foams and honeycombs with metal veneers, laminates, wood, and resins. SMTC customers include ABB Adtranz, AFR, Alstom Transport, Bombardier, Duewag, Evac AB, Fiat Ferroviaria, RATP, Siemens, and SNCF (SMTC Web site)—see Figure B3.
b)	Angel Trains—Mr. Barrie Cottam (TBD).
c)	Metronet BCV—Mr. Barrie Cottam (TBD).
Two Additional European Carriers	
a)	First Group (UK) —Mr. Clive Burrows. RSSB is conducting research to improve the design of seats and tables to minimize passenger injuries (Project T201).
b)	Southwest Trains—Mr. David Sawyer (TBD).



Figure B1. Georgia Rail Workstation Table



Figure B2. Colorado Railcar Table



Figure B3. SMTC Workstation Tables



Figure B4. Colorado Railcar Company, Table Photos